

THE STRUCTURAL GEOLOGY OF THE THOMSON FORMATION:  
CLOQUET AND ESKO QUADRANGLES,  
EAST-CENTRAL MINNESOTA

A THESIS  
SUBMITTED TO THE FACULTY OF THE GRADUATE SCHOOL  
OF THE UNIVERSITY OF MINNESOTA

BY  
RICHARD C. CLARK

IN PARTIAL FULFILLMENT OF THE REQUIREMENTS  
FOR THE DEGREE OF  
MASTER OF SCIENCE

MAY, 1985

## ABSTRACT

The Thomson Formation at the type locality in northeastern Carlton County is composed of a thick sequence of interbedded metagreywacke, slaty greywacke (metasiltstone) and slate. Minor amounts of phyllite and hornfels as well as numerous diabase dikes are also present in the study area.

Despite the lower greenschist-facies regional metamorphism, primary sedimentary structures are very well preserved. Bedding generally strikes within 10 degrees of east-west and dips moderately to the north or more commonly to the south. Sedimentary features such as load structures, convolute bedding, small-scale cross-bedding, and graded bedding are excellently preserved at many locations. Sedimentological studies performed previously have noted a dominant north-south paleocurrent trend with a subordinate east-west paleocurrent trend and a northerly source area for the sediments. This is compatible with deposition in a deep-water basin with the coarser beds being deposited by southward-flowing turbidity currents and the muddy units slowly accumulating during the periods between turbidity currents.

The entire study area has been affected by at least one period of major folding that formed generally open, upright, subhorizontal, symmetric or asymmetric, east-west trending folds that contain an axial-planar cleavage. A boundary between one Penokean deformation to the north and two Penokean deformations to the south extends across the southern portion of the study area with multiple deformation south of the boundary being indicated by the presence of a crenulation cleavage.

Cleavage is very well developed in most of the Thomson Formation and ranges from a fine continuous cleavage in the slate to a coarser disjunctive or rough cleavage in the slaty greywacke. Three varieties of rough cleavage are seen in the study rocks: type A (with poorly-developed mica seams), type B (with well-developed mica seams) and type C (with only isolated zones of well-developed mica seams). Microscopic evidence such as shape-modified quartz grains suggests that the rough cleavage seen here probably formed by a pressure solution mechanism whereby quartz was preferentially dissolved allowing the phyllosilicates to be passively concentrated into mica seams around the detrital grains.

A crenulation cleavage that ranges from a zonal to a discrete crenulation cleavage is present at several localities. The microscopic examination of the cleavage zones indicates that the phyllosilicates were passively concentrated into the cleavage zones as deformation proceeded. This is compatible with a pressure solution origin for the crenulation cleavage. Other effects of pressure solution are seen at several places elsewhere in the study rocks.

Kink-bands are common at the type locality at Thomson Dam. Several models have been proposed to explain their origin; however, the kink-bands in this area have characteristics that seem to fit a combination of the rotation model and the joint-drag model of kinking. The Thomson kink-bands formed late in the structural history of the area and are probably the result of Keweenawan activity. Other features presumably related to Keweenawan events such as several cases

of unusual bedding-cleavage relationships are seen throughout the study area.

Intracratonic models and plate-tectonic models have been proposed for the Penokean orogeny in east-central Minnesota. The intracratonic models suggest that Penokean deformation was the result of vertical remobilization of basement rocks along the boundary between Archean gneiss and granite-greenstone terranes. Several converging plate models with south and/or north-dipping subduction zones have been proposed for the Penokean orogeny although several features of modern plate-tectonics are absent from the Proterozoic rocks. The recent identification of probable nappes in the Thomson Formation provides considerable support to the idea that plate-tectonics was responsible for the Penokean orogeny.

## Table of Contents

Abstract . . . . .	i
Table of Contents . . . . .	iii
List of Figures . . . . .	v
List of Tables . . . . .	viii
List of Plates . . . . .	viii
Acknowledgements . . . . .	ix
Chapter I - Introduction . . . . .	1
Statement of the Problem . . . . .	1
Location . . . . .	1
Method of Study . . . . .	2
Previous Work . . . . .	4
Regional Geology . . . . .	5
Chapter II - Petrology . . . . .	13
Introduction . . . . .	13
Metagreywacke . . . . .	16
Slaty greywacke . . . . .	18
Slate . . . . .	19
Phyllite . . . . .	21
Hornfels . . . . .	21
Concretions . . . . .	23
Quartz veins . . . . .	25
Diabase . . . . .	25
Chapter III - Sedimentology . . . . .	27
Introduction . . . . .	27
Bedding and sedimentary structures . . . . .	27
Paleocurrent analyses . . . . .	29
Provenance . . . . .	31
Environment of deposition . . . . .	32
Stratigraphic relationships . . . . .	33
Chapter IV - Structure . . . . .	34
Introduction . . . . .	34
Folds . . . . .	34
Cleavage . . . . .	37
Lineations . . . . .	41
Faults . . . . .	41
Dikes . . . . .	42
Folded cleavage . . . . .	42
Kink-bands . . . . .	44
Joints and quartz veins . . . . .	48

Chapter V - Structural Interpretation . . . . .	50
Introduction . . . . .	50
Cleavage . . . . .	50
Classification . . . . .	50
Origin of slaty cleavage . . . . .	53
Origin of rough cleavage . . . . .	58
Crenulation cleavage . . . . .	61
Introduction . . . . .	61
Origin of crenulation cleavage . . . . .	61
Other evidence of pressure solution . . . . .	67
Kink-bands . . . . .	69
Introduction . . . . .	69
Kink-band models . . . . .	71
Thomson Formation kink-bands . . . . .	76
Origin of the Thomson Formation kink-bands . . . . .	77
Late-stage deformation . . . . .	81
Chapter VI - Tectonic Interpretation . . . . .	87
Introduction . . . . .	87
Deformation in the Thomson Formation . . . . .	87
Influences of basement rocks . . . . .	91
Intracratonic model . . . . .	92
Plate-tectonic model . . . . .	95
Nappes in the Thomson Formation . . . . .	100
Conclusions . . . . .	103
Chapter VII - Summary . . . . .	105
References Cited . . . . .	107

### List of Figures

Fig. 1	Map showing the location of the thesis field area. . . . .	3
Fig. 2	Inferred location of the Animikie basin. . . . .	7
Fig. 3	Generalized tectonic map of the Lake Superior region. . . . .	10
Fig. 4	Pre-tectonic cross-section through east-central Minnesota. . . . .	11
Fig. 5	Photomicrograph of metagreywacke. . . . .	17
Fig. 6	Photomicrograph of slaty greywacke. . . . .	17
Fig. 7	Small-scale trough cross-bedding in laminated slaty greywacke. . . . .	20
Fig. 8	Photomicrograph of slate. . . . .	20
Fig. 9	Photomicrograph of phyllite. . . . .	22
Fig. 10	Photomicrograph of spotted slate. . . . .	22
Fig. 11	Concretions deformed to an elliptical shape. . . . .	24
Fig. 12	Diabase dike intruding the Thomson Formation. . . . .	26
Fig. 13	Photomicrograph of diabase. . . . .	26
Fig. 14	Equal area projection of 1118 poles to bedding. . . . .	28
Fig. 15	Photomicrograph of a load structure at a slaty greywacke-slate contact. . . . .	28
Fig. 16	Orientation diagrams of sedimentary structures. . . . .	30
Fig. 17	Large-scale, open, upright, subhorizontal fold. . . . .	35
Fig. 18	Photomicrograph of a microfold with axial-planar cleavage. . . . .	35
Fig. 19	Equal area projection of 846 bedding-cleavage intersections. . . . .	36
Fig. 20	Small-scale, tight, vertical folds. . . . .	36
Fig. 21	Equal area projection of 868 poles to cleavage. . . . .	38

Fig. 22	Alternating slate and slaty greywacke beds showing alternating steep and flat cleavage. . . . .	38
Fig. 23	Photomicrograph of crenulation cleavage in slate not visible in hand sample. . . . .	40
Fig. 24	Photomicrograph of crenulation cleavage in slate. . . . .	40
Fig. 25	Photomicrograph of a microfault in slate. . . . .	43
Fig. 26	Diabase dike and pod swarm at Oldenburg Pt. . . . .	43
Fig. 27	Folded cleavage in slate at Oldenburg Pt. . . . .	45
Fig. 28	Field sketches of the folded cleavage at Oldenburg Pt. . . . .	46
Fig. 29	Kink-bands in slate at Thomson Dam. . . . .	47
Fig. 30	Kink-band in slate at Thomson Dam. . . . .	47
Fig. 31	Equal area projection of 110 poles to kink-bands. . . . .	49
Fig. 32	Equal area projection of 807 poles to joints. . . . .	49
Fig. 33	Equal area projection of 95 poles to quartz veins. . . . .	49
Fig. 34	Classification of rock cleavage. . . . .	51
Fig. 35	Photomicrograph of type A rough cleavage. . . . .	54
Fig. 36	Photomicrograph of type B rough cleavage. . . . .	54
Fig. 37	Photomicrograph of type C rough cleavage. . . . .	55
Fig. 38	Photomicrograph of a 'cross-mica' chlorite porphyroblast in slate. . . . .	59
Fig. 39	Photomicrograph of a grain with quartz overgrowths and mica beards. . . . .	59
Fig. 40	Photomicrograph of discrete crenulation cleavage. . . . .	62
Fig. 41	Photomicrograph of zonal crenulation cleavage. . . . .	63
Fig. 42	Idealized model showing the importance of grain position on a microfold. . . . .	66
Fig. 43	Photomicrograph of an opaque mineral deformed by buckling. . . . .	68

Fig. 44	Photomicrograph of opaque minerals deformed by buckling. . . . .	68
Fig. 45	Photomicrograph of the offset in bedding in a silty slate. . . . .	70
Fig. 46	The geometric parameters of kink-bands. . . . .	72
Fig. 47	The migration model of kink-band development. . . . .	73
Fig. 48	The rotation model of kink-band development. . . . .	73
Fig. 49	The joint-drag model of kink-band development. . . . .	75
Fig. 50	The simple shear model of kink-band development. . . . .	75
Fig. 51	Photomicrograph of a kink-band showing the dilation of foliation within the kink-band. . . . .	78
Fig. 52	Photomicrograph of a kink-band showing the continuity of foliation across the kink-band. . . . .	79
Fig. 53	Photomicrograph of a kink-band showing the discontinuity of foliation across the kink-band. . . . .	79
Fig. 54	Photomicrograph of a kink-band with triangular fillings along the kink-band boundary. . . . .	80
Fig. 55	Photomicrograph of a kink-band showing dilation of foliation and the discontinuity of foliation across the kink-band. . . . .	80
Fig. 56	Sketch of a single cleavage plane through a kinked sample. . . . .	82
Fig. 57	'Abnormal' cleavage refraction around a fold. . . . .	84
Fig. 58	Map showing the boundary between one and two Penokean deformations. . . . .	88
Fig. 59	Sketch of a small fold with axial-planar $S_1$ foliation. . . . .	90
Fig. 60	Map showing the boundary between Archean basement types. . . . .	90
Fig. 61	Geologic section across the Animikie basin. . . . .	94
Fig. 62	Diagram illustrating Penokean deformation in Michigan. . . . .	96
Fig. 63	A possible reconstruction of the Penokean orogeny. . . . .	97



Fig. 64	Geometric relations of bedding and cleavage near Mahtowa. . . . .	102
Fig. 65	Diagrammatic cross-section of the Thomson Formation. .	104
Fig. 66	A possible model of the Penokean orogeny in Minnesota.	104

List of Tables

Table 1	Inferred correlation of Middle Precambrian rocks in Minnesota. . . . .	6
Table 2	Inferred correlation of Middle Precambrian rocks in Minnesota, Wisconsin and Michigan. . . . .	6
Table 3	Stratigraphic column for east-central Minnesota. . .	8
Table 4	Point count analyses of selected metagreywackes. . .	14
Table 5	Point count analyses of selected slaty greywackes. .	15
Table 6	Point count analyses of selected slates. . . . .	15

List of Plates

Plate 1	Outcrop map of the Thomson Formation in the Cloquet and Esko quadrangles showing bedding and cleavage. . . . .	in pocket
Plate 2	Outcrop map of the Thomson Formation in the Cloquet and Esko quadrangles showing fold axes and dikes. . . . .	in pocket

#### ACKNOWLEDGEMENTS

I would like to thank Dr. Timothy B. Holst for being my advisor. His continual help, patience and understanding was greatly appreciated. I also extend my appreciation to my thesis committee members, Dr. Peter J. Hudleston and Dr. Richard W. Ojakangas, for their critical review of my writing and their timely suggestions. I also thank Ed Mulligan for his help with the computer work and my fellow graduate students for their help and encouragement throughout my graduate career. This thesis was funded by a grant from the National Science Foundation.

CHAPTER I  
INTRODUCTION

Statement of the problem

The Middle Precambrian Thomson Formation of east-central Minnesota is a thick sequence of interbedded slate, slaty greywacke and metagreywacke. It has been subjected to several metamorphic and deformational events during the Penokean orogeny (1875-1825 m.y., Van Schmus, 1976; 1980) the effects of which are seen to varying degrees throughout the formation. Only one major Penokean deformational event has been recognized at the type locality in the northern portion of the formation (Schwartz, 1942a; Wright and others, 1970) while several workers have recognized two or more deformations in more southerly exposures of the Thomson Formation (Connolly, 1981; Hyrkas, 1982; Neuman, in prep.). This study concentrates on a key area in the northern part of the formation where there appears to be a boundary between one and two Penokean deformations. Field observations of structure combined with microstructure seen in thin section can be used to help determine the type, style and extent of deformation that occurred in this portion of the Thomson Formation. This type of study can furnish information that will be useful in gaining a better understanding of the Penokean orogeny.

Location

The study area is located in the Cloquet and Esko quadrangles, northeastern Carlton and southwestern St. Louis Counties, east-central Minnesota. The area includes major portions of Knife Falls Township (T.49N,R.17W), Thomson Township (T.49N,R.16W), and Twin Lakes Township

(T.48N,R.17W; T.48N,R.16W), a small portion of Midway Township (T.49N,R.15W) and the communities of Cloquet, Scanlon, Carlton and Thomson (Fig. 1). Access to the area can be gained via Interstate 35 and state highways 61, 210 and 33 as well as several county roads.

Much of the area is covered with Pleistocene glacial deposits that range in thickness from 0 to 50 meters (Wright and others, 1970). However, the St. Louis River, acting as a glacial drainageway, has cut through this cover exposing bedrock. Most of the outcrop is found along 15 km of the St. Louis River valley and 7 km of the Little Otter Creek valley. Outcrop density within the valleys is quite good, with the outcrop forming long east-west trending ridges rising as much as 20 meters above the surrounding swamps. These ridges are often dissected by the southward-flowing rivers and north-south trending highways and railroads providing good exposures.

#### Method of study

Most outcrops were located through the use of previous studies (Wright and others, 1970; Kilburg and Morey, 1977); however, others were identified by their characteristic slope and relief on topographic maps and by personal communication with local inhabitants. More time was spent observing river, road and railroad cuts than smaller, more poorly-exposed outcrop since these cuts provided a more complete section and more easily identifiable structure.

About 250 outcrops were examined with notes being taken on lithology and structure. Structural data collected included measurements of bedding, cleavage, joint, fault, quartz vein and fold

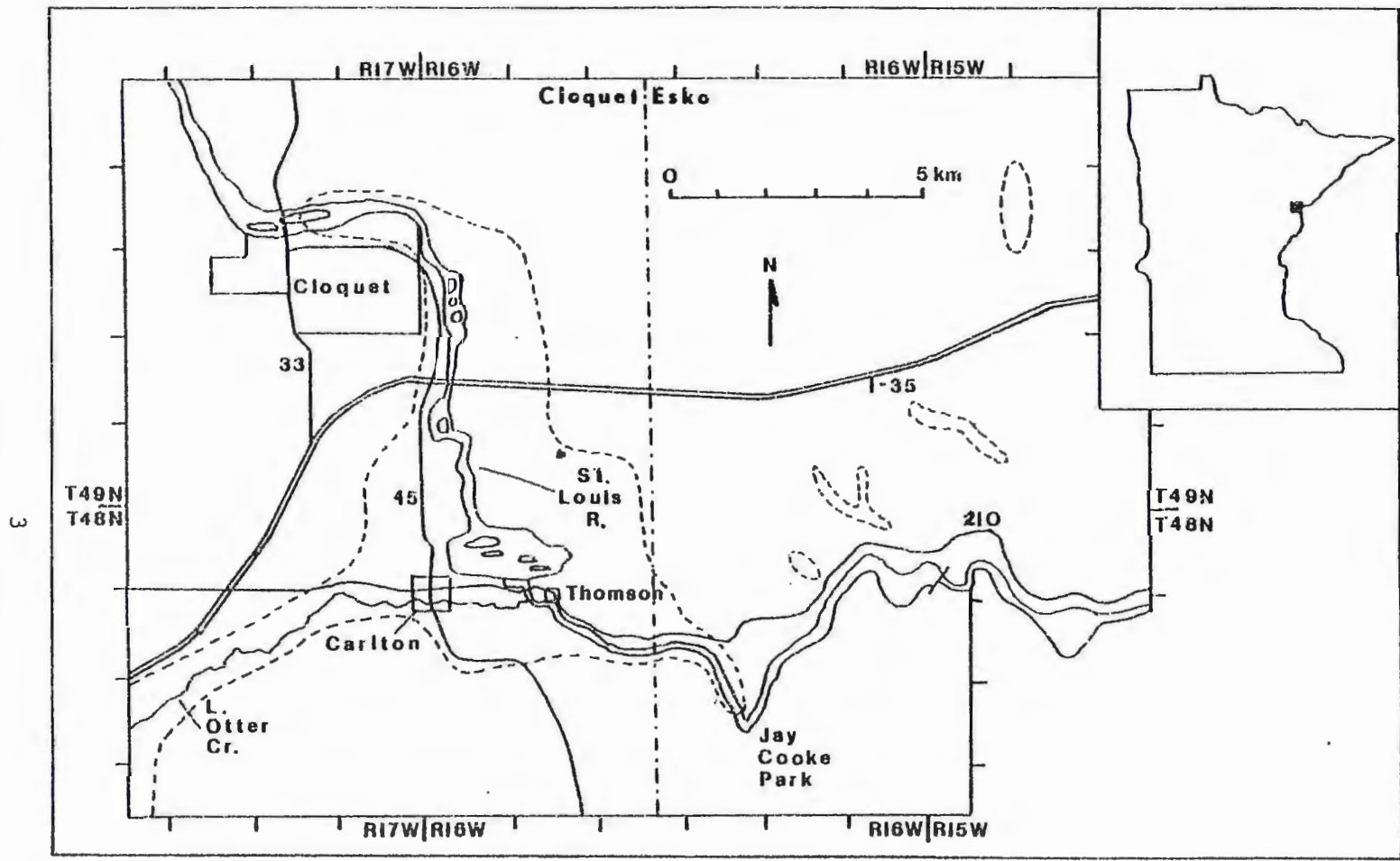


Fig. 1 Map showing the thesis field area consisting of the Cloquet and Esko 7.5' quadrangles, Minnesota. State and county highways are labelled. All outcrop is found within the dashed lines.

orientations. To help process the large number of structural measurements a computer program was used to store and plot the data on equal-area stereonet.

At most locations a representative sample was taken. From these samples a suite of 86 thin sections was made, and detailed descriptions of lithology and particularly microstructure were made. At several outcrops oriented samples were taken for later analysis.

#### Previous Work

Since 1894 when the rocks in and around the village of Thomson were named the 'Thomson Slates' there has been a fair amount of work done on the Thomson Formation. Most of the early work (Spurr, 1894; Hall, 1901; Sandberg, 1938) consisted of the correlation of the Thomson Formation with other formations of east-central and northeastern Minnesota. Schwartz (1942a, 1942b, 1942c) did the first detailed field work of the Thomson Formation and published several papers dealing with the lithology (where he renamed the Thomson Slates the Thomson Formation), structure, metamorphism and carbonate concretions of the area. In the early 1970's several papers were published dealing mainly with the lithology and general structure of the area near the type locality (Wright and others, 1970; Morey and Ojakangas, 1970; Keighen and others, 1972). More southerly exposures of the Thomson Formation in the Moose Lake, Atkinson and Denham areas have been studied as master theses by Connolly (1981), Hyrkas (1982) and Neuman (in prep.). Ojakangas (1976), Morey (1979) and Davidson (1979) have also studied portions of the Thomson Formation with reference to the possible uranium potential of the area.

## Regional Geology

Through the years there has been much debate as to the correlation of the Thomson Formation with other formations in the Lake Superior region. Several writers have suggested a correlation with Middle Precambrian Animikie rocks (Irving, 1883; Van Hise and Leith, 1911; Harder and Johnston, 1918) while others have said the Thomson Formation is older and correlates with Lower Huronian or older rocks (Spurr, 1894; Leith, 1903; Schwartz, 1942b; Grout and others, 1951). Detailed lithology and sedimentology studies showing a correlation with the Animikie Rove Formation by Morey and Ojakangas (1970) as well as radiometric age dating by Goldich and others (1961) seem to confirm an Animikie age for the Thomson Formation.

There have been attempts to show a correlation between the three main iron ranges in Minnesota (Table 1) and between the Minnesota ranges and the Michigan-Wisconsin ranges (Table 2). Because of sedimentological and lithological similarities it is probable that these sediments were deposited in different parts of the same basin (Fig. 2).

The Precambrian rocks of east-central Minnesota can be divided into four distinct terranes: 1) Lower Precambrian rocks; 2) Middle Precambrian stratified rocks; 3) Middle Precambrian plutonic rocks; and 4) Upper Precambrian Keewenawan sedimentary and volcanic rocks (Morey, 1978). A stratigraphic column for east-central Minnesota is given in Table 3. Detailed descriptions of the different rock types can be found in Morey (1978), and a generalized geologic map for east-central Minnesota has been published by Morey, Olsen and Southwick (1981).

GUNFLINT RANGE Minnesota and Ontario (Goldich and others, 1961; Tanton, 1931)	MESABI RANGE Minnesota (White, 1954)	CUYUNA RANGE Minnesota (Groat and Wolff, 1955; Schmidt, 1963)	EAST-CENTRAL MINNESOTA (Goldich and others, 1961; Morey and Ojakangas, 1970)
UPPER PRECAMBRIAN SEDIMENTARY AND IGNEOUS ROCKS (younger than 1.6 b. y.)			
----- unconformity -----			
Rove Formation Gunflint Iron-formation "Kakabeka Quartzite"	Virginia Formation Biwabik Iron-formation Pokegama Quartzite	Rabbit Lake Formation Trommald Formation Mahnomen Formation	Thomson Formation
----- unconformity -----			
Trout Lake formation quartzite and slate			
----- unconformity -----			
LOWER PRECAMBRIAN IGNEOUS AND METAMORPHIC ROCKS (older than 2.6 b. y.)			

Table 1 Inferred correlation of Middle Precambrian sedimentary rocks in Minnesota (Morey, 1972).

MESABI RANGE	CUYUNA RANGE	GOGEBIC RANGE	DICKINSON COUNTY	MARQUETTE RANGE
UPPER PRECAMBRIAN SEDIMENTARY AND IGNEOUS ROCKS (younger than 1.6 b. y.)				
----- unconformity -----				
Virginia Formation	Rabbit Lake Formation	Tyler Slate	Badwater Greenstone Michigamme Slate Hemlock Formation	Bataga Group { Michigamme Slate Geordich Quartzite
Annikie Group Biwabik Iron-formation Pokegama Quartzite	Trommald Formation	Ironwood Iron-formation	Vulcan Iron-formation Felch Formation	
	Mahnomen Formation	Palmis Quartzite		
----- unconformity -----				
	Trout Lake formation quartzite and slate?	Bad River Dolomite Sunday Quartzite	Randville Dolomite Sturgeon Quartzite Fern Creek Formation	Chocoma Group { Wewe Slate Kona Dolomite Mesnard Quartzite Enchantment Lake Formation
----- unconformity -----				
LOWER PRECAMBRIAN IGNEOUS AND METAMORPHIC ROCKS (older than 2.6 b. y.)				

Table 2 Inferred correlation of Middle Precambrian sedimentary rocks in Minnesota, Wisconsin and Michigan (Morey, 1972).



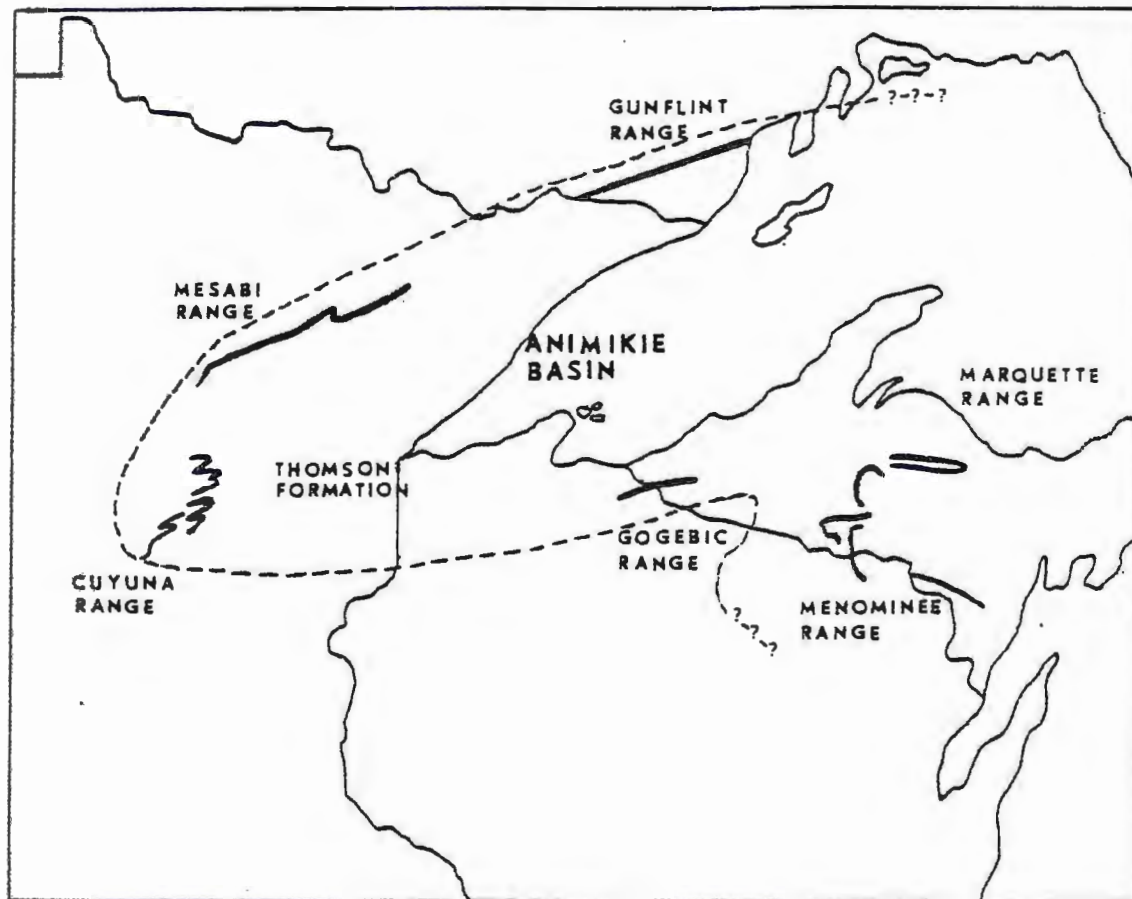


Fig. 2 Inferred location of the Animikie basin showing the locations of the Animikie Group sediments of the Minnesota, Wisconsin and Michigan iron ranges (After Ojakangas, 1983).

Table 3 - Stratigraphic column for east-central Minnesota  
(After Morey, 1978).

UPPER PRECAMBRIAN

Hinckley Sandstone  
 Fond du Lac Formation  
 - - - unconformity - - -  
 Chengwatana Volcanic Group  
 - ? - unconformity - ? -  
 North Shore Volcanic Group - Ely's Peak Basalts  
 Nopeming Sandstone  
 - - - major unconformity - - -

MIDDLE PRECAMBRIAN

Stearns Granitic Complex  
     St. Cloud Granite  
     Rockville Granite  
 Post-Penokean Granites  
     Isle, Warman, Pierz and Reformatory Granites  
 Late-Penokean Plutonic Rocks  
     Bradbury Creek Granodiorite  
     Freedhem Granodiorite  
     Unnamed dioritic and gabbroic rocks  
 - - - major unconformity - - -  
 Animikie Group  
     Rabbit Lake Formation; Thomson Formation  
     Trommald Formation  
     Mahnomen Formation  
     - - - unconformity - - -  
 Mille Lacs Group  
     Trout Lake Formation  
     Little Falls Formation  
     Randall Formation; Glen Township Formation  
     Denham Formation  
     - ? - unconformity - ? -  
 Hillman Migmatite  
 - - - major unconformity - - -

LOWER PRECAMBRIAN

Granite-Greenstone rocks  
     Granitic, metasedimentary, metavolcanic rocks  
 - - - major unconformity - - -  
 McGrath Gneiss  
 Sauk Rapids Metamorphic Complex  
     St. Wendel Metagabbro  
     Watab Amphibolite  
     Sartell Gneiss  
 Richmond Gneiss

The Lower Precambrian terrane consists of a northern segment with rocks similar to a granite-greenstone terrane (2700 m.y.), a southern highly deformed gneiss segment (3550 m.y.) and a central sheared, schistose segment (Morey, 1978) also known as the Great Lakes tectonic zone (Sims and others, 1980) (Fig. 3). Along this zone at the end of the Archean, granite plutons acted as a weld between the Lower Precambrian northern and southern segments forming a relatively stable craton (Morey, 1978).

This craton was capable of supporting a large sedimentary basin during the Middle Precambrian, known as the Animikie basin. Sedimentation began about 2100 m.y. ago (Van Schmus, 1976), with deposition proceeding through five phases: prequartzite (conglomerate, quartzite, pillow basalt), quartzite (quartzite, dolomite, argillite), shelf (iron formation), transition (carbonaceous argillite, iron formation, volcanics) and flysch (greywacke, slate, argillite) phases (Morey, 1978) (Fig. 4).

The Penokean orogeny which occurred near the close of Middle Precambrian time (1875-1825 m.y., Van Schmus, 1976; 1980)) caused the deformation and metamorphism of much of the Animikie basin sediments, with both deformation and metamorphism increasing in grade from the north (granite-greenstone basement) to the south (sheared schistose and gneissic basement) perhaps suggesting that the basement rock (and possible relative motions of the basement rock) had some effect on the degree of deformation (Morey, 1978).

During and after the Penokean orogeny plutonic rocks were intruded into Middle Precambrian stratified rocks. These plutonic rocks consist

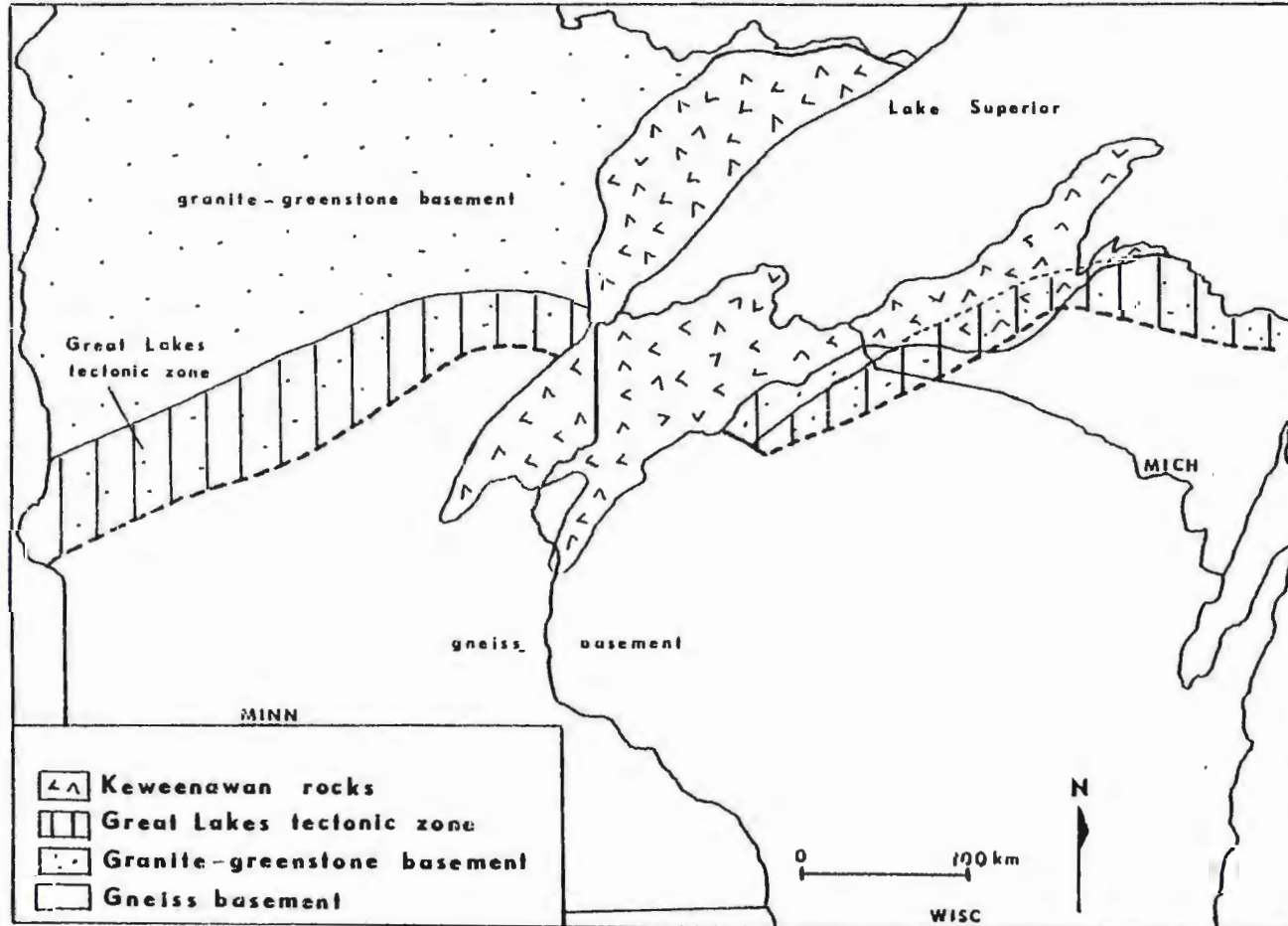


Fig. 3 Generalized tectonic map of the Lake Superior region showing the location of the Great Lakes tectonic zone (After Sims and Peterman, 1983).

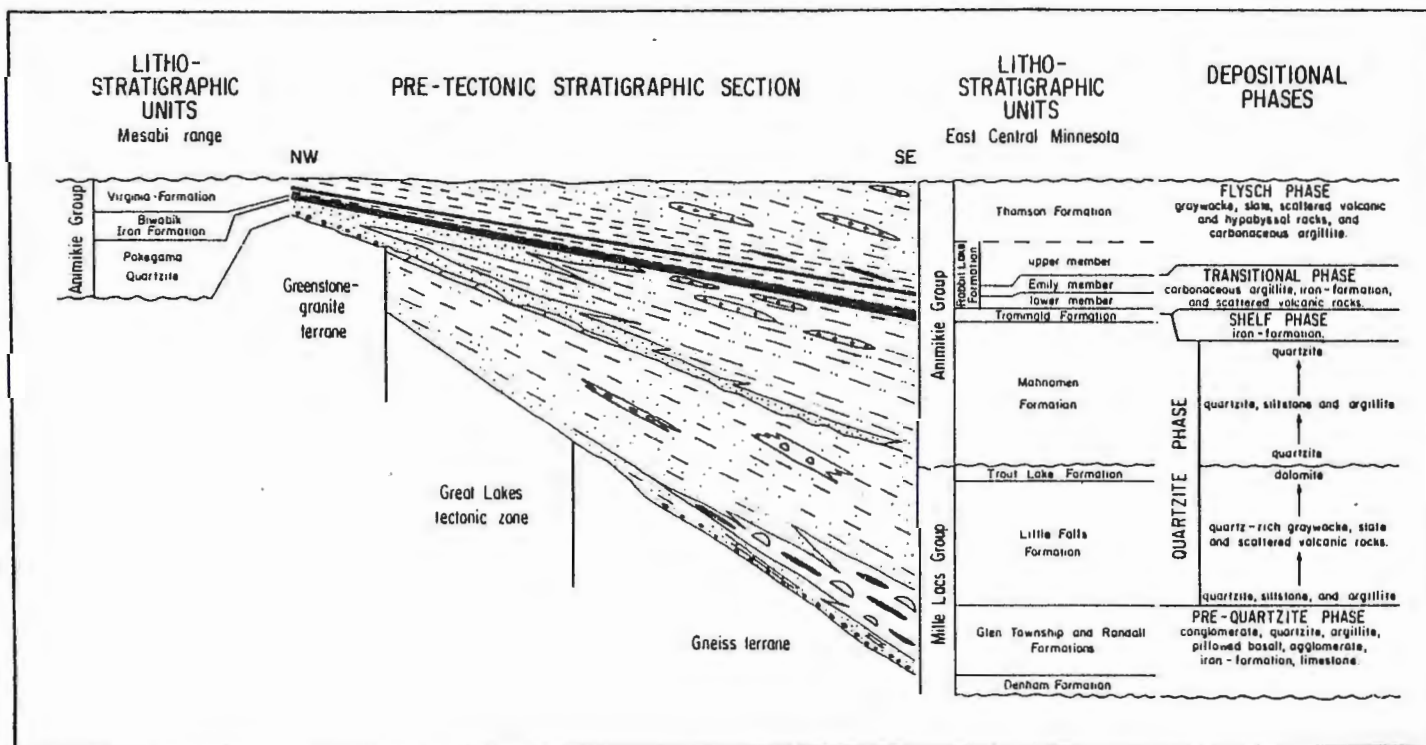


Fig. 4 Pretectonic north-south cross section showing the lithostratigraphic nomenclature and depositional phases of the Middle Precambrian stratified rocks in east-central Minnesota (Morey, 1979).

of syn-orogenic gabbro, diorite and granodiorite and post-orogenic granites (Morey, 1978).

The Precambrian history of east-central Minnesota ended with the deposition of the Upper Precambrian Keweenaw System consisting of volcanic rocks (1100 m.y.) and slightly younger sedimentary rocks. Keweenaw-age syn-volcanic dikes are quite common, especially in the study area in the northern part of east-central Minnesota.

Phanerozoic rocks are absent from the rock record of east-central Minnesota. However, Pleistocene glacial deposits of varying types provide nearly continuous coverage of the underlying Precambrian rocks. The lithology and stratigraphy of the Pleistocene of the Cloquet quadrangle has been studied in some detail by Wright and others (1970).

## CHAPTER II

### PETROLOGY

#### Introduction

The Thomson Formation in the study area consists of a thick sequence of laterally continuous, interbedded metagreywacke, slaty greywacke and slate. Estimates of the proportions of rock types at the type locality have been given previously as approximately 34 to 48% metagreywacke, 25 to 43% slaty greywacke (metasiltstone) and 23 to 31% slate (Schwartz, 1942a; Wright and others, 1970; Morey and Ojakangas, 1970). There doesn't appear to be any relationship between stratigraphic position and relative abundance of the rock types (Morey and Ojakangas, 1970).

Also found in the study area are minor amounts of phyllite and hornfels, as well as numerous mafic dikes. Concretions and quartz veins are common in many of the sedimentary beds. Modal mineralogy of the metagreywacke, slaty greywacke and slate is given in Tables 4, 5 and 6.

The rocks in the study area have been regionally metamorphosed to the lower greenschist facies. Metamorphic grade has been noted to increase towards the southwest (Schwartz, 1942b; Morey, 1979).

The total thickness of the Thomson Formation is not known with any degree of certainty because of the strong deformation, the paucity of recognizable marker beds, the lack of continuous exposure, and because neither the top nor the bottom of the formation is exposed. Estimates of the formation thickness range from an early estimate of more than 6500 meters (Schwartz, 1942b) to a more recent estimate of about 1000

Table 4 - Point Count Analyses (500 grains) - Metagreywacke

Sample number	<u>5a2</u>	<u>79b</u>	<u>129d</u>
Quartz	40	22	34
strained	26	15	23
polycrystalline	9	1	4
recrystallized*	5	6	7
Feldspar	14	27	22
plagioclase	13	19	16
orthoclase	1	7	4
microcline	-	1	2
Rock Fragments	7	7	8
felsic VRF**	2	3	4
quartzite	2	3	3
mafic VRF**	2	1	1
schist	1	tr	tr
granite	-	-	tr
slate	tr	tr	-
Matrix	38	44	36
chlorite-sericite	26	28	27
quartz-feldspar	9	10	7
calcite	2	3	tr
epidote	1	3	1
opaques	tr	1	tr
Miscellaneous	tr	tr	tr
QFL (Dickinson, 1970)	Q <sub>66</sub> F <sub>23</sub> L <sub>12</sub>	Q <sub>39</sub> F <sub>48</sub> L <sub>13</sub>	Q <sub>53</sub> F <sub>34</sub> L <sub>13</sub>
QFM***	Q <sub>44</sub> F <sub>15</sub> M <sub>41</sub>	Q <sub>23</sub> F <sub>29</sub> M <sub>48</sub>	Q <sub>37</sub> F <sub>24</sub> M <sub>39</sub>

\* Quartz grains showing various stages of recrystallization.

\*\* VRF = volcanic rock fragments.

\*\*\* QFM = % quartz-feldspar-matrix.



Table 5 - Point Count Analyses (500 grains) - Slaty Greywacke

Sample number	<u>140</u>	<u>145c</u>	<u>179x</u>	<u>204x</u>
Quartz	30	31	21	26
strained	26	30	20	25
polycrystalline	3	1	1	1
recrystallized*	1	-	-	-
Feldspar	16	17	20	23
plagioclase	9	14	14	17
orthoclase	7	3	6	6
microcline	-	-	tr	-
Rock fragments	4	1	4	1
felsic VRF*	2	1	2	1
quartzite	2	tr	2	tr
mafic VRF*	-	-	tr	-
Matrix	50	51	55	51
chlorite-sericite	32	34	37	37
quartz-feldspar	12	12	14	11
calcite	2	tr	1	1
epidote	4	5	2	2
opaques	tr	tr	tr	tr
organics	-	tr	-	-
Miscellaneous	tr	tr	tr	tr
QFL (Dickenson, 1970)	Q <sub>60</sub> F <sub>33</sub> L <sub>7</sub>	Q <sub>63</sub> F <sub>35</sub> L <sub>2</sub>	Q <sub>47</sub> F <sub>44</sub> L <sub>9</sub>	Q <sub>52</sub> F <sub>46</sub> L <sub>2</sub>
QFM*	Q <sub>31</sub> F <sub>17</sub> M <sub>52</sub>	Q <sub>31</sub> F <sub>17</sub> M <sub>52</sub>	Q <sub>32</sub> F <sub>21</sub> M <sub>57</sub>	Q <sub>26</sub> F <sub>23</sub> M <sub>51</sub>

\* Definitions as in Table 4.

Table 6 - Point Count Analyses (500 grains) - Slate

Sample number	<u>52a</u>	<u>174x</u>	<u>201x</u>
Chlorite-sericite	59	67	70
Quartz-feldspar	17	22	23
Epidote	2	6	3
Calcite	2	1	1
Carbonaceous material	11	2	3
Pyrite	-	tr	-
Chlorite porphyroblasts	tr	1	1
Quartz veins	8	2	-

meters based on the folding of a presumed marker horizon (Wright and others, 1970). Greenhalgh (1981) has noted, through the use of seismic profiling, a constant velocity sequence that is approximately 1000 meters thick in this region.

The sediments of the Thomson Formation were probably deposited in relatively deep water with the coarser greywacke and slaty greywacke being deposited by southward-flowing turbidity currents and the mud accumulating slowly in the calm periods between turbidity currents (Morey and Ojakangas, 1970.) Sedimentological and provenance studies by Morey and Ojakangas (1970) indicate that these sediments were derived from a mainly plutonic terrane located to the north.

#### Metagreywacke

Massive metagreywacke commonly occurs in beds that range in thickness from two centimeters to nearly 10 meters. The metagreywacke, being more resistant than the other rock types, tends to form long, topographically prominent ridges. Most of the metagreywacke is fine or medium-grained, but some is coarse-grained. Locally, small lenses of intraformational conglomerate are found at the base of the beds, with the pebbles consisting of 1 to 5 centimeter fragments of slate. The rock is grey to greenish-grey in color on a fresh surface and tends to be very massive with little or no evidence of internal laminations or foliations. Normal grading is evident in many beds while cross-bedding is rare. In thin section it can be seen that the most common detrital grains are quartz, feldspar, and rock fragments (Fig. 5). Quartz comprises 20 to 40% of the samples, with most grains being angular, unsorted, monocrystalline quartz. The effect of deformation is evident

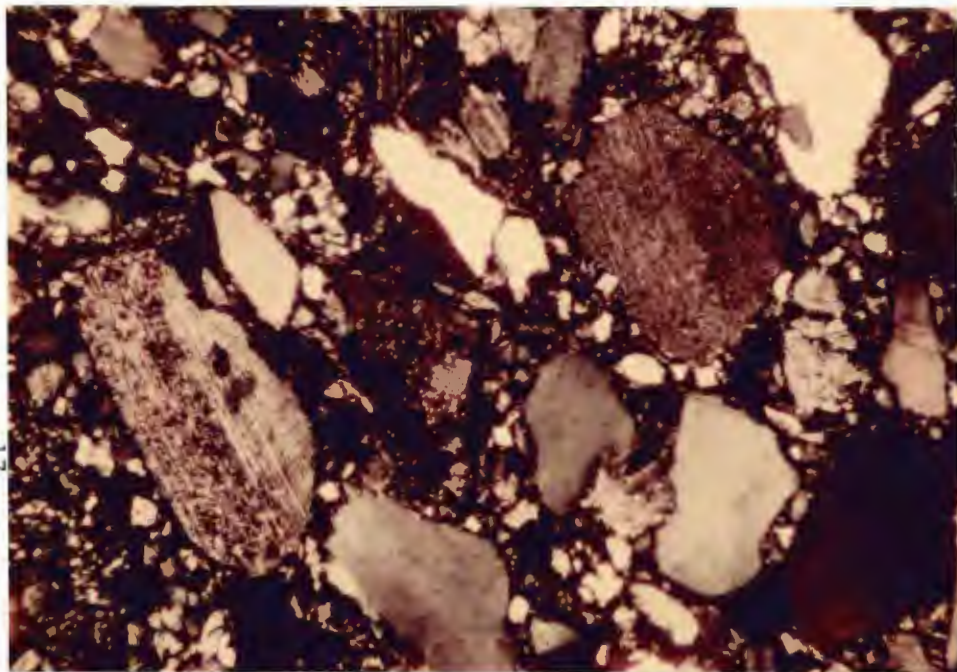
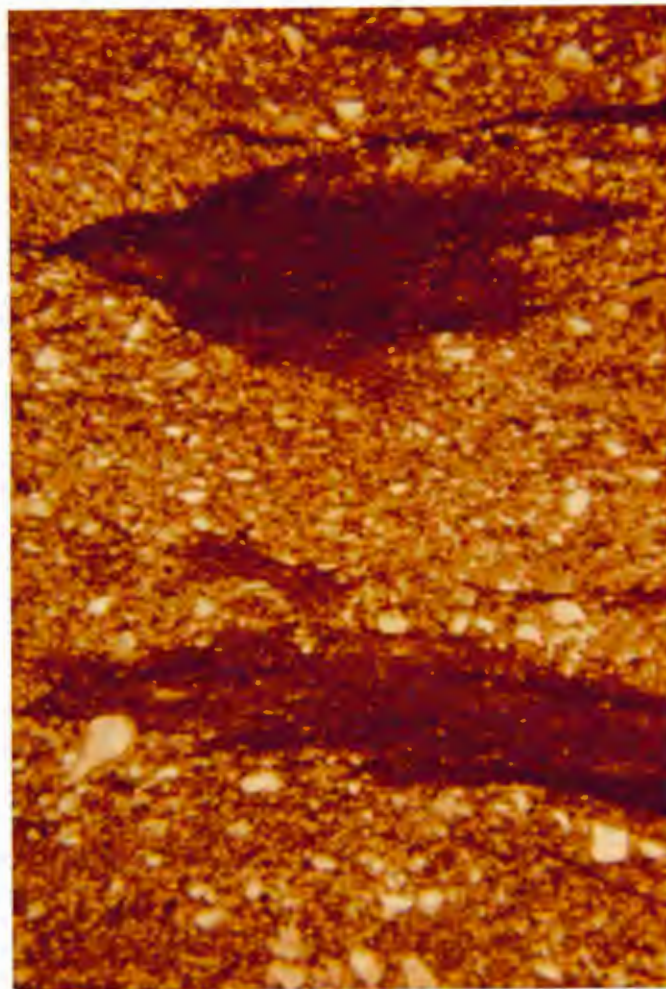


Fig. 5 Photomicrograph of metagreywacke showing quartz, and feldspar grains. 2.2 km E. of Thomson Dam. Field of view is 3.8mm X 2.6mm. Crossed nichols.

Fig. 6 Photomicrograph of slaty greywacke. Note the presence of a cleavage and the presence of rip-up clasts of slate. 3.5 km WSW of Carlton. Field of view is 3.8mm X 2.6mm. Plain light.



in most samples; the grains are cracked, usually have strong undulatory extinction and some show the effects of recrystallization to some degree.

Feldspar comprises 15 to 25% of the rock with the actual percentage being greater in the coarser grained metagreywacke. The feldspar is dominantly sodic plagioclase with small amounts of orthoclase, microcline and perthite. All occur as angular to subrounded, unsorted, moderately to intensely seriticized grains.

Rock fragments make up only about 7 to 10% of the rock and generally consist of subrounded to rounded quartzite and felsic volcanic grains with lesser amounts of basalt, schist, chert, granite and slate fragments.

The matrix of the metagreywacke makes up 35 to 45% of the samples and is dominantly composed of chlorite, sericite, quartz and feldspar with minor amounts of calcite, epidote, pyrite and carbonaceous material. The present matrix is probably derived from the recrystallization of an original clayey matrix (Morey and Ojakangas, 1970).

#### Slaty Greywacke

Slaty greywacke is an intermediate rock type between slate and metagreywacke (Fig. 6). It is found in two centimeter to two meter thick beds as well as in the upper portion of some of the metagreywacke beds. It is usually grey to greenish-grey in color on a fresh surface and commonly has internal laminations as well as a poorly to moderately well-developed cleavage. Grading and small-scale sedimentary structures are commonly present (Fig. 7).

In thin section it can be seen that the slaty greywacke consists of 20 to 30% quartz, 15 to 20% feldspar and less than 5% rock fragments which is roughly similar to the composition of the metagreywacke. The matrix, which makes up about 50% of the rock, is again composed of chlorite, sericite, quartz and feldspar with minor amounts of calcite, epidote, pyrite and carbonaceous material. The laminations of the slaty greywacke can be identified by the relative predominance of either quartz-feldspar or chlorite-sericite.

### Slate

Slate occurs throughout the formation either as up to two centimeter thick layers between graded metagreywacke and slaty greywacke beds or in less than two centimeter to nearly 10 meter thick repetitive beds. It is less resistant than the metagreywacke and thus is often found only along the flanks of the metagreywacke ridges. The slate is usually dark greenish-grey in color on a fresh surface and nearly always shows excellent slaty cleavage. The individual slate beds are usually composed of numerous laminations showing small-scale sedimentary structures such as cross-bedding and soft sediment deformation; however, some beds are massive and show no laminations.

The slate (or silty slate) is composed of 0 to 20% very fine quartz and feldspar grains in a matrix of chlorite, sericite and quartz-feldspar with minor amounts of calcite, pyrite, epidote and carbonaceous material (Fig. 8). Small metamorphic porphyroblasts of chlorite and patches of authigenic calcite are commonly present. The authigenic calcite content is significantly greater in the southern



Fig. 7 Small-scale trough cross-bedding in laminated slaty greywacke. Thomson Dam.

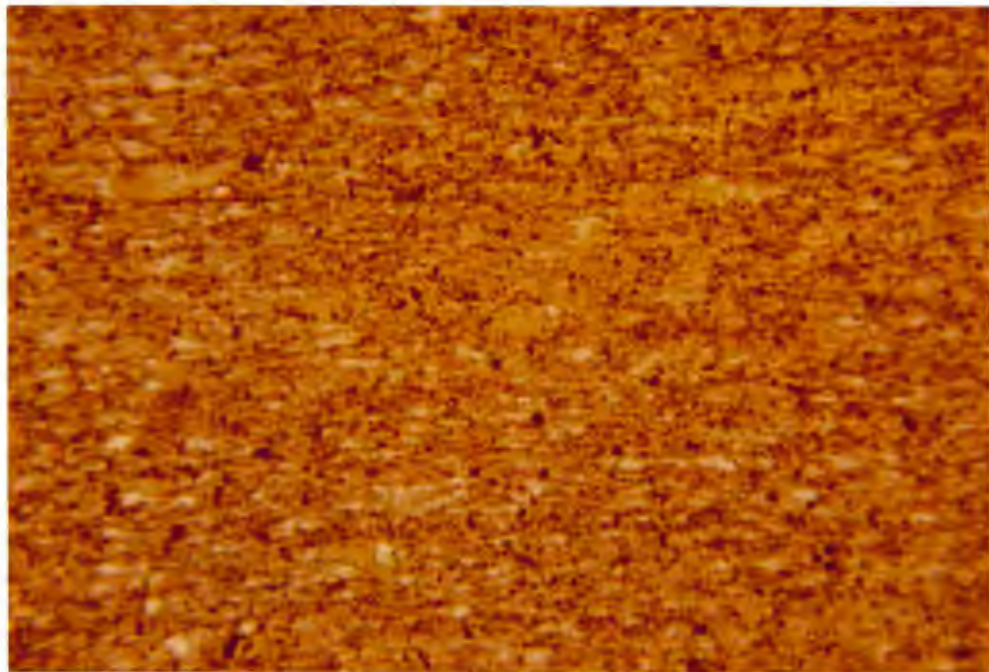


Fig. 8 Photomicrograph of slate showing the preferred orientation of phyllosilicates and elongated chlorite porphyroblasts and quartz grains. 0.8 km SSE of Carlton. Field of view is 0.95mm X 0.65mm. Plain light.

portion of the study area than in the northern part. The laminations within the slate can be recognized in thin section as slightly coarser, less mica-rich layers.

#### Phyllite

A fine-grained 'incipient' phyllite is exposed in the extreme southwestern corner of the field area. This phyllite is an indication of the metamorphic progression that increases in grade towards the southwest (Schwartz, 1942b). The phyllite is silver-grey in color on a fresh surface and has a composition very similar to the previously described slaty greywacke. A well-developed foliation is defined by the preferred orientation of relatively coarse chlorite and sericite and the presence of mica films (Fig. 9).

#### Hornfels

A spotted slate of the hornblende-hornfels facies indicative of incipient low-grade contact metamorphism is found in the northwestern corner of the field area. The outcrop is located stratigraphically just below Keweenaw mafic flows and intrusions, and has probably been metamorphosed by the heat that emanated from these rocks. In hand sample the fresh spotted slate appears as a black, fine-grained, partly recrystallized slate or slaty greywacke still showing relict bedding. In thin section it takes on a distinct spotted appearance, consisting of about 40% small, incipient porphyroblasts of cordierite set in a very fine matrix of mainly chlorite, sericite and opaque minerals (Fig. 10). Bedding can be seen as a change in matrix grain size and as bands of opaque minerals overprinting the other constituents of the rock. The change in grain size probably represents a grain size reversal due

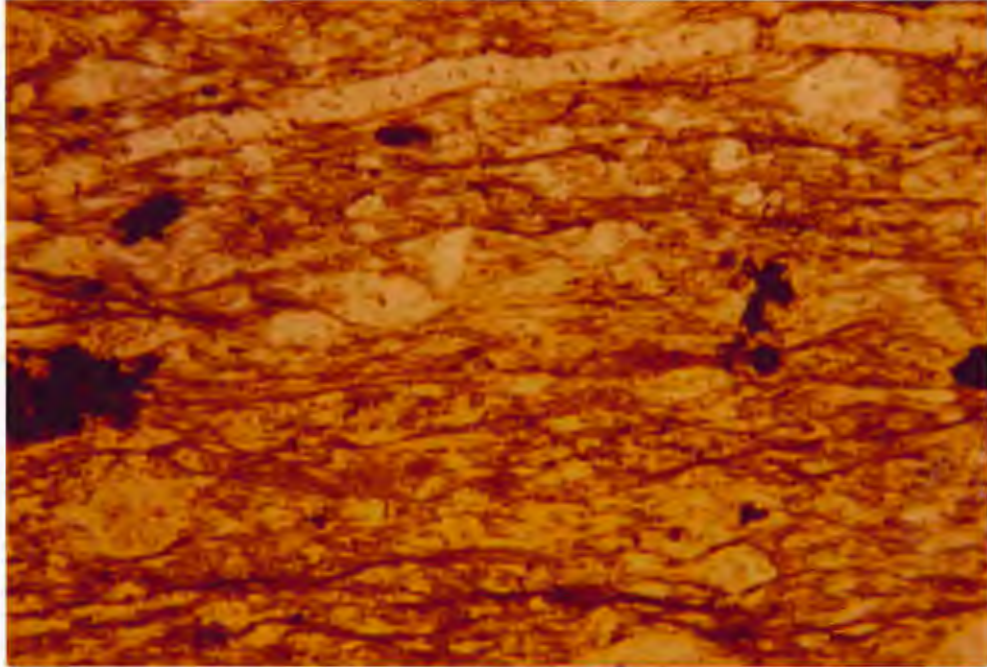


Fig. 9 Photomicrograph of phyllite showing the extremely well-developed preferred orientation of chlorite and the presence of mica films. 6.0 km WSW of Carlton. Field of view is 0.95mm X 0.65mm. Plain light.

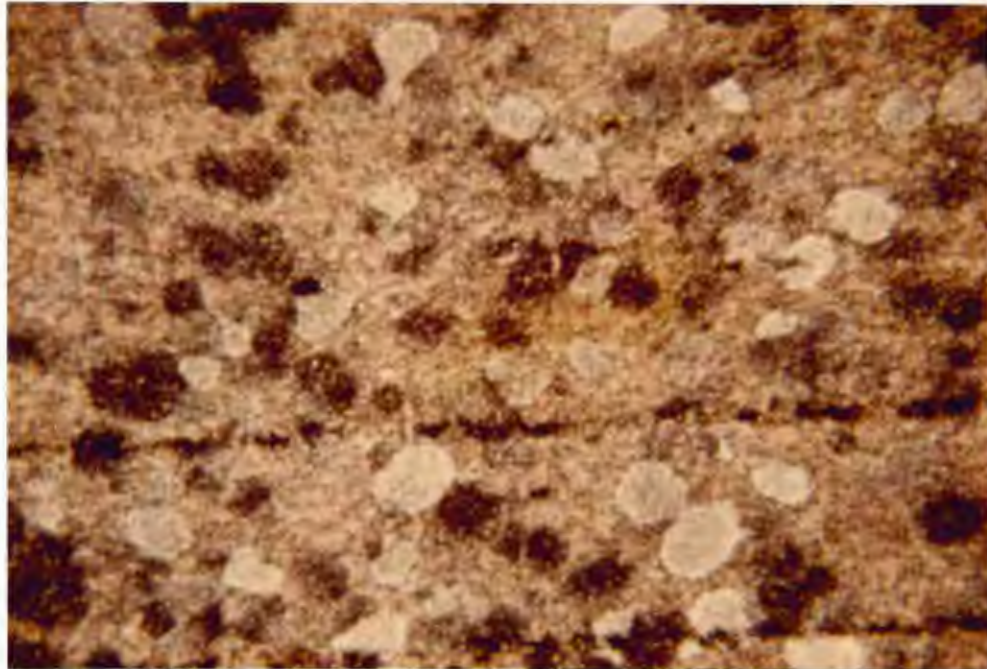


Fig. 10 Photomicrograph of a spotted slate showing incipient porphyroblasts of cordierite in a phyllosilicate matrix. 11.6 km NE of Thomson Dam. Field of view is 3.8mm X 2.6mm. Crossed nichols.



to the fact that the fine-grained slate was more susceptible to recrystallization than the coarser slaty greywacke. The ubiquitous dusting of opaque minerals shows a faint foliation at an angle to bedding and probably represents relict cleavage.

#### Concretions

Carbonate concretions are common throughout the formation and range in size from less than one centimeter to over one meter. They are commonly found along bedding planes and are therefore useful in determining bedding attitudes in otherwise massive beds. They are often flattened in the plane of the cleavage (Fig. 11). Detailed measurements of the concretions' elliptical shapes have been made to help determine the finite strain and strain history of the surrounding rocks (Holst, 1983). As the concretions are less resistant than their host rocks, they tend to weather preferentially leaving behind deeply pitted concretions or holes. The concretions are probably diagenetic and formed after the deposition of the surrounding sediments (Schwartz, 1942c; Weiblen, 1964; Morey and Ojakangas, 1970). In hand sample it can be seen that they are composed of light grey to reddish-brown fine-grained calcite. Bedding laminations can be seen to pass right through the concretion and a moderately well-developed anastomosing cleavage is usually present. In thin section the concretions consist of greater than 90% calcite with only minor amounts of quartz, chlorite, sericite and epidote.

#### Quartz Veins

Quartz veins and pods that range in width from less than a millimeter to over a meter are present throughout the field area. They



Fig. 11 Concretions deformed to an elliptical shape. Concretions are flattened in the plane of the cleavage. Looking due west. State highway 45 roadcut in Carlton.

are found along joint sets and along bedding planes where they may resemble ptigmatic folds due to the presence of remnant sedimentary structures along the bedding planes. They are primarily composed of vein quartz with very minor amounts of calcite, pyrite and chalcopyrite.

#### Diabase

The study area has been dissected by numerous mafic dikes that range in width from a few centimeters to 30 meters or more (Fig. 12). The dikes are composed of fine to medium-grained, greenish-black diabase that weathers to a distinctive rusty-brown color. The diabase is composed of 45 to 60% labradorite plagioclase, 20 to 40% augite, 8 to 13% former olivine grains, 1 to 5% hornblende, 5 to 10% magnetite and ilmenite and less than 2% apatite (Fig. 13). The diabase typically exhibits a well developed ophitic texture. Alteration ranges from light to moderate with the plagioclase altering to sericite and calcite, the augite altering to hornblende and uralite and the olivine completely altering to chlorite, iddingsite, serpentine and bowlingite.

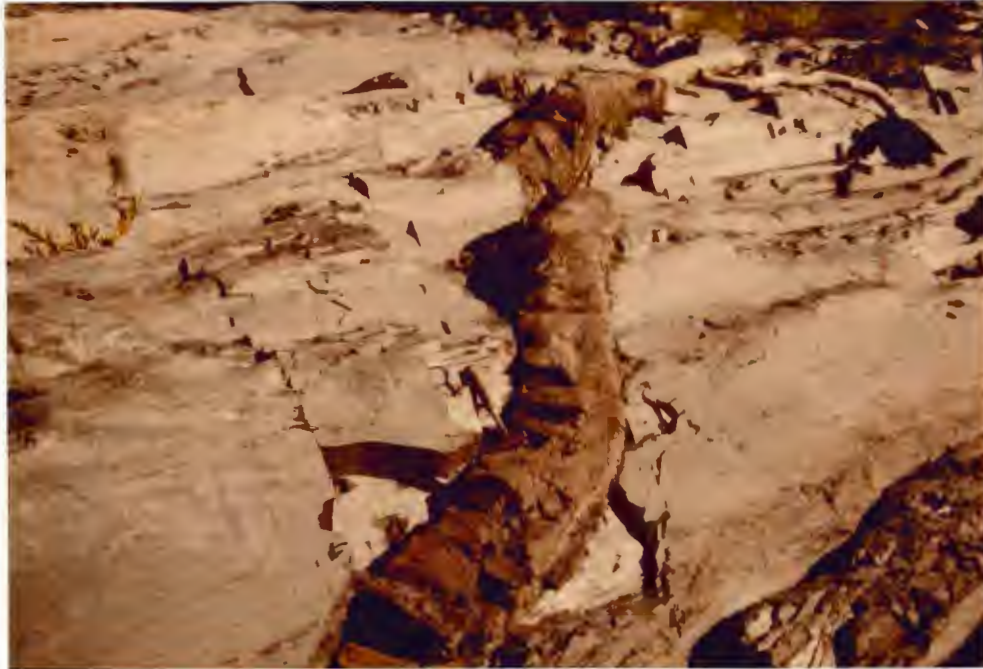


Fig. 12 Diabase dike intruding the Thomson Formation. Dike strikes N30E. Thomson Dam.

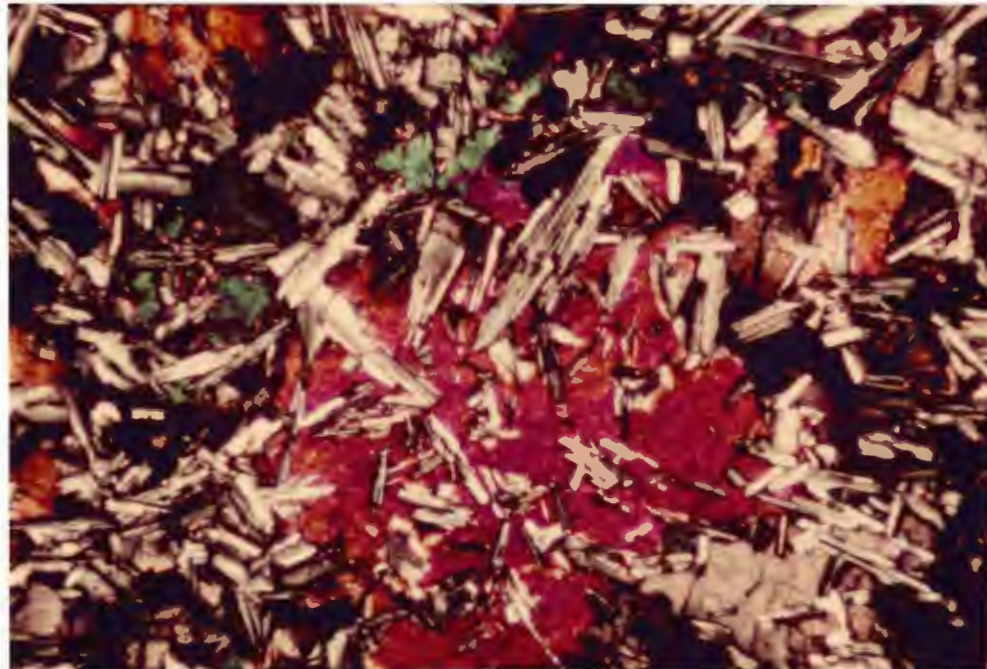


Fig. 13 Photomicrograph of diabase showing an ophitic texture of augite and plagioclase. 1.4 km NNE of Thomson Dam. Field of view is 3.8mm X 2.6mm. Crossed nichols.

CHAPTER III  
SEDIMENTOLOGY

Introduction

The main emphasis of this study is on structural aspects and not on the sedimentology of the Thomson Formation. However, some observations were made on the bedding and sedimentary structures of the study area. Previous work by Wright and others (1970) and Morey and Ojakangas (1970) provides detailed sedimentological information that will be summarized here.

Bedding and Sedimentary Structures

Because of the low grade of metamorphism in this part of the Thomson Formation bedding and primary sedimentary structures are very well preserved. Bedding can be determined at most outcrops by the physical differences (e.g. grain size and cleavage type) of the different rock types or by the presence of very fine-scale laminations within the beds. In some outcrops where the evidence for bedding is otherwise absent, it can be determined by the presence of concretions along bedding planes.

Bedding orientations are very consistent throughout the study area. Beds generally strike within 10 degrees of east-west and dip 40 to 70 degrees to the south or 50 to 90 degrees to the north with the south dip being predominant (Fig. 14, Plate 1). In a few areas, especially around the noses of the larger folds, bedding attitudes are noticeably different, striking more north-south and dipping to the east or more rarely to the west.

Primary sedimentary features are seen in numerous locations. Load

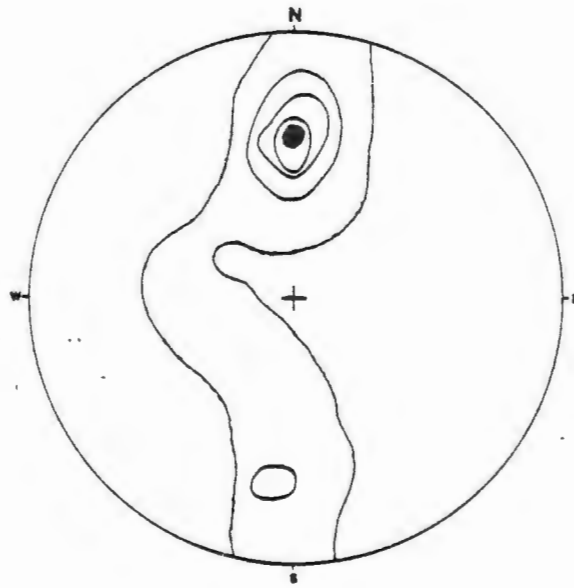


Fig. 14 Equal area projection of 1118 poles to bedding. Readings from entire field area. Contours at 1-5-10-15-20% of data per 1% area.

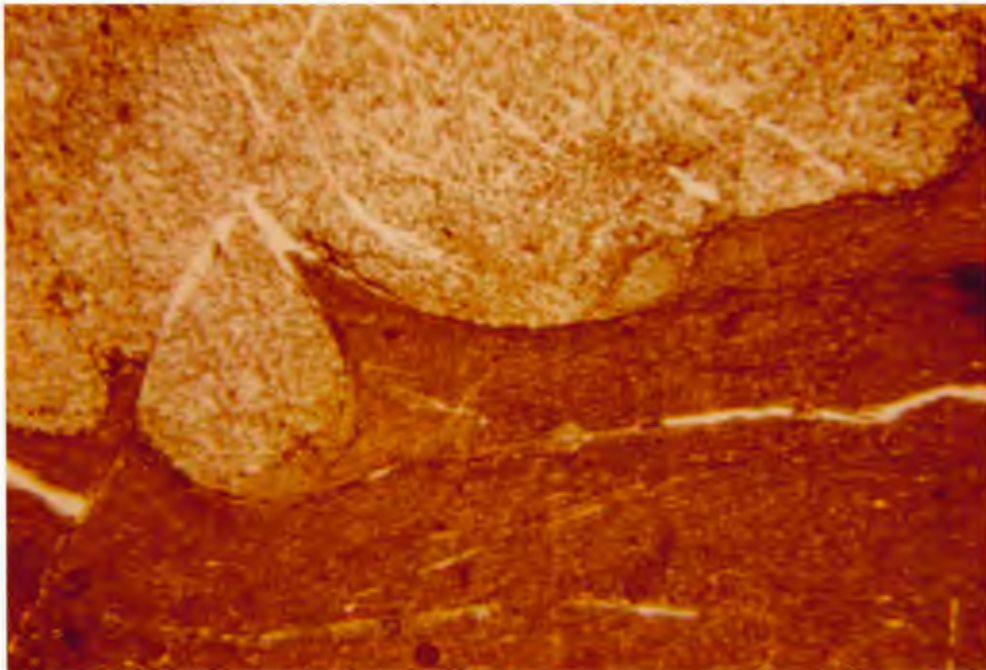


Fig. 15 Photomicrograph of a load structure at a slaty greywacke-slate contact. The load structure has been 'altered' by the cleavage to some extent. 1.6 km NNW of Thomson Dam. Field of view is 3.8mm X 2.6mm. Plain light.

structures and flame structures are present at greywacke-slate contacts on a scale of several centimeters to a few millimeters (Fig. 15). Small ball structures are common and are especially well preserved on an island in the Thomson Reservoir. Trough cross-bedding that ranges in width from nearly a meter to less than a centimeter is found in many beds (Fig. 7). The large-scale cross-beds are relatively rare; most cross-beds occur on a scale of several centimeters. Ripple marks are occasionally seen in some of the finer-grained units.

Graded bedding is a very common feature on a meter to centimeter scale. A typical graded bed consists of a coarse-grained metagreywacke grading up to a finer-grained slaty greywacke, occasionally with a thin layer of mud on top.

Evidence for penecontemporaneous deformation is shown by the presence of convolute bedding in many of the slate and slaty greywacke beds. These folds do not appear to have a common fold axis or axial surface orientation suggesting that the deformation occurred in unconsolidated sediments.

#### Paleocurrent analysis

Morey and Ojakangas (1970) measured 201 cross-beds near the type locality which showed a consistent paleocurrent trend from north to south and a vector mean dip direction (Potter and Pettijohn, 1976, p. 376) of 172 degrees. The orientations of 17 flute casts and 26 groove casts indicate a more variable east-west paleocurrent trend (Fig. 16). Despite the fact that the trend of flute casts and groove casts is similar to the strike of cleavage in the area (suggesting that some of the measured sole marks may be in fact tectonically related 'pseudo-

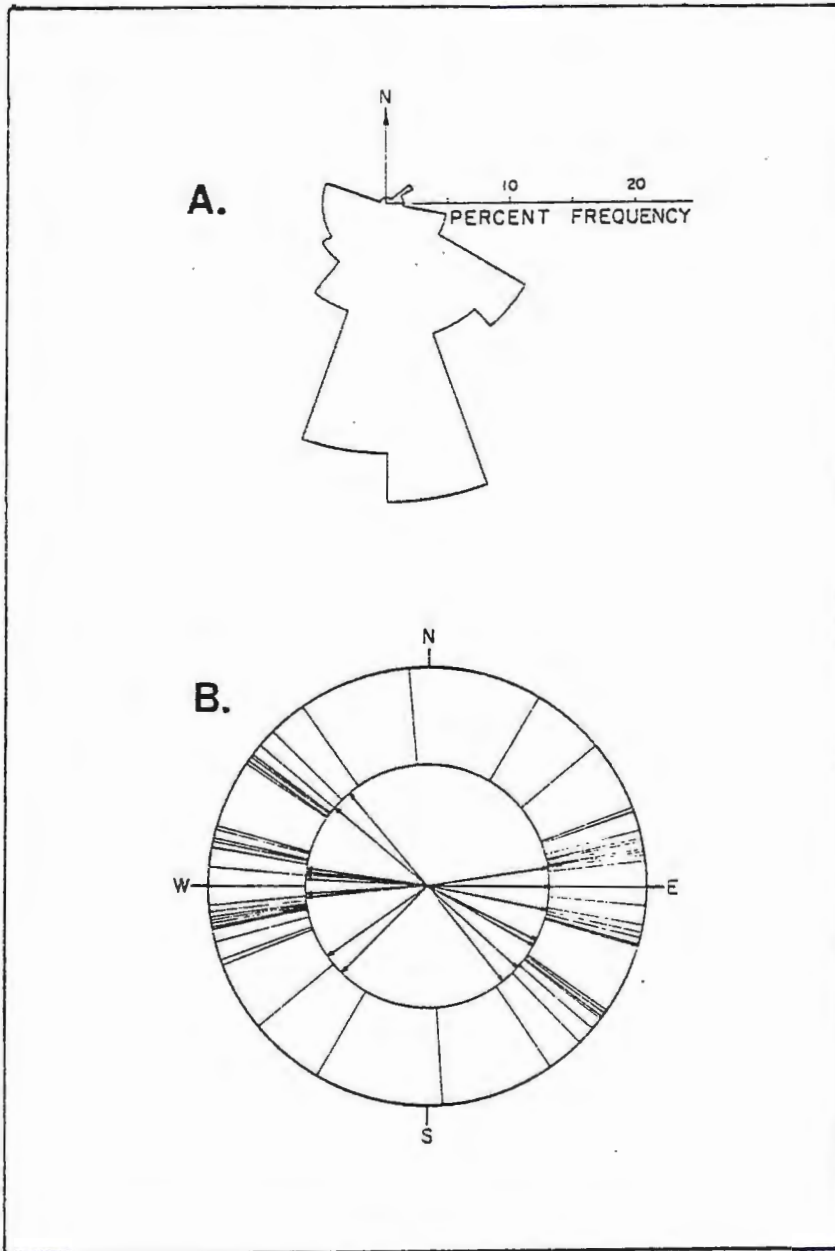


Fig. 16 Rose diagram of 201 cross-bedding measurements (a) and orientation diagram of 17 flute casts and 26 groove casts measurements (b) taken along the St. Louis River near the type locality. (Morey and Ojakangas, 1970).



groove casts formed by differential weathering of bedding-cleavage intersections on exposed bottoms of beds and not true sole marks (Morey and Ojakangas, 1970)), they determined that most of the measured sole marks were truly sedimentational and not tectonic structures. They also observed eight greywacke beds that contained both sole marks and cross-beds at high angles to each other confirming a bimodal paleocurrent trend. Morey and Ojakangas (1970) explain the bimodal nature of the paleocurrent trend in the light of regional paleogeography (and the inferred correlation of the Thomson Formation with the Rove Formation in northeastern Minnesota) by suggesting that the cross-beds were formed by currents flowing down the paleoslope perpendicular to the shore and that the sole marks were formed by either 'normal' bottom currents moving parallel to shore or by diverted turbidity currents.

#### Provenance

Paleocurrent studies previously mentioned suggest a northerly source for the Thomson Formation sediments. Source rocks of suitable age and composition are found north of the Mesabi Range in northeastern Minnesota (Morey and Ojakangas, 1970). The Archean Giants Range batholith, composed largely of granodiorite (Sims and Viswanathan, 1972) was capable of supplying the large amounts of 'plutonic' quartz and sodic plagioclase found in the sediments. Minor constituents of the sediments such as volcanic rock fragments and quartzite are also common Archean rock types of northeastern Minnesota.

Heavy mineral analysis performed by Hyrkas (1982) for an area just south of the study area was inconclusive in determining a source

terrane for the sediments since the only four detrital nonopaque minerals separated (zircon, apatite, rutile and garnet) are rather common in many different potential source rocks.

#### Environment of deposition

The current sedimentational model for the Thomson Formation is deposition by turbidity currents in a relatively deep-water basin. The coarser-grained greywacke was probably deposited by the main body of the turbidity current whereas the finer siltstone (later metamorphosed to slaty greywacke) was deposited by the tail portion of the turbidity current. Extremely fine-grained mud (slate) slowly accumulated on top of the coarser sediments during the long, calm time periods between turbidity currents (Wright and others, 1970; Morey and Ojakangas, 1970). Evidence for deposition by turbidity currents include the presence of soft-sediment slump structures, rip-up clasts of slate in the coarser greywacke units, prevalent graded bedding in greywacke and slaty greywacke beds with internal features characteristic of Bouma beds and the general lack of ripple marks, large-scale cross-bedding and other shallow water features. The textural and mineralogical immaturity of the rocks suggests that the sediments were deposited in a tectonically unstable environment. This instability was probably the result of the foundering of the Animikie basin during the Middle Precambrian.

No ideal, complete Bouma beds (Bouma, 1962) were found, but abundant 'A', 'AB', 'BC' and rarer 'ABC' sequences were identified. Many of these sequences had a thin 'E' (or clayey) layer deposited over

them. The abundance of the coarser, graded 'A' portion of the Bouma bed indicates that the main body of individual turbidity currents commonly reached this part of the basin (Morey and Ojakangas, 1970). Further to the south the ratio of Bouma 'A' to 'B' beds decreases (Hyrkas, 1982) suggesting that the deposits to the north are more proximal according to Walker's (1967) proximity index  $P = A + 0.5B$ . This would agree with the source area of the sediments being located to the north of the Mesabi Range.

#### Stratigraphic relationships

The interpretation of stratigraphic relationships between individual beds of the Thomson Formation is complicated by the general absence of identifiable marker beds. One marker unit, referred to as the Otter Creek Unit (a 17-19 foot unit of thin interbedded slate and metagreywacke) was recognized in three places along the banks of the St. Louis River and the Thomson Reservoir by Wright and others (1970). This unit helped in their structural interpretation of the area. Due to very high water levels of the Upper St. Louis River and the Thomson Reservoir only the type locality near the mouth of Otter Creek was observed in this study, leaving the stratigraphic relationship rather speculative.

## CHAPTER IV

### STRUCTURE

#### Introduction

The orientations of various structural features such as folds, cleavage, lineations, faults, kink bands and joints can be used to determine regional patterns of deformation. This chapter will only describe these structures; a discussion of the structural significance will be given in the following chapter.

#### Folds

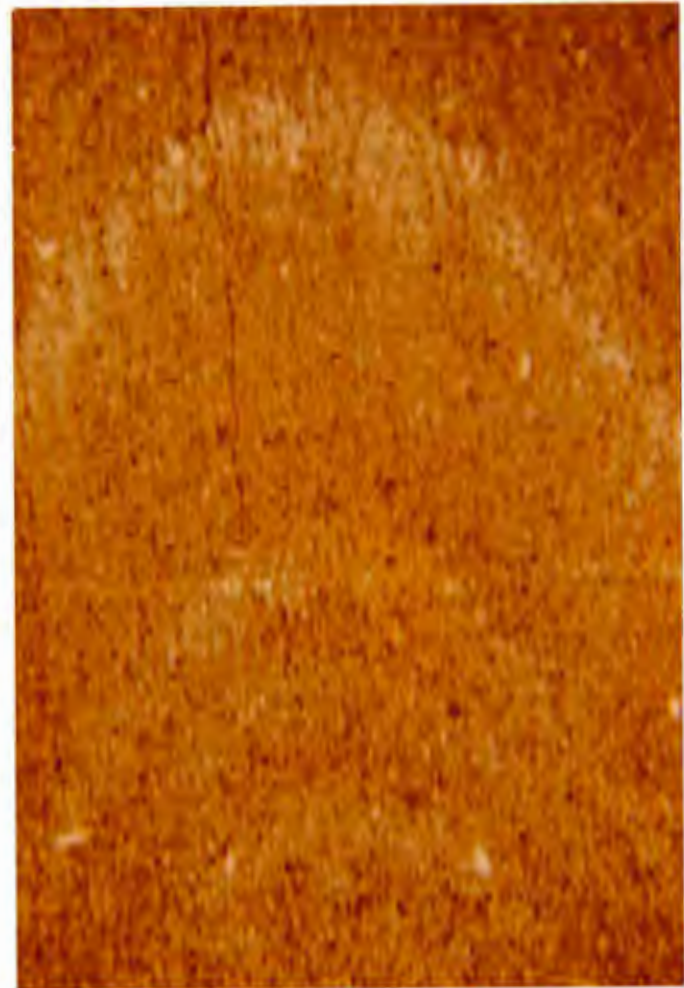
The Thomson Formation in the study area has been affected by a period of major folding. The folds developed have an open, rounded, nearly upright, subhorizontal geometry and range in wavelength from hundreds of meters to a few centimeters, and in amplitude from tens of meters to a few centimeters. They generally have an interlimb angle of 60 to 120 degrees (although more open folds exist) and have a symmetric or, more typically, an asymmetric shape (Fig. 17) with shallow-dipping south limbs and more steeply-dipping north limbs. The folds, regardless of their size, commonly contain an axial-planar cleavage (Fig. 18). As seen by actual fold axis measurements and by bedding-cleavage intersections, fold axes usually trend within 10 degrees of due east or west and usually plunge 0 to 20 degrees to the east or west (Fig. 19, Plate 2). Locally, however, fold axes have plunges of up to 50 degrees, mainly to the east, where the folds die out. Axial planes of the folds strike nearly east-west and dip vertically or steeply to the south. The fact that bedding-cleavage intersections are of a consistent attitude at all positions on the fold substantiates the

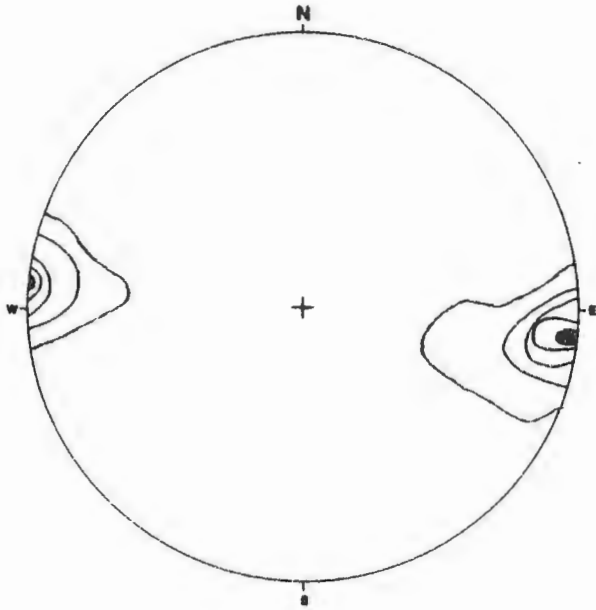


35

Fig. 17 Large-scale, open, upright, horizontal fold. Looking due west. Thomson Dam.

Fig. 18 Photomicrograph of a microfold in silty slate showing axial-planar cleavage. 4.8 km N. of Carlton. Field of view is 3.8mm X 2.6mm. Plain light.





36

Fig. 19 Equal area projection of 846 bedding-cleavage intersections. Readings from entire field area. Contours at 2-10-20-30-40% of data per 1% area.

Fig. 20 Small-scale, tight, vertical folds in alternating fine and coarser beds. Fold axial surfaces strike nearly east-west and dip nearly vertically. Looking due east at a 45 degree exposure. St. Louis River 0.1 km E. of the Potlatch paper mill in Cloquet.



axial-planar nature of the cleavage (Borradaile, 1978).

Tight, near-vertical folds are found in a narrow (less than 10 meters wide) east-west striking zone just east of Cloquet (Plate 1) (Fig. 20). These folds have an amplitude of approximately one to two meters and consist of alternating one to two centimeter 'beds' of greywacke and slate. The fold axes of these folds trend about S80E and plunge vertically or steeply to the east. Their axial planes strike S80E-N80W and dip about 80 degrees to the south.

### Cleavage

Cleavage is generally quite well developed in this part of the Thomson Formation, existing as a slaty cleavage in the slate and as a spaced, rough or fracture cleavage in the coarser-grained slaty greywacke. In fact, at the turn of the century several slate quarries producing roofing slate were active in and around the village of Thomson. As previously stated, the cleavage is axial-planar. Cleavage usually strikes between S80E-N80W and S85W-N85E and dips between 80 degrees north and 80 degrees south (Fig. 21, Plate 1). Most cleavage is steeper than bedding indicating that the beds have not been overturned during this phase of folding. In some places, however, there is a deviation from the average orientations. Cleavage with a dip as low as 40 degrees is not uncommon, and in a few isolated outcrops nearly horizontal cleavage in slate beds alternating with a much steeper 'normal' cleavage in more competent beds can be seen (Fig. 22).

In the fine-grained slate units cleavage is defined by a preferred orientation of chlorite and sericite and by the elongation of quartz

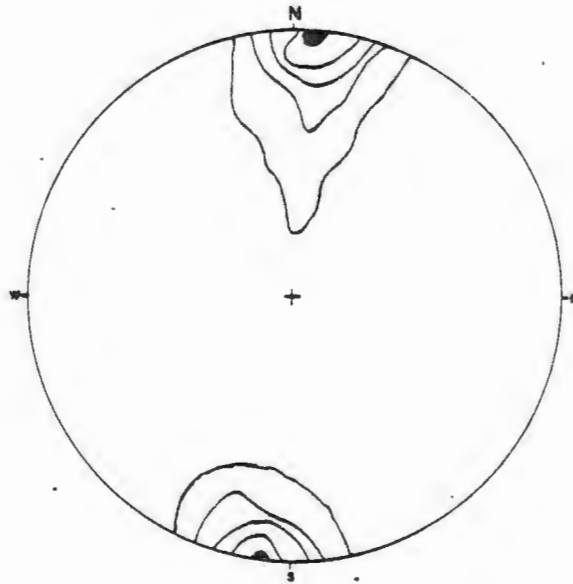


Fig. 21 Equal area projection of 868 poles to cleavage. Readings from entire field area. Contours at 1-5-10-20-30% of data per 1% area.



Fig. 22 Alternating slate and slaty greywacke beds exhibiting 'abnormal' cleavage refraction with horizontal and steeply-dipping cleavage attitudes. Looking due west. Oldenburg Pt., Jay Cooke Park.



grains forming a continuous slaty cleavage (Fig. 8). In the coarser grained slaty greywacke the cleavage is defined by a preferred orientation of the chlorite and sericite forming a fracture, rough or spaced cleavage with spacing generally less than 0.5 mm as seen in thin section (Fig. 6) and less than one centimeter as seen in outcrop.

A poorly to moderately well-developed crenulation cleavage is found in a small portion of the study area, particularly in the southernmost exposures (Plate 1). It is easily seen in the field only in the extreme southwestern and southeastern corners of the field area; otherwise, it can only be identified in thin section (Fig. 23). A very poorly-developed crenulation cleavage can be detected in some of the isolated outcrops with horizontal cleavage. The crenulation cleavage has an orientation very similar to that of the cleavage already described, that is, striking approximately S85E-N85W and dipping vertically or very steeply to the south.

The crenulation cleavage is exclusively found in slates that have a previous well-developed cleavage, and it is the result of microscopic folding or crenulation of that earlier foliation. The crenulations consist of asymmetric, open folds with an interlimb angle of 120 to 170 degrees (Fig. 24). They have an amplitude ranging from less than 0.02 mm to approximately 0.1 mm and a wavelength ranging from approximately 0.05 mm to about 0.3 mm. The crenulation cleavage itself is defined by a relative concentration of phyllosilicates along the short limb of the crenulation forming a mica-rich zone or a mica film (Fig. 24). The earlier slaty cleavage generally tends to have an orientation that is not parallel to bedding (although exceptions occur), while the

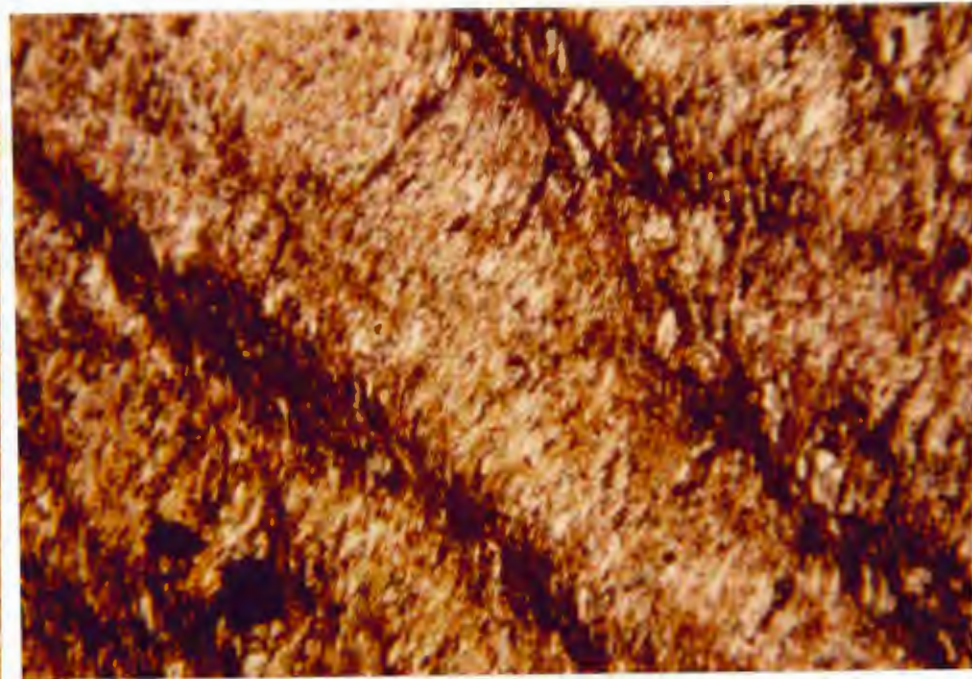
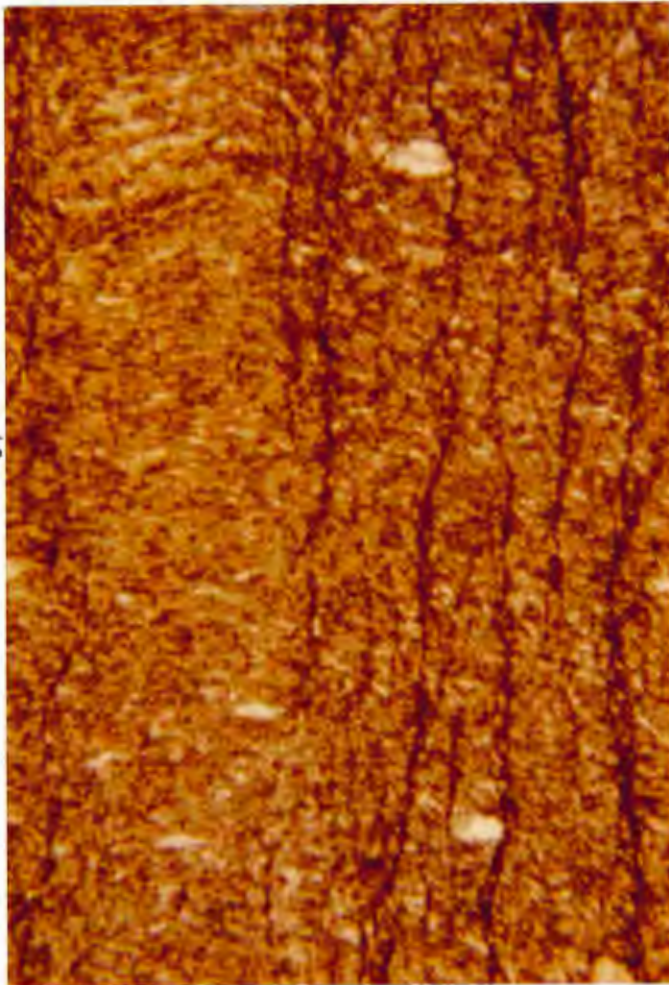


Fig. 23 Photomicrograph of crenulation cleavage in slate not visible in outcrop but visible in thin section. 1.6 km S. of Thomson Dam. Field of view is 0.38mm X 0.26mm. Plain light.

Fig. 24 Photomicrograph of crenulation cleavage in slate. Note the asymmetric crenulations and the relative concentration of phyllosilicates in the short limb. Oldenburg Pt., Jay Cooke Park. Field of view is 0.38mm X 0.26mm. Crossed nichols.

crenulation cleavage intersects the first cleavage at an angle ranging from approximately 40 to 90 degrees (Fig. 23) with the greatest concentration being at 60 to 75 degrees.

### Lineations

Bedding-cleavage intersections defining a non-penetrative lineation are present, and as previously mentioned, they define the orientation of the fold axis and help to establish the axial-planar nature of the cleavage. The bedding-cleavage intersections have a bearing of approximately S85E or N85W and plunge generally less than 20 degrees (Fig. 19) although plunges of up to 50 degrees were observed.

A stretching lineation can occasionally be seen on the cleavage surfaces of the slaty units. It usually has a plunge that approaches 90 degrees on the near-vertical slaty cleavage surfaces.

### Faults

Faults are present in this part of the Thomson Formation, but their displacements, where measurable, appear to be 10 meters or less. Recognition of large-scale faulting is complicated by the lack of marker beds and by incomplete exposure, but indirect evidence such as the inferred offset of fold axes and greywacke ridges can be used to identify the faults.

Several reverse faults with displacements of 5 meters or less strike within 10 degrees of S85E-N85W and dip variably to the north or south at angles of 45 to 75 degrees. Normal faults with unknown displacements strike approximately N30E-S30W and dip vertically. Some of the faults, both normal and reverse, have associated breccia zones and shear zones. Alteration involving the complete breakdown of the

feldspar grains and matrix into clay was usually more intense along these zones, and many were later filled with quartz. Diabase dikes were commonly intruded along the N30E normal faults as indicated by the offset greywacke ridges and fold axes on either side of the dikes. Microfaults with displacements of a few millimeters or less are very common, and include both normal and reverse faults and are commonly quartz filled (Fig. 25).

### Dikes

Numerous diabase dikes of presumed Keweenawan age intrude the Thomson Formation (Fig. 12, Plate 2). Most of these have a strike of approximately N30E-S30W and are very nearly vertical. They range in width from less than a meter to 30 meters or more and appear to have been intruded along zones of weakness such as the N30E fault set. The dikes commonly have a fine-grained chill margin of several centimeters and have moderately well-developed columnar jointing perpendicular to the dike contact.

In the Oldenburg Point area of Jay Cooke State Park (Plate 1) there is a dramatic increase in the number and volume of diabase dikes. Some of the dikes in this area are much larger than elsewhere in the study area and tend to have much more irregular lens or pod shapes and variable orientations (Fig. 26). However, the diabase 'complex', when viewed as a whole has a definite N30E-S30W strike.

### Folded Cleavage

The cleavage in the slates in the vicinity of the large diabase dike and pod swarm just described has been folded into rounded, open

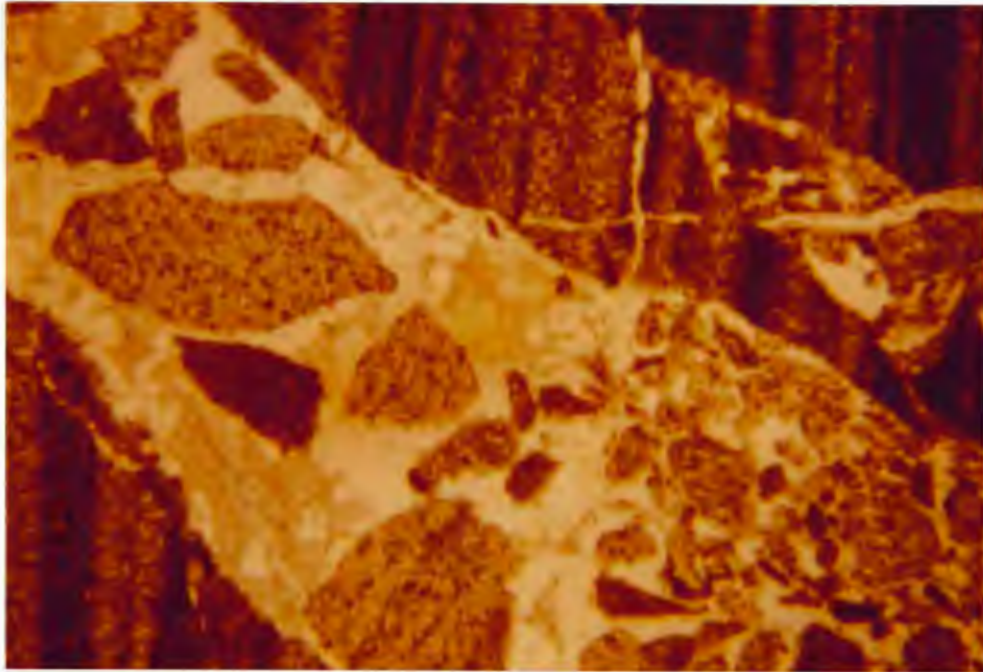


Fig. 25 Photomicrograph of a quartz-filled microfault in slate. Note fault gouge. 2.1 km N. of Carlton. Field of view is 3.8mm X 2.6mm. Plain light.



Fig. 26 Diabase dike and pod swarm. Ki = Keweenawan diabase. Looking north. Oldenburg Pt., Jay Cooke Park.

folds with an interlimb angle of 90 to 150 degrees (Fig. 27). The folds formed have an amplitude and wavelength ranging from a few centimeters to more than a meter. There is a joint set that is approximately axial-planar to many of the folds, and occasionally there is some shear or offset along it (Fig. 28). The folds display a rather large degree of variability in their orientation; however, a definite concentration of axial surfaces striking approximately N30E-S30W is evident. Fold axes have an approximate trend of S30W and a plunge of 10 to 45 degrees.

In the vicinity of the dike swarm many of the slate beds are intensely jointed, especially along bedding and cleavage planes, instead of showing the folded cleavage described above. Also in this area there are isolated outcrops showing the alternating flat-steep cleavage previously mentioned (Fig. 22).

#### Kink-bands

Kink-bands are a prominent feature of the Thomson Formation particularly at the type locality at Thomson Dam (Plate 1, Fig. 29). They are much more common in the fine-grained slates than in the coarser units. Kink-bands involve the folding of the cleavage laminae into open (interlimb angle of 120 to 175 degrees), angular, asymmetric folds (Fig. 30). The axial surfaces of these folds define the kink-band boundaries, and the short limb of the asymmetric fold constitutes the kink-band. The kink-bands are subplanar features and range in width from less than a millimeter to several centimeters. The density of kink-bands in a given section ranges from near zero to approximately 10 kink-bands per 10 centimeters. Individual kink-band boundaries may



Fig. 27 Folded cleavage in slate near the diabase dike swarm. Field of view in foreground is about 10 meters. Looking south. Oldenburg Pt., Jay Cooke Park.

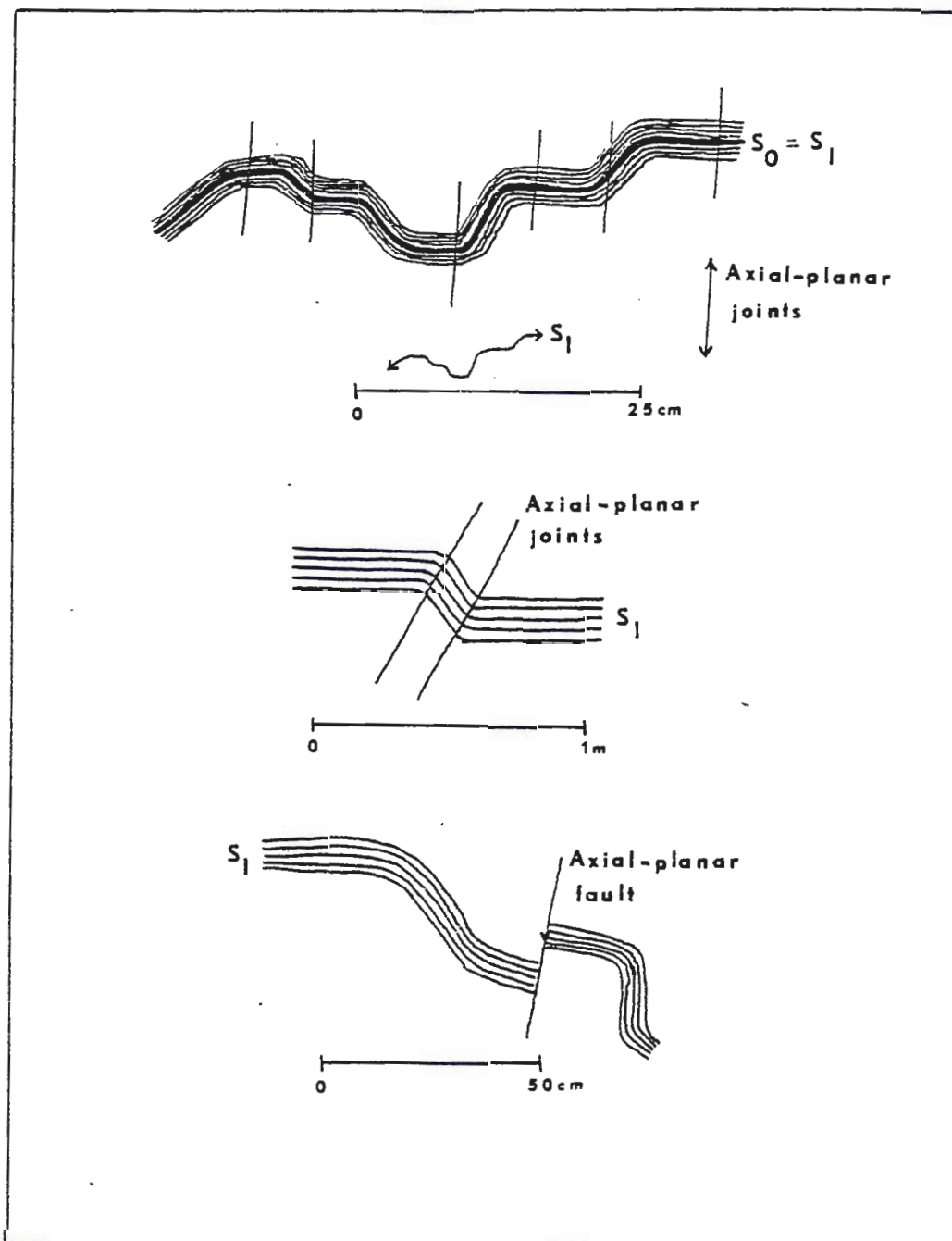


Fig. 28 Field sketches showing the relationship of the axial-planar joint set to folded cleavage. Oldenburg Pt., Jay Cooke Park.





Fig. 29 Kink-bands in slate. Note the curvi-planar nature of the kink-bands. Field of view in foreground is about one meter. Looking due west at a vertical exposure. Thomson Dam.



Fig. 30 Kink-band in slate showing the angular, asymmetric nature of folding. The kink-band in center of photo is about 1 cm wide. Looking due east at a vertical exposure. Thomson Dam.

or may not show brittle behavior (i.e. breakage or shear along the boundary).

Due to their curvi-planar nature the orientation of the kink-bands displays some variability. However, a general strike of approximately N70E-S70W and a dip of about 20 degrees to the south can be ascertained (Fig. 31). Many of the kink-bands intersect; however, the angle of intersection appears to vary randomly between 0 and 30 degrees. Also, no definite cross-cutting patterns between the intersecting kink-bands could be determined.

#### Joints and Quartz Veins

Joints are abundant throughout the study area. They exhibit a varied degree of development and a varied density, and range from less than one joint per linear meter to more than 10 per linear meter. Three joint sets can be identified on an equal-area stereonet plot for the entire the map area (Fig. 32), although individual outcrops seldom display more than two joint sets. Two major sets are present; one striking north-south and dipping vertically, and the other striking between N20E and N30E and dipping steeply to the west. A minor set strikes approximately N30W and dips near vertically.

Quartz veins that range in width from less than a millimeter to nearly a meter are commonly found along joints, particularly the N30E joint set (Fig. 33).

The diabase dikes that intrude the Thomson Formation have joint sets that are independent of those of the surrounding rock. One set is parallel to the dike contact, while the others define columnar jointing perpendicular to the dike walls.

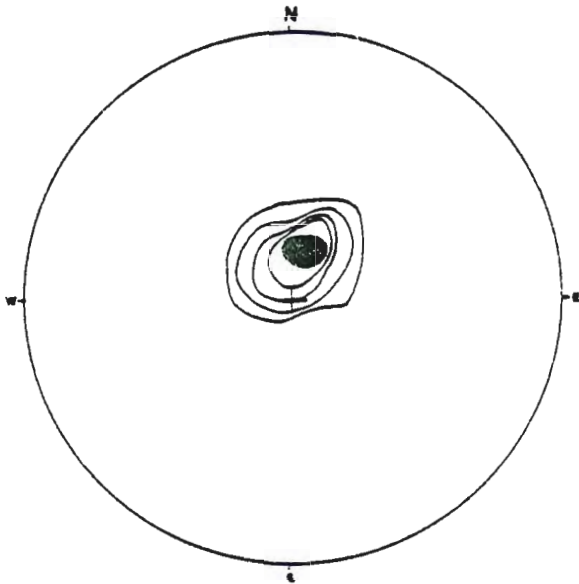


Fig. 31 Equal area projection of 110 poles to kink-bands. Readings from Thomson Dam area. Contours at 5-10-15-20-30% of data per 1% area.

Fig. 32 Equal area projection of 807 poles to joints. Readings from entire field area. Contours at 3-4-5-6% of data per 1% area.

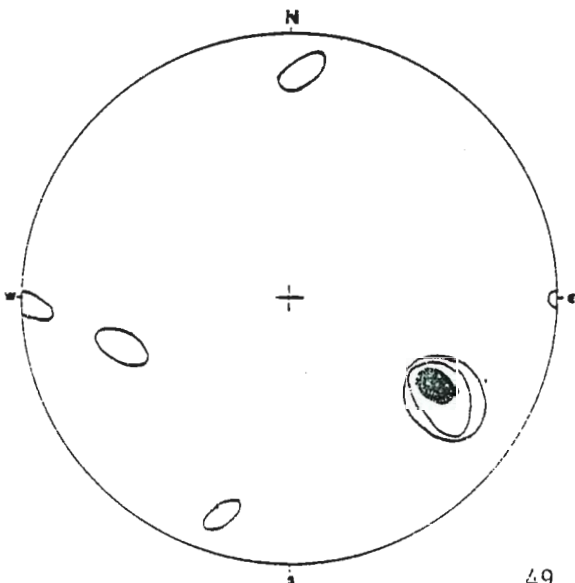
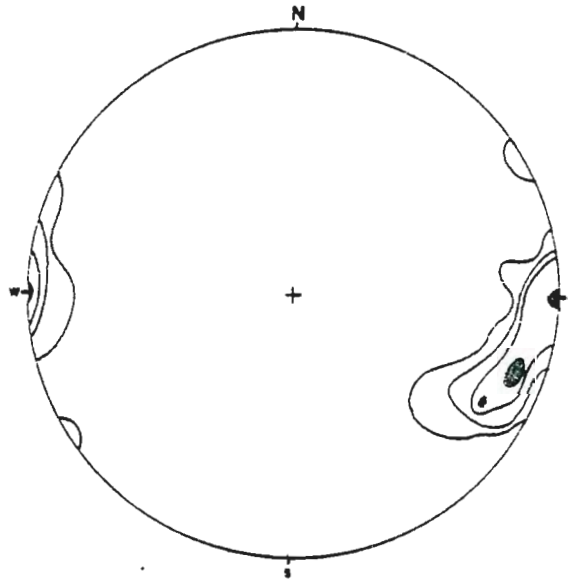


Fig. 33 Equal area projection of 95 poles to quartz veins. Readings from entire field area. Contours at 4-8-12% of data per 1% area.

## CHAPTER V

### STRUCTURAL INTERPRETATION

#### Introduction

This chapter will attempt to explain the significance of the structural data of the Thomson Formation presented in the previous chapter. A discussion of larger-scale mesoscopic features as well as a detailed discussion of microstructure will be given. Possible mechanisms of formation of some of the microstructure will also be presented. These observations, although at times speculative, can be useful in gaining a better understanding of the deformational history of the Thomson Formation.

#### Cleavage

##### Classification

The cleavage in this study will be morphologically classified using a system that combines the classification schemes of Powell (1979) and Gray (1977b, 1978) (Fig. 34). Because the origin of cleavage is still being debated, a morphologic classification is preferred over a genetic one.

Most cleaved rocks have zones of strongly preferred mineral orientation (cleavage seams or films) separated by zones of differently or usually nonoriented minerals (microlithons) (Powell, 1979). The presence or absence of this domainal structure can be the primary subdivision of rock cleavage (Fig. 34). If a domainal structure is not apparent at the scale of observation (usually the scale of a standard petrographic microscope), then the rock can be said to have continuous cleavage. Continuous cleavage can be subdivided on the basis of grain

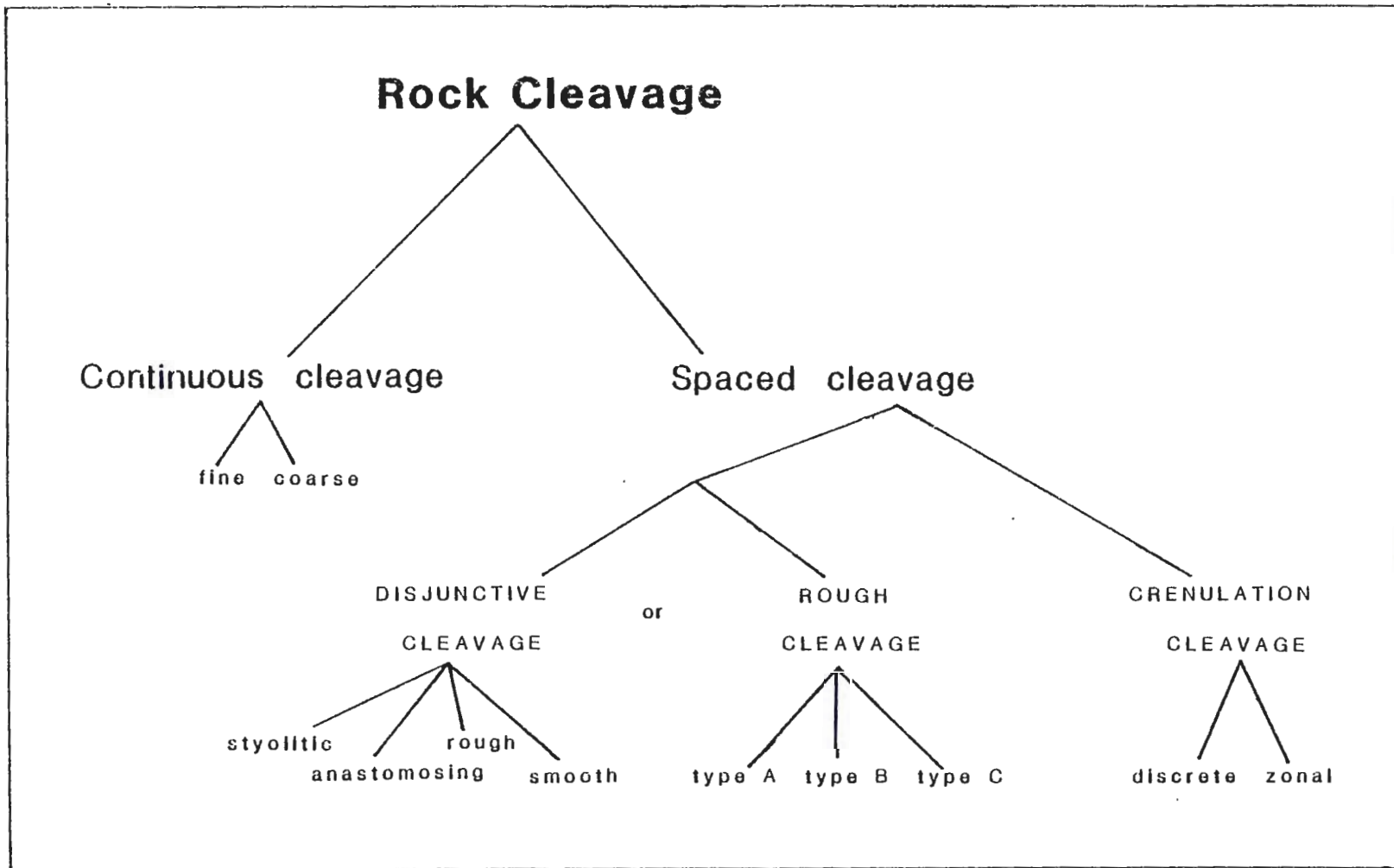


Fig. 34 Classification of rock cleavage. See text for descriptions of the cleavage types. (After Gray, 1977b; 1978 and Powell, 1979).

size: fine as in slates or coarse as in schists and gneisses. If the rock has a domainal structure with cleavage seams and microlithons then the rock has a spaced cleavage.

Subdivisions of spaced cleavage are based on whether there is a pre-existing planar anisotropy (or pre-existing preferred mineral orientation) in the rock (Powell, 1979). If so, the cleavage is a crenulation cleavage and may be further classified as a zonal or discrete crenulation cleavage. If a pre-existing planar anisotropy is absent in a rock with a spaced cleavage, then the cleavage can be called a disjunctive cleavage (in all rock types) (Powell, 1979), or more specifically, a rough cleavage in psammites (Gray, 1978). Disjunctive cleavage is further subdivided on the basis of the shape of the cleavage domains ranging from stylonitic through anastomosing and rough to smooth. Rough cleavage can be subdivided on the basis of the degree of cleavage film development into type A (poorly-developed), type B (well-developed) and type C (well-developed only in specific isolated zones) (Gray, 1978).

A fine continuous cleavage is present in many of the slates in the study area. The cleavage results from the statistical dimensional parallelism of the platy minerals in the slate such as chlorite and sericite (Fig. 8). Many slates and silty slates have a cleavage that grades into a very closely-spaced, slightly rough to smooth disjunctive cleavage, with the cleavage seams separated by tiny grains of quartz.

The slaty greywacke of the study area displays all three types of rough cleavage as described by Gray (1978). Type A rough cleavage has short, discontinuous cleavage seams developed around the non-oriented

quartz and feldspar grains, especially in the coarser slaty greywacke (Fig. 35). Type B rough cleavage has well-developed, continuous cleavage seams forming around elongated detrital grains (Fig. 36). The slaty greywackes with type B rough cleavage are usually finer grained and have a much better developed fissility than those with type A cleavage. The third type of rough cleavage, type C, has well-developed, continuous cleavage seams in isolated zones separated by zones where the fabric has no or only weakly-developed, discontinuous cleavage seams (Fig. 37). The three types of rough cleavage described are end member types, hence, transition forms may occur in between them. Rocks in the study area also contain the two types of crenulation cleavage outlined above. These will be described in a later section.

#### Origin of slaty cleavage

The origin of slaty cleavage has been a highly debated subject ever since 1838 when De la Beche proposed that cleavage formed from electric currents and earth magnetism. In recent years several theories of cleavage formation have been introduced.

Maxwell (1962) proposed that slaty cleavage in the Martinsburg Slate in Pennsylvania was formed by tectonic dewatering of the slate. He stated that during tectonic movements excess water under high pore pressure was forced from the unconsolidated sediments. As the water escaped, platy minerals were mechanically rotated into a direction parallel to the flow of the escaping fluid. He cited the apparent parallelism of clastic dikes with cleavage as evidence that the cleavage

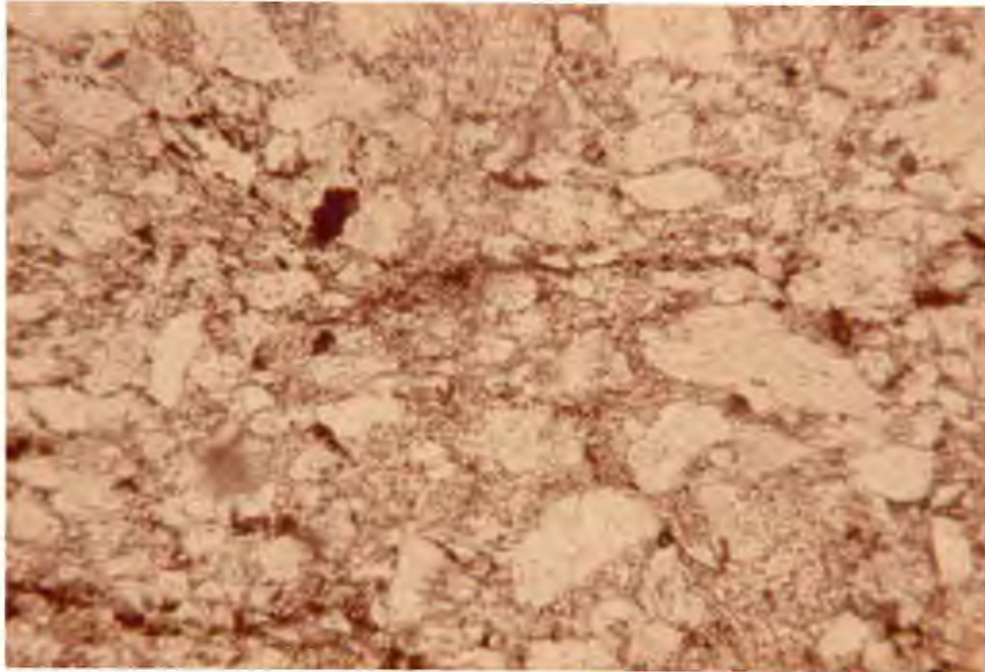


Fig. 35 Photomicrograph of type A rough cleavage in coarse slaty greywacke showing the short, discontinuous cleavage seams developed around the non-oriented quartz and feldspar grains. 1.2 km SSW of Thomson Dam. Field of view is 0.95mm X 0.65mm. Plain light.

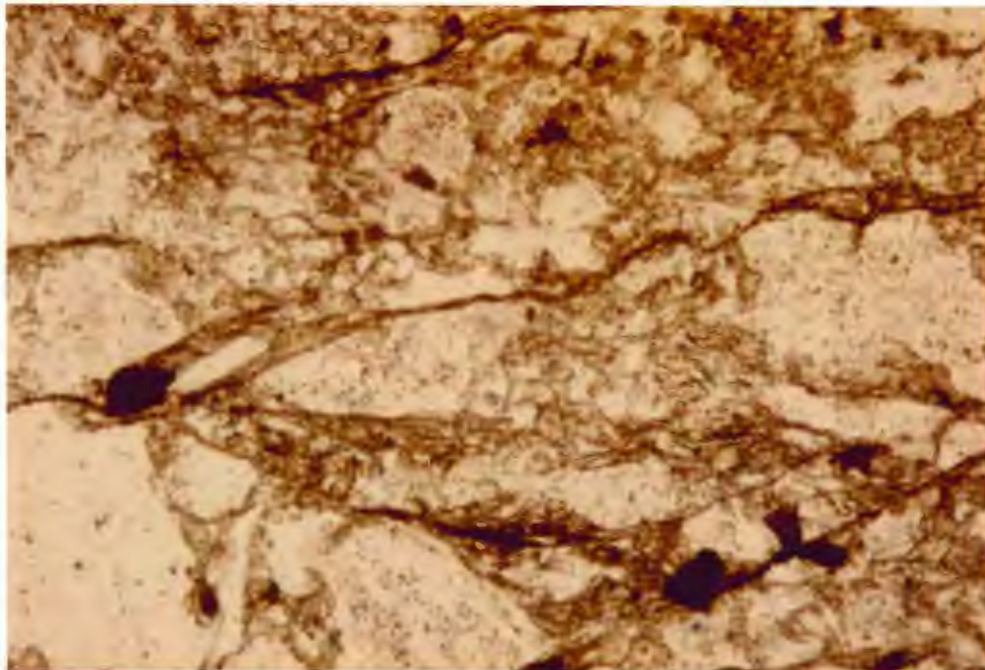


Fig. 36 Photomicrograph of type B rough cleavage in finer slaty greywacke showing the well-developed, continuous cleavage seams forming around elongated detrital grains. 0.6 km N. of Thomson Dam. Field of view is 0.95mm X 0.65mm. Plain light.



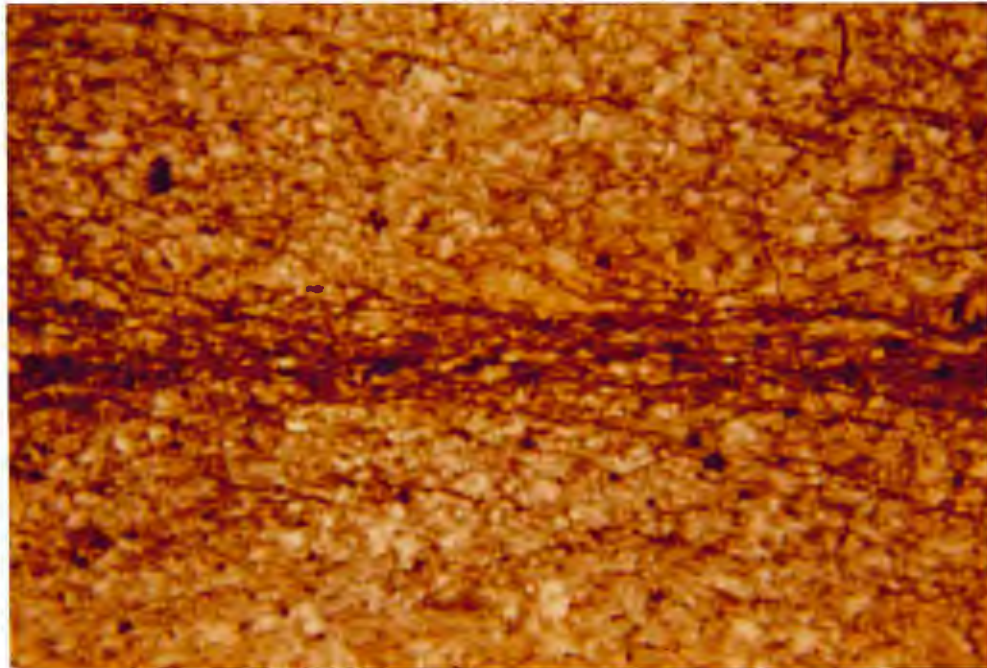


Fig. 37 Photomicrograph of type C rough cleavage in slaty greywacke showing the well-developed, continuous cleavage seams only in isolated zones. 4.3 km N. of Carlton. Field of view is 3.8mm X 2.6mm. Plain light.

formed prior to lithification and metamorphism.

Tectonic dewatering is purported to be the mechanism of cleavage formation in Precambrian rocks in Colorado (Braddock, 1970), the Early Proterozoic Siamo Slate in Northern Michigan (Powell, 1969) and the Early Proterozoic Michigamme Formation (which is approximately correlative to the Thomson Formation) in Northern Michigan (Powell, 1972).

The tectonic dewatering hypothesis has attracted considerable objections from many workers. Strain measurements made in the Martinsburg Slate (Groshong, 1976; Beutner, 1978) have shown that there was sufficient strain associated with the folding of the rocks to deform the clastic dikes into a position approximately parallel to cleavage. Geiser (1975) and Gregg (1979) have also shown how pre-cleavage clastic dikes are redistributed by folding. Beutner (1980) found that clastic dikes and cleavage are not actually parallel in the Siamo Slate nor the Michigamme Formation, but in fact the dikes are cut by the cleavage. He concludes that the clastic dikes were introduced prior to tectonic deformation, and that the cleavage formed during regional strain and low-grade metamorphism.

Another theory of cleavage formation is that of pressure solution accompanied by recrystallization of platy minerals (Durney, 1972; Williams, 1972; Gray, 1978). Quartz, being more soluble than most phyllosilicates, is preferentially dissolved allowing the platy minerals to rotate passively into a position perpendicular to the principal compression direction forming the slaty cleavage. This may be accompanied by crystallization/recrystallization of phyllosilicates

in the same preferred orientation as the rotated minerals. Gray (1978) did most of his work on rough cleavages in psammites, but he noted that since most slaty cleavage is actually domainal in nature (as is rough cleavage), slaty cleavage is a morphological equivalent of rough cleavage, and that the same processes are active in both. In fact, pressure solution may be more important in slates, although not as visible as in coarser-grained rocks, because of the shorter diffusion paths in slates (Durney, 1972). In addition, Ramsey and Wood (1973) have demonstrated that the development of a slaty cleavage may involve volume losses of up to 20%.

A related theory supported by electron microscopic studies (White and Knipe, 1978) suggests that cleavage development is primarily a metamorphic crystallization process where stable phyllosilicates form in zones of intense micro-deformation of the original fabric (zones of high strain energy). These phyllosilicates are aligned approximately perpendicular to axial planes of host micro-kinks thus forming the slaty cleavage. Minor pressure solution is suggested to accompany this process.

Another theory is that inequidimensional particles with an initial random orientation passively rotated into a preferred orientation in a plane of flattening during deformation (March, 1932). The well-aligned grains in the plane of flattening thus define the slaty cleavage. Furthermore, it has been suggested by March that the degree of preferred orientation can be mathematically predicted for a given amount of strain (and vice versa). The major problem with this theory

is that a truly random fabric in an undeformed rock is very rarely seen.

In some slates the continuous slaty cleavage is accompanied by larger (0.1-0.2mm) grains of chlorite that are elongated in the direction of cleavage but have their mineral cleavage at a high angle to the rock cleavage (cross-micas) (Fig. 38). These grains commonly have strain shadows or beards of quartz and chlorite. Borradaile (1982) has suggested that these grains are porphyroblasts that formed in the early stages of cleavage development, whereas Beutner (1978) has suggested that similar-looking grains represent remnants of an earlier bedding plane fabric.

#### Origin of rough cleavage

Many of the coarser slates and slaty greywackes of the Thomson Formation contain a rough cleavage and show good evidence for cleavage formation by solution transfer. Rough cleavage has previously been known as fracture cleavage, however, there is little or no evidence of brittle deformation such as cataclasis or granulation of material along the cleavages (Williams, 1972).

Many of the detrital quartz grains near cleavage seams have undergone shape modification. They tend to have truncated sides along the cleavage seams and appear to be elongated in the direction of cleavage. Grains not in contact with cleavage seams are more equant and have less distinct grain boundaries. These features have been observed by Geiser (1975), Means (1975) and Gray (1978) and suggest a solution transfer deformation mechanism. This mechanism requires dissolution of more soluble minerals such as quartz and feldspar,



Fig. 38 Photomicrograph of a 'cross-mica' chlorite porphyroblast in slate. Note the elongation of the porphyroblast parallel to rock cleavage, the orientation of the mineral cleavage perpendicular to the rock cleavage and the strain shadows at the ends of the porphyroblast. 0.8 km SSE of Carlton. Field of view is 0.24mm X 0.17mm. Plain light.

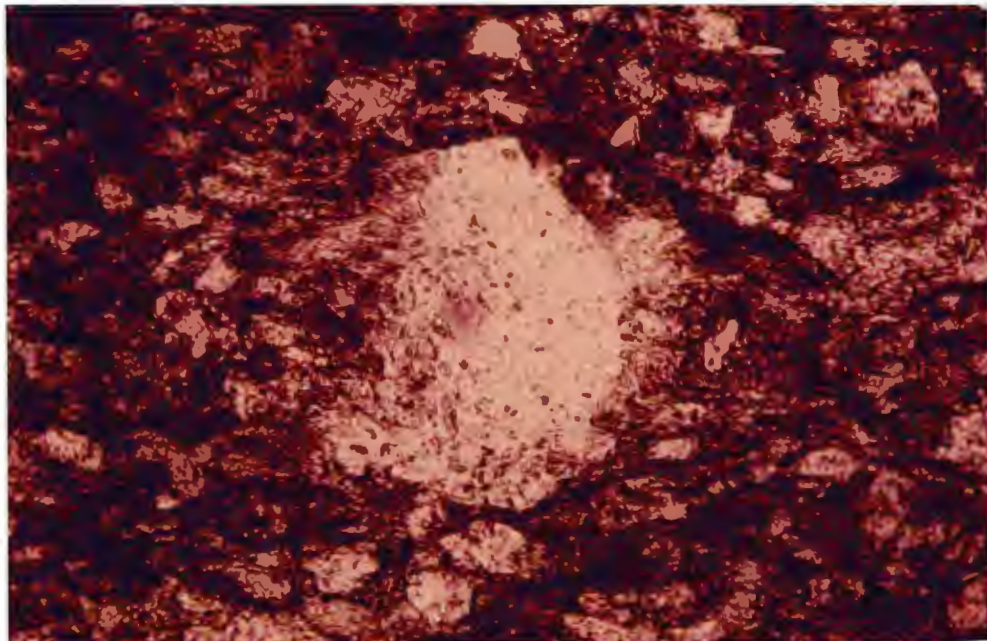


Fig. 39 Photomicrograph of a quartz grain in a slaty greywacke with quartz overgrowths and mica beards. Note the elongation in the direction of cleavage of some of the smaller quartz grains adjacent to the cleavage seams. 1.5 km S. of Carlton. Field of view is 0.38mm X 0.26mm. Plain light.

transfer by diffusion of the solutions along grain boundaries and precipitation as overgrowths or mica beards on grains (Fig. 39) or in quartz veins (Gray, 1978).

If a granular fabric is differentially stressed, solution will occur on grain boundaries subject to a high normal stress (maximum normal stress occurs on grain boundaries that are perpendicular to the principal compression direction) and growth occurs on boundaries with a low normal stress (Durney, 1976). As solution proceeds on the boundary with a high normal stress, quartz and feldspar are dissolved away and phyllosilicates are passively concentrated (with their long dimension parallel to the boundary) forming a cleavage seam. The areas of low normal stress have development of overgrowths on the detrital grains and the crystallization of phyllosilicates as mica beards adjacent to the grain (Fig. 39). The phyllosilicates of the mica beards have a preferred orientation approximately parallel to the cleavage seams (Williams, 1972; Means, 1975).

Once a cleavage seam has been established, it may propagate along its length because of stress concentrations at the ends of the seam (Cosgrove, 1976). Therefore, subparallel seams develop around the largest grains and extend laterally, eventually linking up into an irregular network of cleavage seams (Gray, 1978).

The type A rough cleavage previously described (Fig. 35) with its short, discontinuous cleavage seams represents an early stage of rough cleavage development. With continued stress and subsequent solution type B rough cleavage (Fig. 36) forms with long, well-developed, continuous cleavage seams. Type C rough cleavage (Fig. 37) shows

dissolution acting only in a particular zone, perhaps reflecting some anisotropy in the original fabric (Gray, 1978).

### Crenulation cleavage

#### Introduction

A crenulation cleavage is found in several outcrops, usually in the extreme southern portion of the field area. It is found only in fine-grained slates and can usually be identified only in thin section.

The crenulation cleavage can be classified according to Gray's (1977a, 1977b, 1978) scheme into discrete and zonal crenulation cleavage. Zonal crenulation cleavage (Fig. 40) is defined as wide cleavage domains coincident with fold limbs having gradational boundaries, and having relict traces of pre-existing foliation being continuous through the cleavage zone. Discrete crenulation cleavage (Fig. 41) is defined as a thin, sharply defined cleavage discontinuity that truncates the pre-existing foliation in a crenulated fabric.

#### Origin of crenulation cleavage

Early work on crenulation cleavage suggested that the cleavage formed by faulting or passive-slipping along a plane of shear thus explaining the apparent offset of features across the cleavage surface (Donath and Parker, 1964). However, very little evidence of brittle deformation (granulation of grains or cataclasis) has been found along the cleavage surfaces (Gray, 1977b; 1978). Furthermore, strain measurements preclude shear alone being responsible for the cleavage (Gray and Durney, 1979b). They suggested that apparent offsets across the cleavage can be explained by volume reduction due to pressure

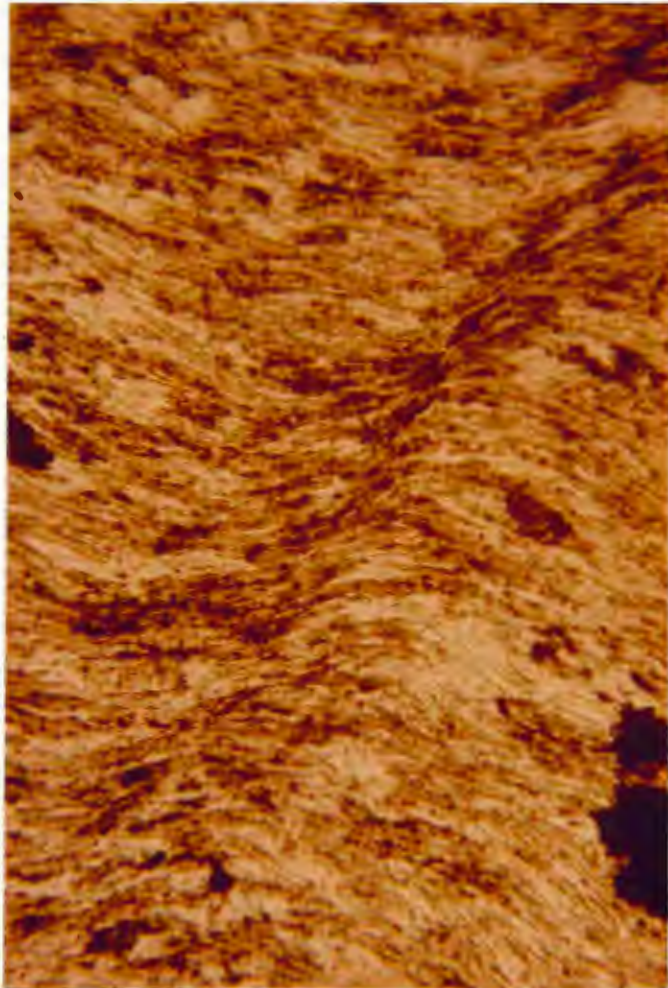


Fig. 40 Photomicrograph of zonal crenulation cleavage in slate. Note the wide zone of phyllosilicate concentration and the continuity of the pre-existing foliation. Oldenburg Pt., Jay Cooke Park. Field of view is 0.38mm X 0.26mm. Plain light.



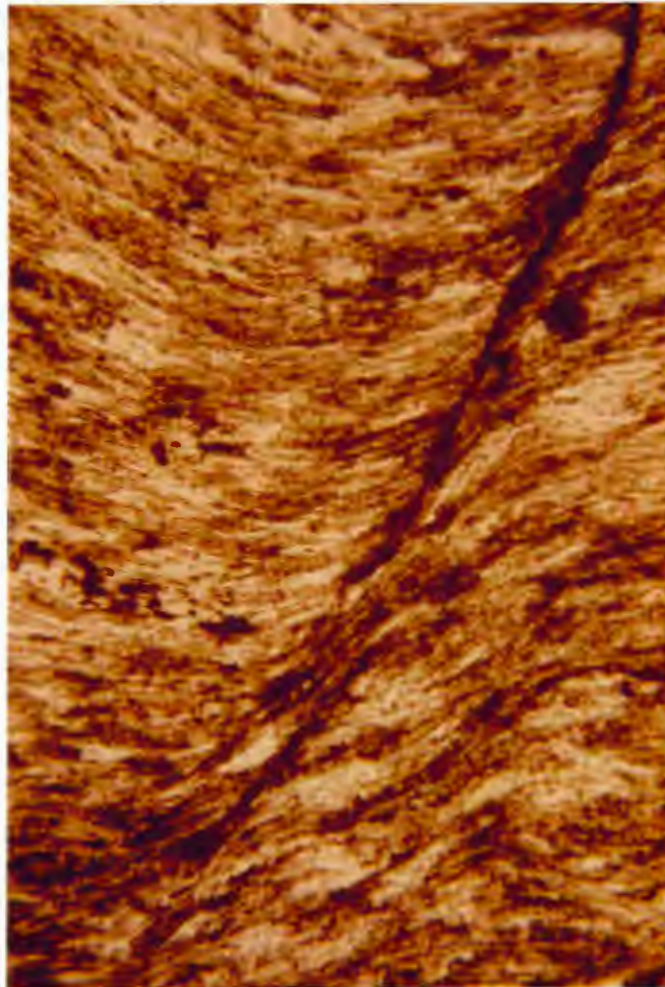


Fig. 41 Photomicrograph of discrete crenulation cleavage in slate. Note the sharply defined cleavage seams truncating the pre-existing foliation. Also note the gradual transition from a zonal crenulation cleavage in the lower left of the picture. Oldenburg Pt., Jay Cooke Park. Field of view is 0.38mm X 0.26mm. Plain light.

solution.

There has been a lot of work presented in recent years suggesting metamorphic differentiation due to pressure solution as an origin for crenulation cleavage (Cosgrove, 1976; Gray, 1977b; 1978; 1979a; 1979b; Gray and Durney, 1979a; 1979b). The basic principle behind the pressure solution process is the solution transfer of soluble minerals from sites of high chemical potential to sites of low chemical potential. The differences in chemical potential can be directly related to stress variations around microfolds (crenulation-folds) (Fletcher, 1977; Gray and Durney, 1979a).

It has been noted that crenulation cleavages coincide with the limbs of microfolds, and that crenulation cleavage development involves the transfer of dissolved phases from microfold limbs to hinges (Cosgrove, 1976; Gray, 1979b). Therefore it has been suggested that crenulation-folds are a necessary prerequisite for the development of crenulation cleavage (Gray, 1979b). The fold geometry does not determine the cleavage type; just the cleavage position and spacing (Gray, 1977b). These microfolds may form from buckling instabilities in an anisotropic medium (such as is found in slate) (Cosgrove, 1976; Gray, 1979b).

As the crenulation-folds develop the stresses acting on the individual mineral grains of the rock vary, depending on the exact location of the grain on the microfold. The chemical potential (and therefore the solubility) of a stressed mineral phase at any point along its boundary is directly related to the magnitude of the normal stress at that point (Gray and Durney, 1979b). Variations in normal

stress occurring on individual grains around the microfold depend on the grain's orientation with respect to the principal compressive stress (Fig. 42). The grains along the limbs of the microfolds, being oriented with their long dimension at an angle to the principal stress, are subject to a higher normal stress than the grains in the hinge which have their long dimension parallel to the principal stress. Therefore, the chemical potential is greater on grains in the limbs than in the hinges, so there will be transfer of dissolved species (usually quartz) from the limbs to the hinges of the microfolds (Fletcher, 1977; Gray and Durney, 1979b). When the quartz is removed from the limbs the phyllosilicates are passively concentrated into a mica-rich zone (zonal crenulation cleavage) coincidental with the microfold limb. As solution-deposition differentiation proceeds the limbs become more normal to the principal stress (the fold tightens), so that normal stresses increase causing further differentiation (Gray and Durney, 1979b). As pressure solution continues the quartz is entirely removed from the limbs and the folds 'lock up'. The former limb zone (now a discrete crenulation cleavage) becomes a pressure-solution surface defined by a concentration of parallel phyllosilicates forming a distinct cleavage seam (Gray, 1979b).

There is commonly a transition from zonal crenulation cleavage to discrete crenulation cleavage over the length of the cleavage (Fig. 41). In fact, discrete crenulation cleavages are thought to propagate lengthwise due to continual differentiation of microfolds ahead of the cleavage (Gray, 1977b; 1979b).

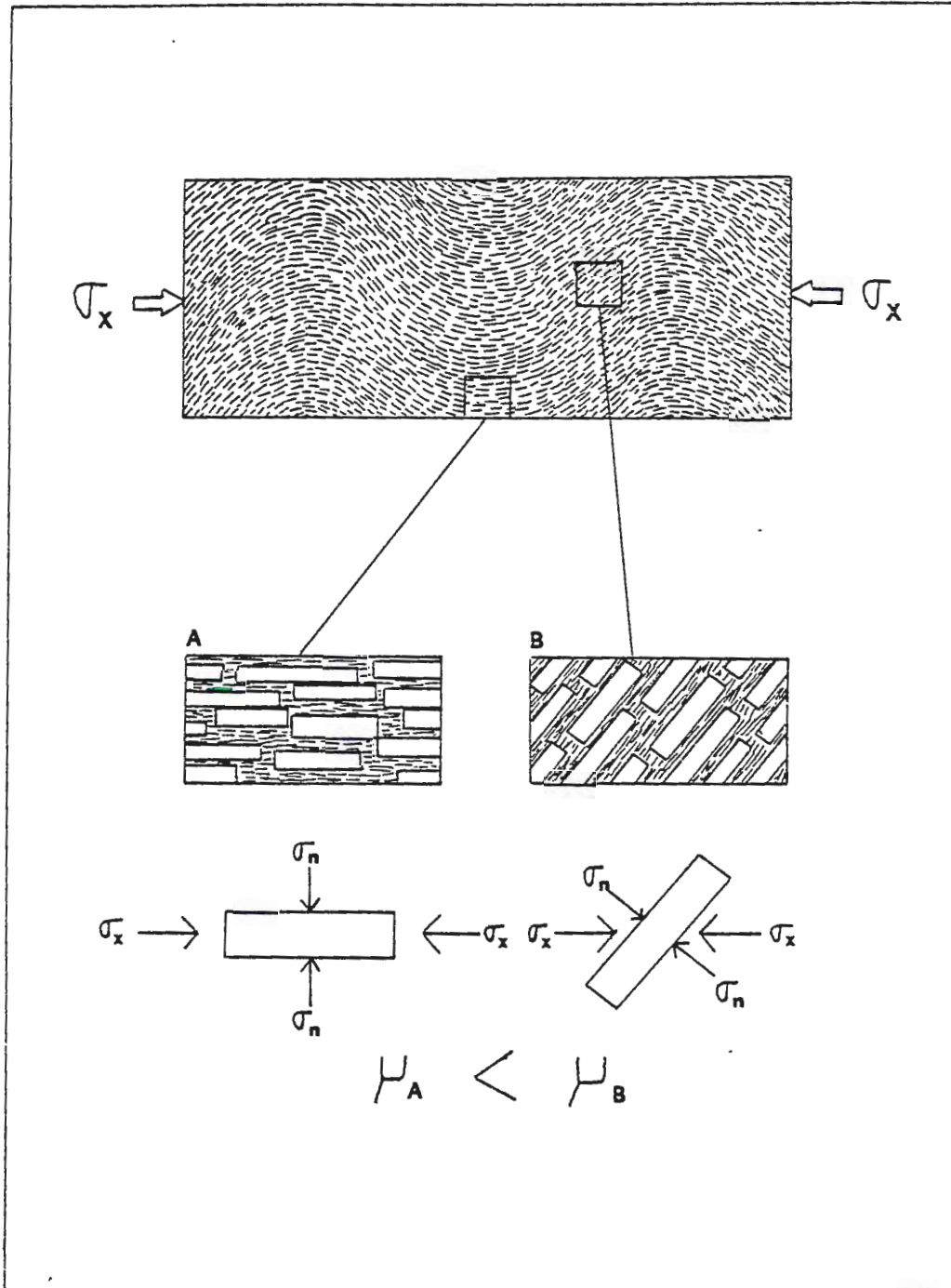


Fig. 42 Idealized model showing the importance of a grain's position on the microfold in a crenulated fabric. (After Gray and Durney, 1979b).

Discrete crenulation cleavage is most common in slates subjected to relatively low-grade metamorphism. The fine-grain size of the slates allows the crenulation fold to 'lock up' (and thus form a discrete crenulation cleavage) sooner than they do in coarser rocks. Low metamorphic grades are indicated since recrystallization would obliterate the crenulation cleavage at higher grades (Gray, 1977b).

The formation of crenulation cleavage by pressure solution is accompanied by significant reduction of rock volume resulting in shortening normal to cleavage. The total shortening value of 50-60% is composed of two components: a buckle shortening (due to microfolds) of 40-50% and a pressure-solution shortening of 10-20% (Gray, 1979a).

It must be emphasized that although the dominant mechanism of crenulation cleavage formation is differentiation due to pressure solution, the cleavage is usually enhanced by some degree of recrystallization of phyllosilicates during prograde metamorphism (Gray, 1979a).

#### Other evidence of pressure solution

In some slates in the study area more competent grains were deformed in a different manner than the rest of the rock. Large, elongated, non-detrital, opaque grains didn't undergo the effects of pressure solution as did the rest of the rock. Instead, they accommodated the shortening by buckling and folding (Fig. 43). At the ends of opaque grains where stresses were highest, pressure solution was most active causing the passive concentration of phyllosilicates into mica seams which drape over the ends of the opaque grains (Fig. 44). The more competent opaque grains also caused the formation of

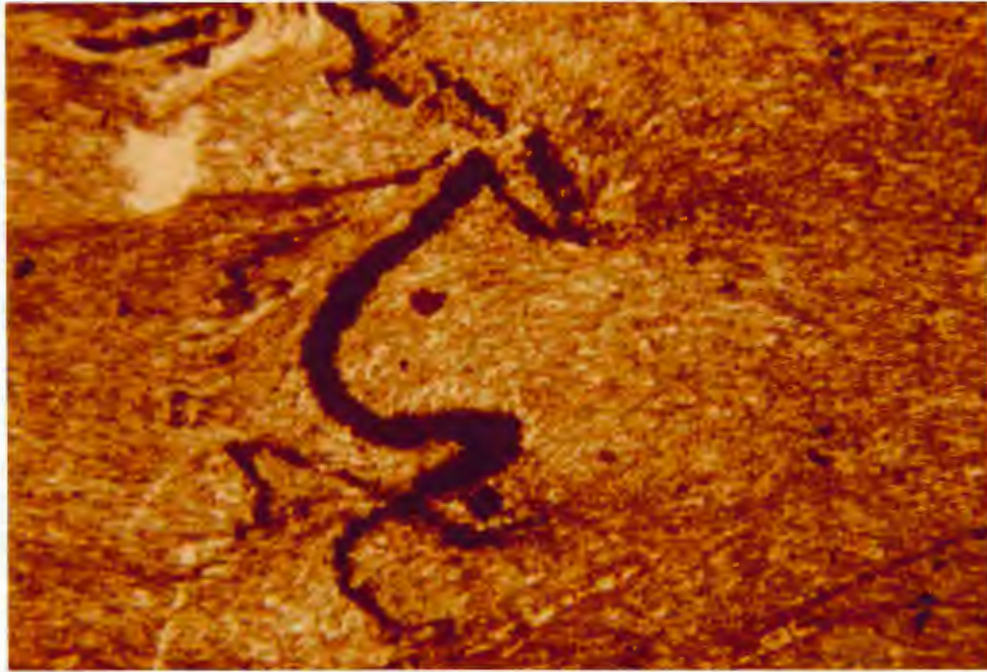


Fig. 43 Photomicrograph of an opaque mineral deformed by buckling in slate that has elsewhere been deformed by pressure solution. 0.3 km E. of Thomson Dam. Field of view is 0.95mm X 0.65mm. Plain light.

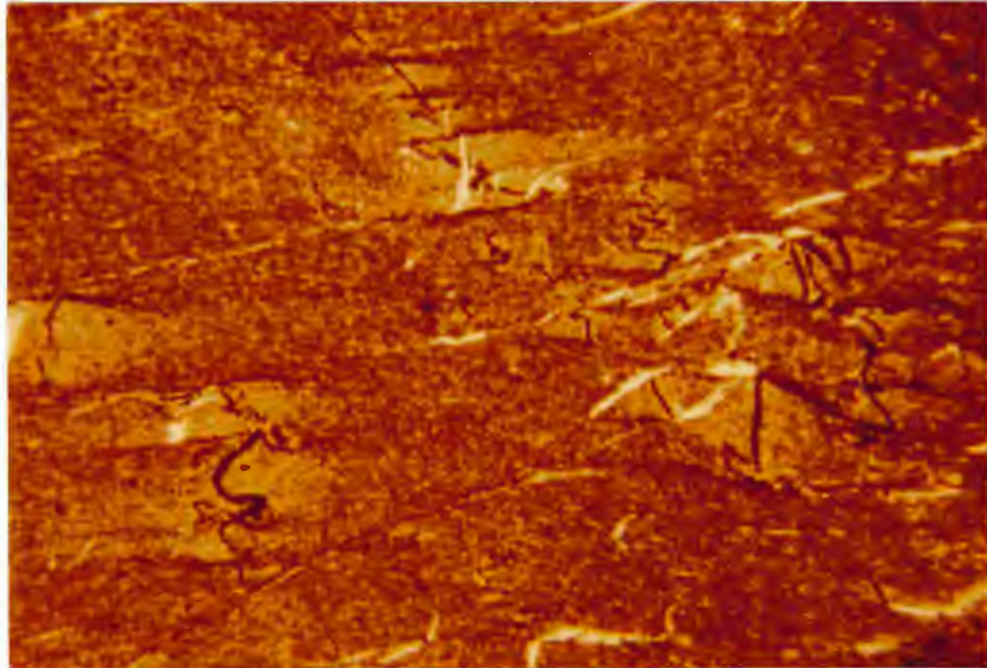


Fig. 44 Photomicrograph of the same slate as in Fig. 43 deformed by pressure solution. Note the concentration of phyllosilicates in mica seams which drape over the ends of the opaque minerals and the presence of strain shadows adjacent to the opaque grains. 0.3 km E. of Thomson Dam. Field of view is 3.8mm X 2.6mm. Plain light.

strain shadows where the proportion of quartz to chlorite is greater than in the rest of the rock (Fig. 44). The greater amount of quartz is due to the less severe effects of pressure solution within the strain shadows. (The quartz is 'protected' by the competent opaque grains.)

It is not uncommon to see bedding or other features that appear to be offset across a cleavage surface (Fig. 45). There is some microfaulting in these rocks, but it is usually in a plane that is not parallel to cleavage. Also, in the rocks where offsets are most noticeable, there is strong evidence for deformation by pressure solution elsewhere in the rock such as well-developed mica seams and partially dissolved quartz grains.

### Kink-bands

#### Introduction

Kink-bands are common in the metasediments of the Thomson Formation, especially at the type locality at Thomson Dam (Plate 1). Kink-bands are commonly described as small-scale monoclinical folds having planar limbs and angular hinge zones normally found in rocks with a definite planar anisotropy such as cleavage or bedding (Verbeek, 1978). As stated previously they are subplanar features that range in width from less than a millimeter to several centimeters, and they are usually oriented at a high angle to the foliation outside the kink-band.

Kink-bands can be classified as to whether there is shortening parallel to foliation outside the kink-band (reverse or negative kink-bands) or if there is extension (normal or positive kink-bands) (Dewey,

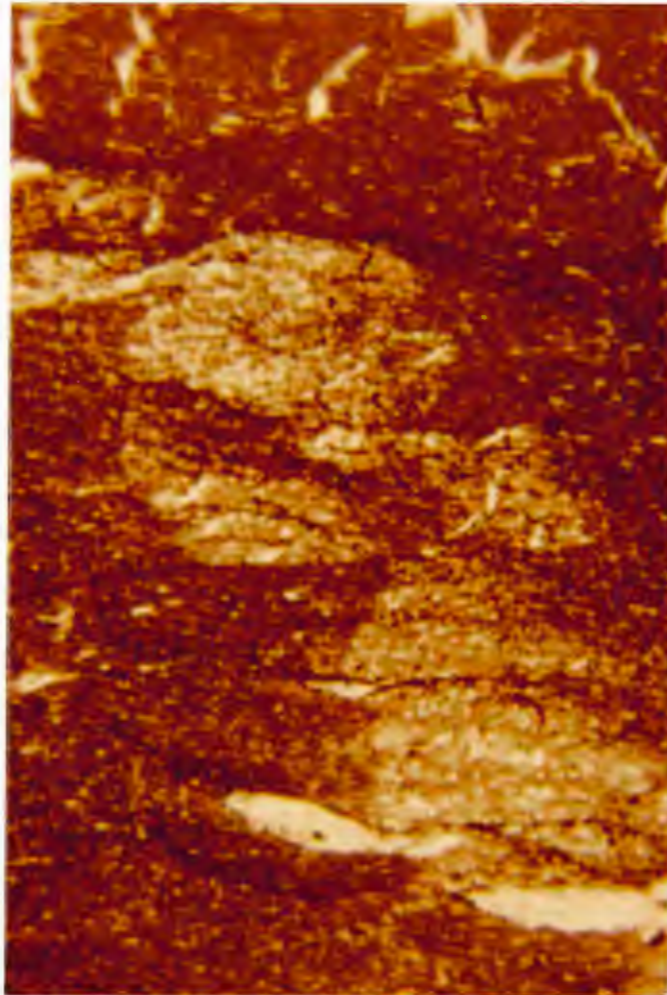


Fig. 45 Photomicrograph of silty slate showing the offset of bedding across cleavage due to pressure solution. Bedding is from upper left to lower right in the picture. Note the extremely well-developed cleavage seams where the offset is the greatest. 0.3 km E. of Thomson Dam. Field of view is 3.8mm X 2.6mm. Plain light.



1965; 1969). All observed kink-bands in the study area are reverse or negative kink-bands resulting in a shortening parallel to foliation outside the kink-band.

Measurements of various geometric aspects of kink-bands, illustrated in Fig. 46, can help determine the mode of kink-band formation. Some of the parameters include the angles  $\alpha$  (the angle between the kink-band boundary and the unkinked foliation),  $\beta$  (the angle between the kink-band boundary and the kinked foliation) and  $\gamma$  (the angle of rotation of the kinked foliation) and the distances AB (the thickness of the unkinked foliation) and CD (the thickness of the kinked foliation) (Anderson, 1964).

#### Kink-band models

Several theories have been advanced to explain the formation of kink-bands. Paterson and Weiss (1962, 1966) proposed the migration model on the basis of experimental deformation of phyllite. In this model kink-bands nucleate at a point or line source and grow in width by the outward migration of kink-band boundaries into adjacent undeformed rock (Fig. 47). It is geometrically necessary for the angle  $\alpha$  to be equal to  $\beta$  and for the distance AB to be equal to CD (volume is conserved). Also, as kinking progresses it is necessary for each point of the kink-band to have been the position of a hinge, meaning that it must have been sharply folded and unfolded as the kink-band boundary migrated through it (Paterson and Weiss, 1966).

In the rotation model of kinking the location of the kink-band boundaries are fixed early in the deformation, and they define a kink-

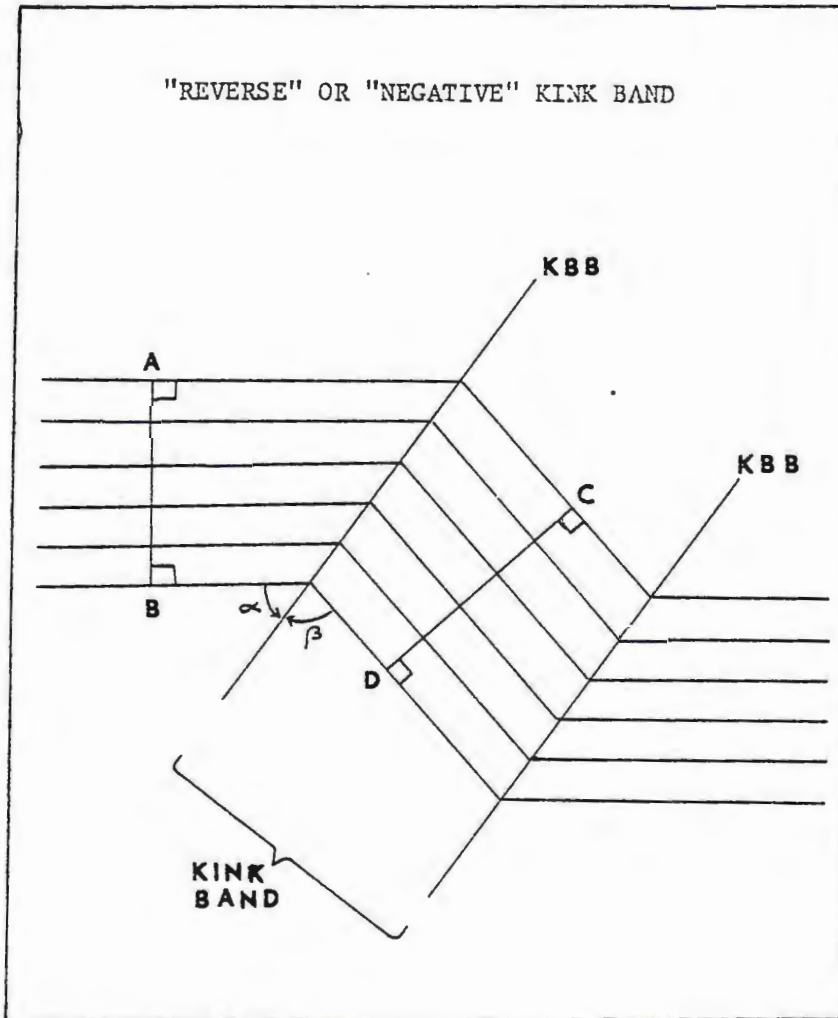


Fig. 46 Idealized diagram showing the various geometric aspects of kink-bands. See text for the descriptions of the various parameters. (After Anderson, 1964).

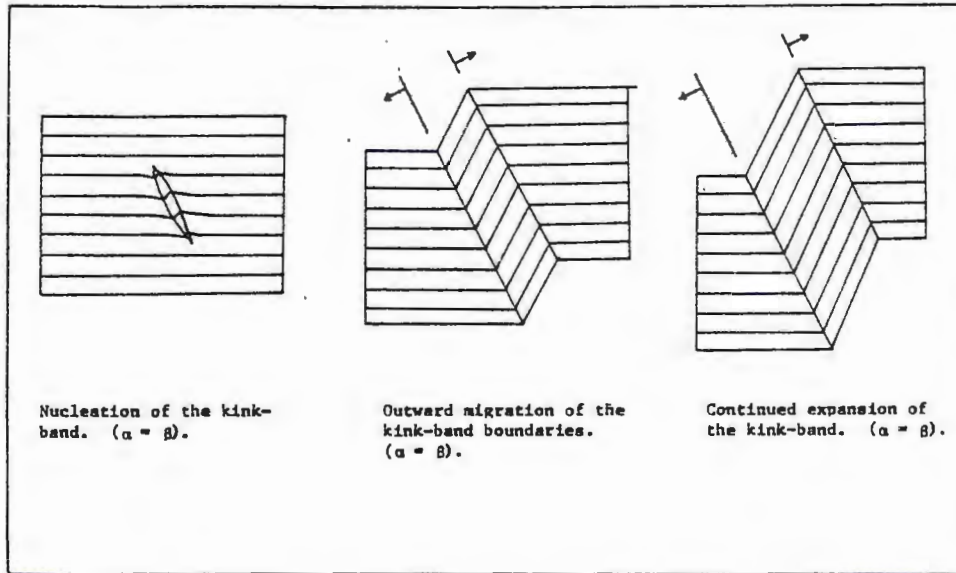


Fig. 47 Idealized diagram showing the migration model of kink-band development. (After Paterson and Weiss, 1966).

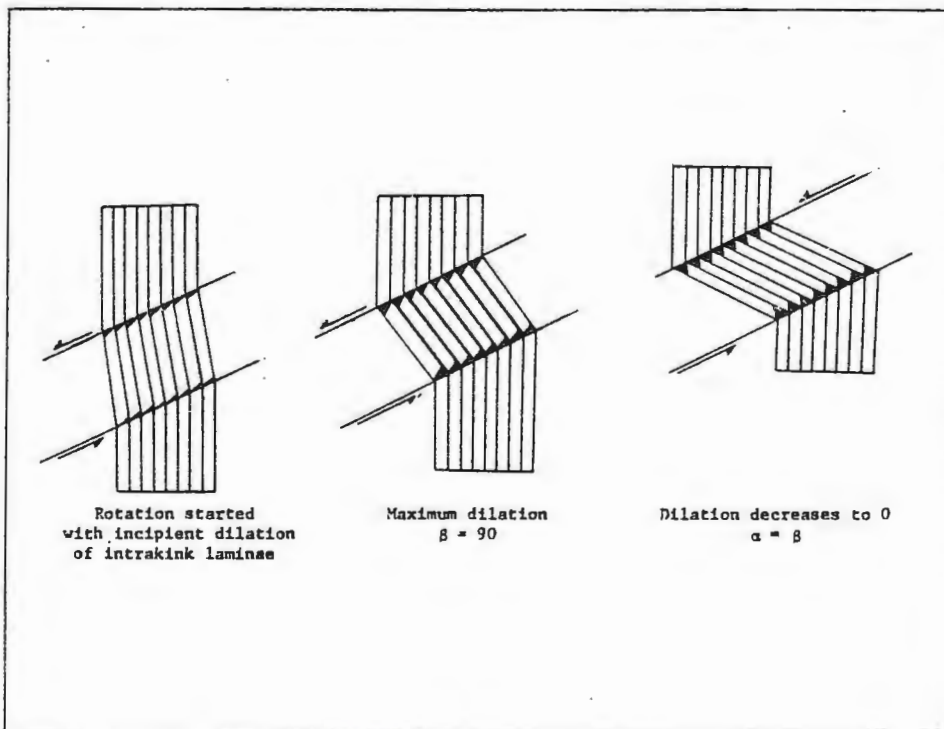


Fig. 48 Idealized diagram showing the rotation model of kink-band development. (After Ramsey, 1967).

band of constant width (Donath, 1968; Clifford, 1968). As deformation proceeds the foliation within the kink-band is rotated to progressively lower  $\beta$  values (Fig. 48). Since the foliation is actually hinged at the kink-band boundary it is geometrically necessary for the foliation to part or dilate as rotation occurs (Clifford, 1968); that is, distance CD must be greater than AB. As rotation passes a critical point ( $\beta = 90^\circ$ ), the foliation begins to close again until  $\alpha = \beta$  when the kink-band becomes locked ( $AB = CD$ ). It is possible, however, for the spaces between the dilated foliation to be filled by precipitating minerals such as quartz or calcite thus 'jamming' the kink-band at a stage where  $\beta > \alpha$  and  $CD > AB$  (Verbeek, 1978). It has also been suggested that the kink-band could collapse, 'jamming' the rotation at an intermediate stage ( $\beta > \alpha$ ) (Clifford, 1968). Since dilation occurs there is a corresponding volume expansion of the rock in which the kink-band has formed.

The joint-drag model of kinking describes kink-bands where the foliation is actually broken and offset by shear along the kink-band boundary. The location of the kink-band is defined early in the deformation by the breakage of foliation along the kink-band boundary, and like in the rotation model, the kink-band retains a constant width (Dewey, 1965). Further deformation causes rotation of the kinked foliation accompanied by slip along the foliation (which remain in contact; that is,  $AB = CD$ ) within the kink-band (Fig. 49). Triangular-shaped voids develop along the kink-band boundary causing volume expansion of the rock. Since the foliation within the kink-band is not connected with the foliation outside there are no angular constraints

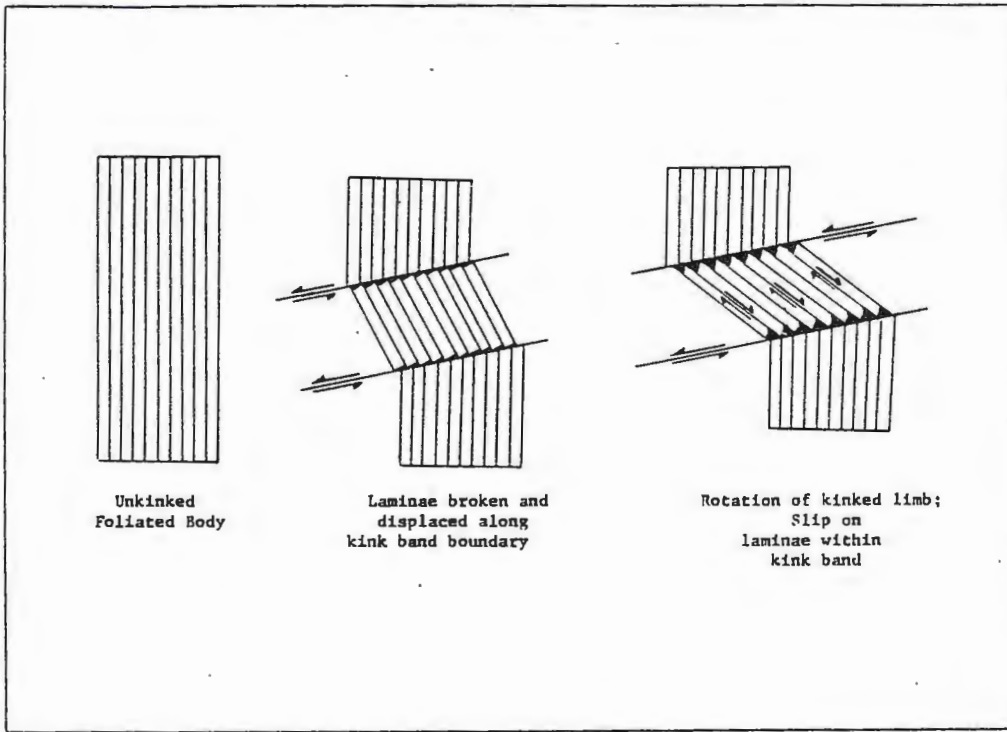


Fig. 49 Idealized diagram showing the joint-drag model of kink-band development. (After Dewey, 1965).

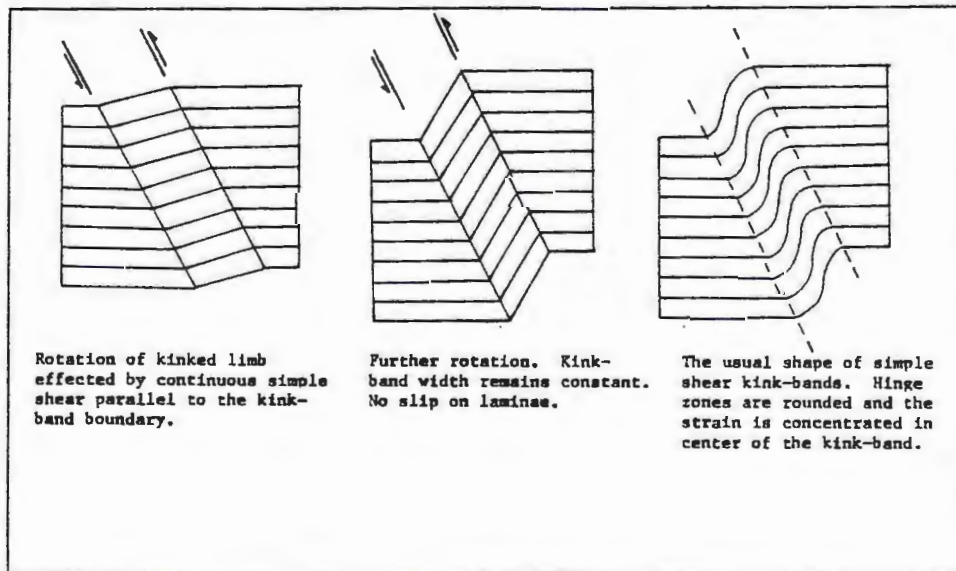


Fig. 50 Idealized diagram showing the simple shear model of kink-band development. (After Dewey, 1965).

between  $\alpha$  and  $\beta$  (Dewey, 1965).

In the simple shear model simple shear parallel to and confined within a tabular zone is responsible for kink-bands (Fig. 50). Whereas angular folds are a geometric possibility this method is much more likely to produce rounded folds due to end effects against the undeformed long limb of the kink folds (strain would be concentrated in the center of the kink-band) (Dewey, 1965).

#### Thomson kink-bands

The models presented above are idealized end members. No one model can be used to describe all the kink-bands in the Thomson Formation. Combinations of these and perhaps other mechanisms are responsible for kink-band development in these rocks.

The migration model probably doesn't apply to the kink-bands in the study area. Few examples of kink-bands pinching out in a lens shape could be found; most appear to die out without changing their width significantly. Additional strain is accommodated by the development of new, incipient kink-bands according to the migration model; thus kink-bands in various stages of development (with each stage represented by a kink-band of a different width) would be expected. However, within an outcrop, each individual kink-band had approximately the same width as the others, although the width of a single kink-band could vary along its length. Also,  $\alpha$  was not equal to  $\beta$  in most kink bands as is required for this model. Likewise, no kink-bands with rounded hinges were seen so the simple shear model is probably not important in this area.

Kink-bands studied in this area contain characteristics of both the rotation model and the joint-drag model. Some show aspects of just the rotation model such as precipitation of quartz in the dilated intrakink foliation (Fig. 51), the continuity of foliation across the kink-band boundary (Fig. 52) and  $\beta > \alpha$ . Other individual kink-bands display attributes of the joint-drag model such as discontinuity of foliation across the kink-band boundary (Fig. 53), the development of triangular-shaped voids along the kink-band boundary (now filled in with quartz) (Fig. 54) and the lack of angular constraints between  $\alpha$  and  $\beta$ . Characteristics of both models can be found within the same kink-band (Fig. 55) where the intrakink foliation is dilated and there is discontinuity of foliation across the kink-band boundary.

The relationship between  $\alpha$  and  $\beta$  angles was not distinctive of a particular model. In addition, the  $\alpha$  angles ranged from 57 degrees to 90 degrees, and the  $\beta$  angles ranged from 34 degrees to 90 degrees.  $\alpha = \beta$ ,  $\alpha > \beta$ , and  $\beta > \alpha$  values were all observed.

#### Origin of the Thomson kink-bands

The origin of the Thomson kink-bands may possibly be similar to that of the kink-bands in the Sompart Slate of the Pyrenees as described by Verbeek (1978). First, early strain occurred nearly parallel to the cleavage as indicated by the presence of microfaults and tension cracks. In the Thomson Formation these microfaults are not as common as in the Sompart Slate, but they are present to some extent. Eventually strain is accommodated by the formation of kink-bands, the exact location of which is probably due to some local instability in

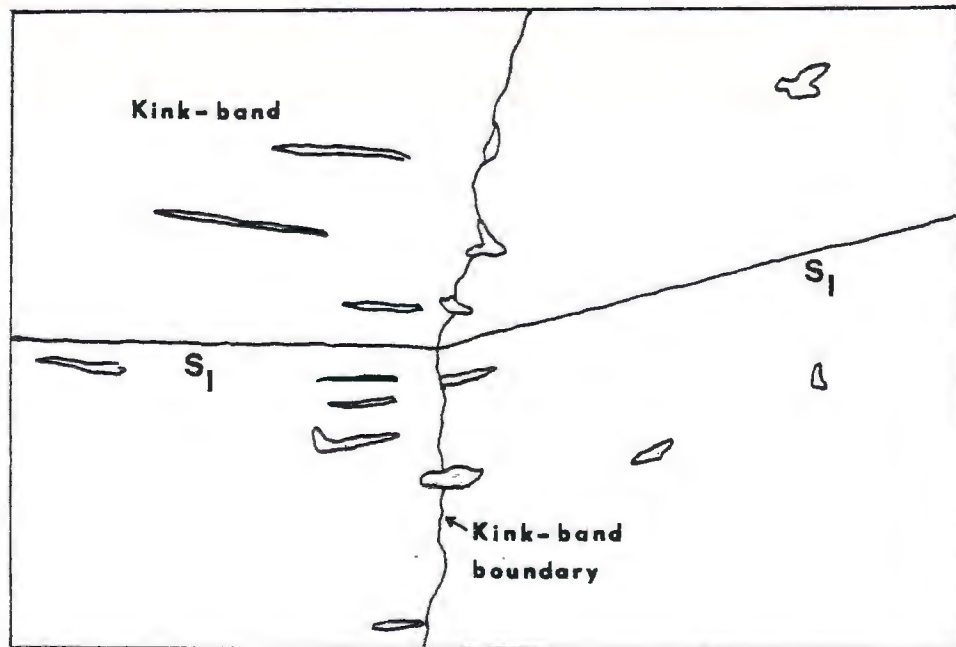
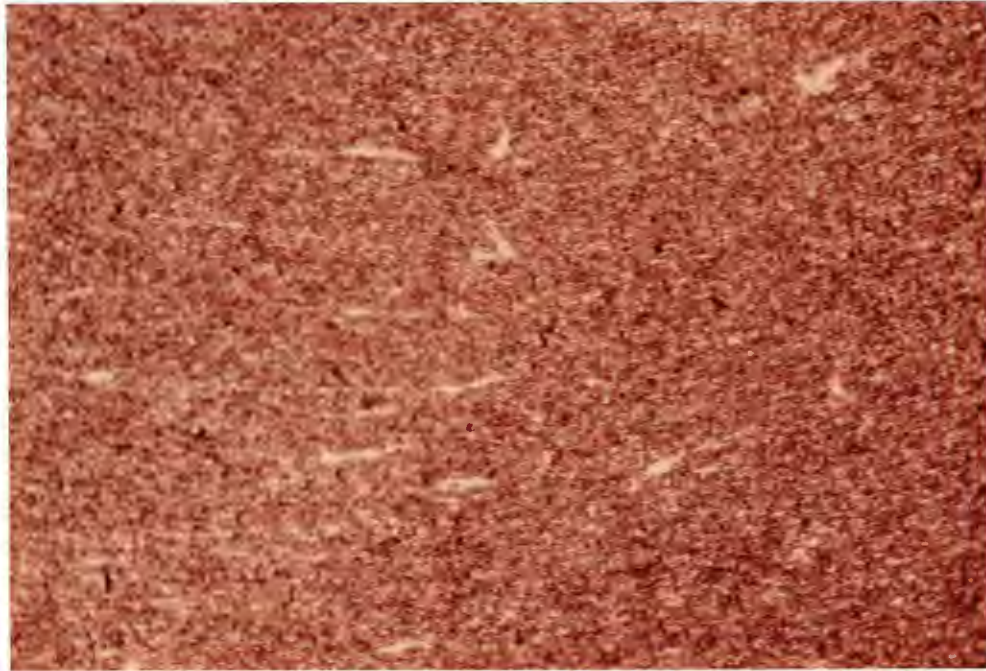


Fig. 51 Photomicrograph of a kink-band in slate showing the early stages of dilation of cleavage within the kink-band. The poorly-developed kink-band is in the left side of the picture. Thomson Dam. Field of view is 0.95mm X 0.65mm. Plain light.



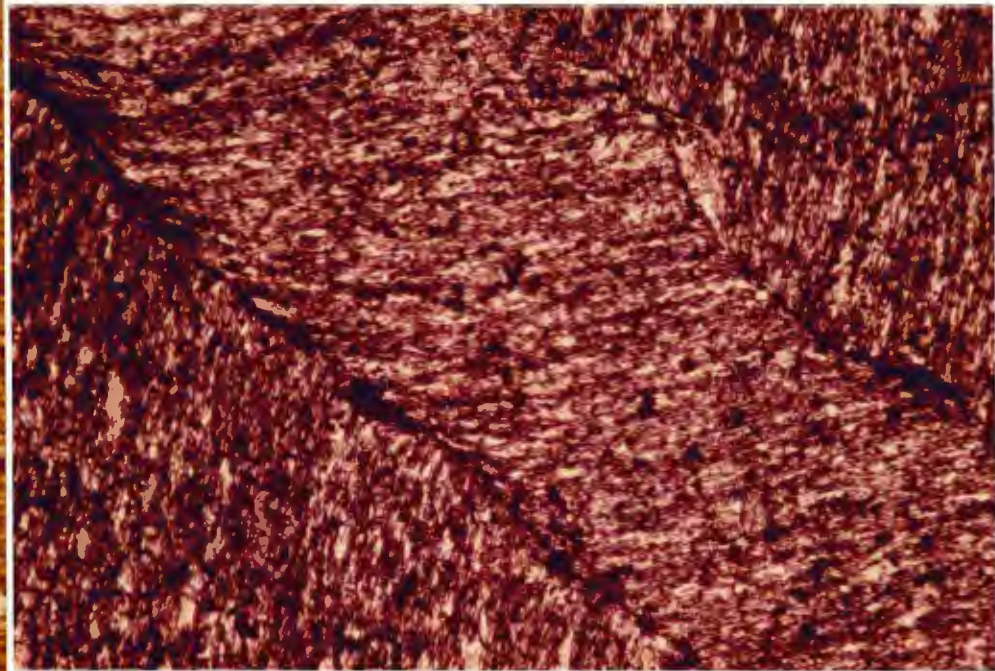
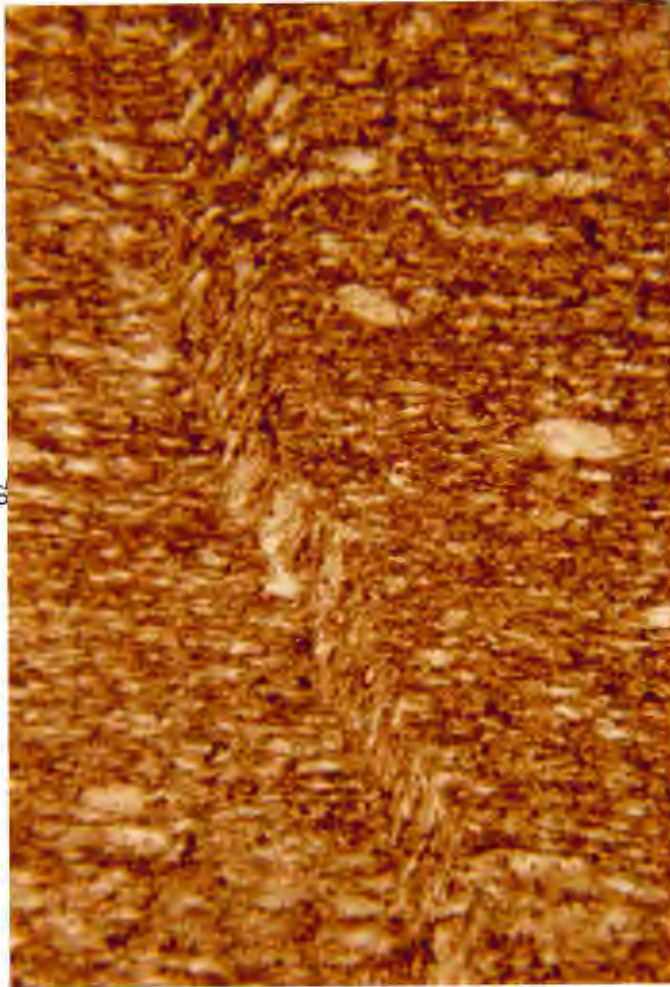


Fig. 52 Photomicrograph of a kink-band in slate showing the continuity of foliation across the kink-band boundary. Thomson Dam. Field of view is 0.95mm X 0.65mm. Plain light.

Fig. 53 Photomicrograph of a kink-band in slate showing the discontinuity of foliation across the kink-band boundary. Thomson Dam. Field of view is 0.95mm X 0.65mm. Plain light.

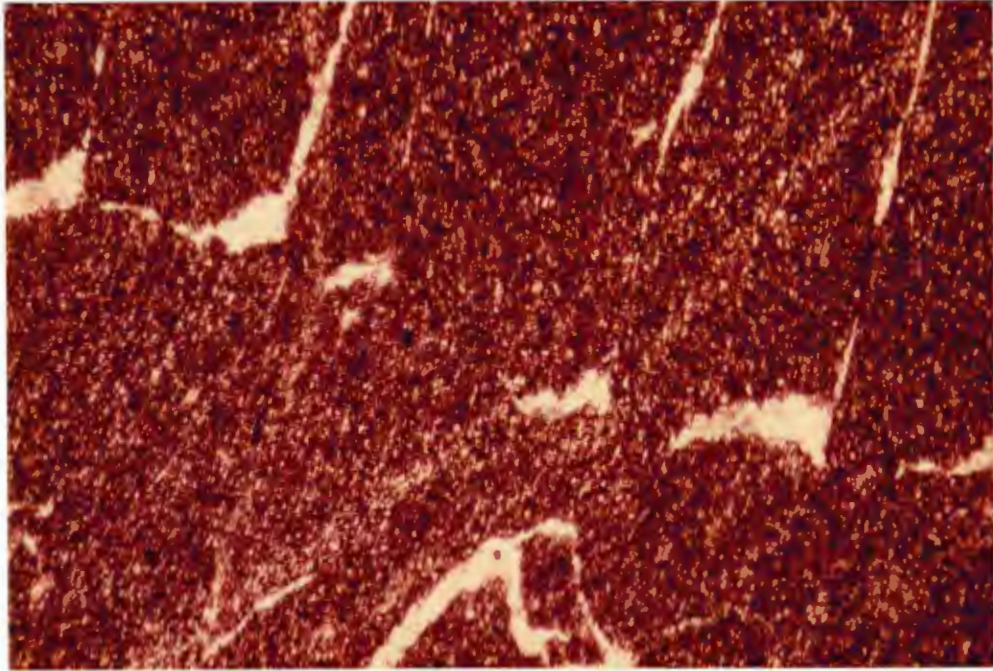


Fig. 54 Photomicrograph of a kink-band in slate showing the triangular shaped quartz fillings along the kink-band boundary. The kinked foliation is in the upper part of the picture. Thomson Dam. Field of view is 0.95mm X 0.65mm. Plain light.

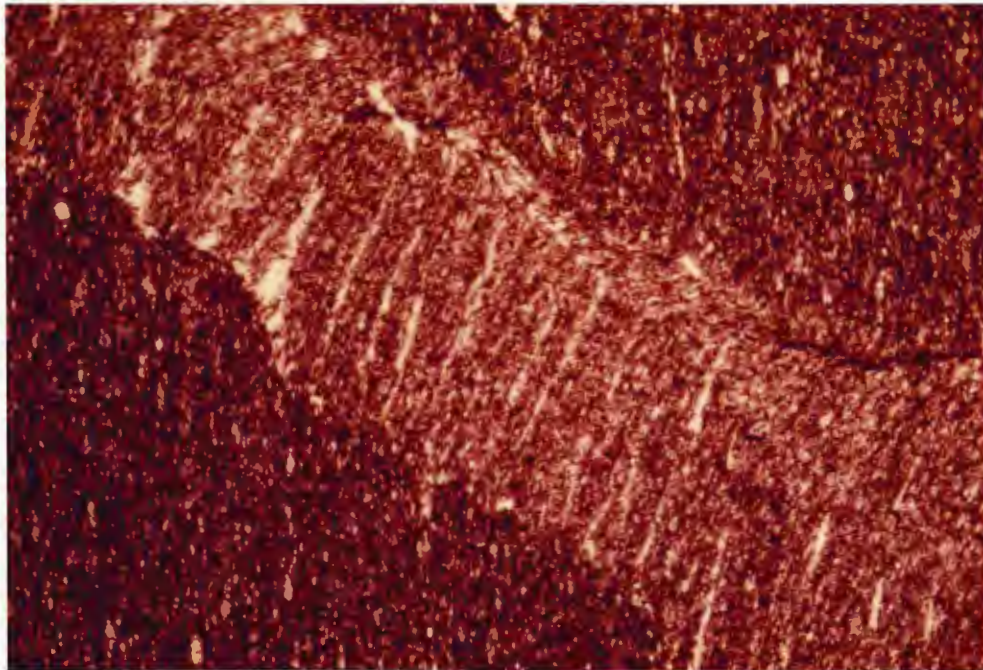


Fig. 55 Photomicrograph of a kink-band in slate showing the dilation of foliation within the kink-band and the discontinuity of foliation across the kink-band boundary. Thomson Dam. Field of view is 0.95mm X 0.65mm. Plain light.

the rock. These kink-bands probably developed by some combination of the rotation and the joint-drag mechanisms. Discontinuity of foliation across the kink-band boundary, dilation of intrakink foliation and triangular-shaped void formation all took place. Some kink-bands were [jammed] by precipitating quartz in the dilation zones, and further strain may have been accommodated by minor rotation of the long limb of the kink-band (that is, the areas between kink-bands) or by pressure solution along the kink-band boundary (Fig. 53) causing the wide variability of the  $\alpha$  and  $\beta$  values.

One cleavage trace was followed through a sample containing six kink-bands (Fig. 56), and it was determined there was approximately 3% shortening due to the kinking. Paterson and Weiss (1966) and Donath (1968) suggest that kink-bands begin to form at about 2% shortening. Thus, total shortening parallel to the principal compressive direction (subparallel to the vertical cleavage) is approximately 5%.

Since the formation of kink-bands by the suggested mechanisms involves volume expansion of the rock in a horizontal direction they must have formed at a high structural level where confining pressures were low (Verbeek, 1978). They are also thought to have formed late in the structural history of the area (Dewey, 1965), perhaps in response to Keweenawan activity such as the sagging of the basin over the Keweenawan rift or the emplacement of igneous rocks stratigraphically above the Thomson Formation.

#### Late-stage deformation

There are several isolated outcrops where the cleavage deviates from its usual near-vertical attitude. In these outcrops the cleavage

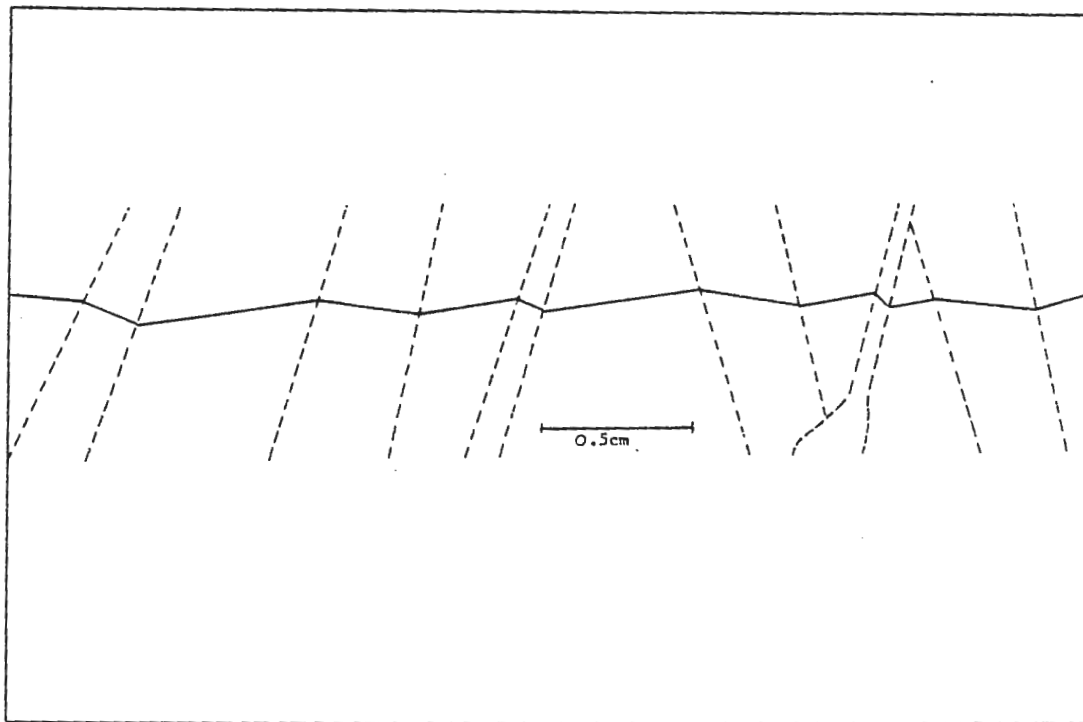


Fig. 56 Sketch of a single cleavage trace through a slate specimen with six kink-bands. The total shortening due to kinking is about 3%.

is refracted nearly 90 degrees from approximately vertical in relatively competent slaty greywacke beds to nearly horizontal in slate beds (Fig. 22). The cleavage orientation closely correlates to lithology, abruptly changing at bedding contacts. It is very limited in extent, typically extending over a distance of less than 10 meters within an individual outcrop.

This refraction is different from normal cleavage refraction seen elsewhere in the field area. The change in orientation is far too great, and the cleavage attitude is reversed from what would be expected with normal refraction. That is, the cleavage in the slate is refracted away from the vertical instead of the usual case of the more competent slaty greywacke cleavage being refracted. This refraction has somewhat similar characteristics to giant kink-bands. Other than scale, the major difference is that 'kinking' in the refracted cleavage areas is controlled by lithology (the 'kink-bands' occur at bedding contacts) which is not the case for the more conventional kink-bands discussed above. These localized areas of intense refraction are difficult to interpret. They are probably due to late-stage tectonic readjustments, possibly related to nearby Keweenawan activity.

Another area of unusual cleavage refraction is found in a railroad cut southeast of Carlton at the northern edge of the area affected by two Penokean deformations. The cleavage in an exposed anticline doesn't appear to be axial-planar to the fold, nor does it fan in a manner usually ascribed to cleavage refraction around a fold (Fig. 57). The cause of this cleavage pattern is not known with any degree of certainty, but it may be related to the outcrop's location right at the

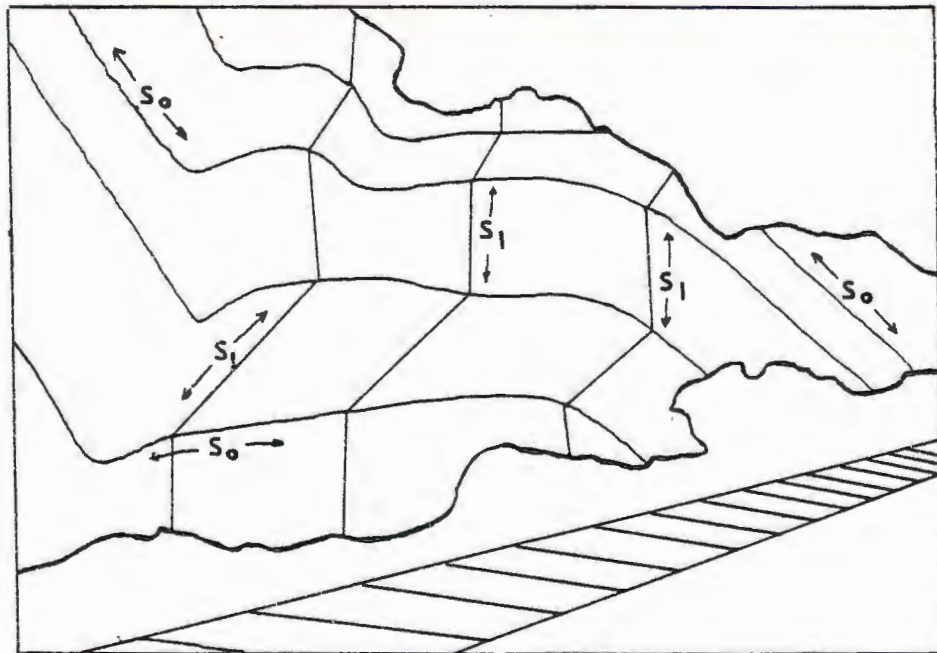


Fig. 57 Outcrop showing 'abnormal' cleavage refraction around a fold. Looking due west. Old Northern Pacific grade 1.6 km south of Thomson Dam.

boundary between one and two Penokean deformations or to later Keweenawan 'readjustments'.

In the Oldenburg Point area of Jay Cooke State Park (Plate 1) there are areas where the cleavage has been deformed (Fig. 27). The deformation is located adjacent to a large diabase dike and pod swarm and involves the folding of cleavage into open folds of variable size with approximately axial-planar joints striking N30E-S30W, the intense jointing of the rock and faulting of the rock along shear zones. The close proximity of the diabase dike and pod swarm (which is much larger and more extensive than anywhere else in the study area) and the overall N30E orientation of the fold axial planes and joint sets (which is parallel to the general strike of Keweenawan dikes in the field area) strongly suggests that this deformation is, again, in response to Keweenawan events.

Variably developed joint sets are abundant throughout the Thomson Formation. Joint sets striking N30E and N30W may define a conjugate joint system that formed at the time of folding. The set striking approximately north-south may be an a-c joint set also developed during folding. The joint set striking between N20E and N30E is probably related to later deformation, possibly associated with Keweenawan activity.

Quartz veins are commonly present along the N30E joint set. These quartz veins may represent final precipitation sites for quartz that was dissolved by pressure solution during cleavage formation.

Both reverse and normal faults are present in the Thomson Formation. The reverse faults normally strike approximately east-west

and involve small displacements of less than 5 meters. They are probably related to and are an alternate expression of the same Penokean event that compressed the rocks in a north-south direction and formed the east-west trending folds with axial-planar cleavage. The normal faults strike approximately N30E and have unknown but probably much greater displacements than the reverse faults. The normal faults offset the east-west trending fold axes and greywacke ridges of the Thomson Formation in places, and they provided a zone of weakness that was later intruded by the Keweenaw diabase dikes. The normal faults are probably the result of later Keweenaw rifting or other extensional activity.



CHAPTER VI  
TECTONIC INTERPRETATION

Introduction

This chapter will attempt to explain some of the structures seen in the study area in the light of regional tectonic activity. The origin of structures in the study area will be compared with those seen elsewhere in the Thomson Formation. Current regional tectonic models for the Penokean orogeny will also be discussed.

Deformation in the Thomson Formation

The rocks in the study area show various degrees of deformation during the Penokean orogeny. Those in the northern area (Fig. 58) show the effects of only one major Penokean deformation. These rocks have been folded into open, asymmetric, upright, east-west trending folds accompanied by a steeply-dipping axial-planar cleavage. The rocks in the extreme southern portion of the study area, on the other hand, show the effects of two major Penokean deformations in places. These rocks contain an earlier slaty cleavage as well as a faint, later crenulation cleavage (often visible only in thin section) that is axial-planar to the open, upright folding. The earlier cleavage is generally dipping much less steeply than the later axial-planar cleavage and is parallel to bedding only in a few places. The later folding and axial-planar crenulation cleavage has nearly the same style and orientation as the single deformation observed in the northern area.

An approximate boundary between the rocks showing the effects of one and two Penokean deformations can be extended in an east-northeastwardly direction across the study area (Fig. 58). The

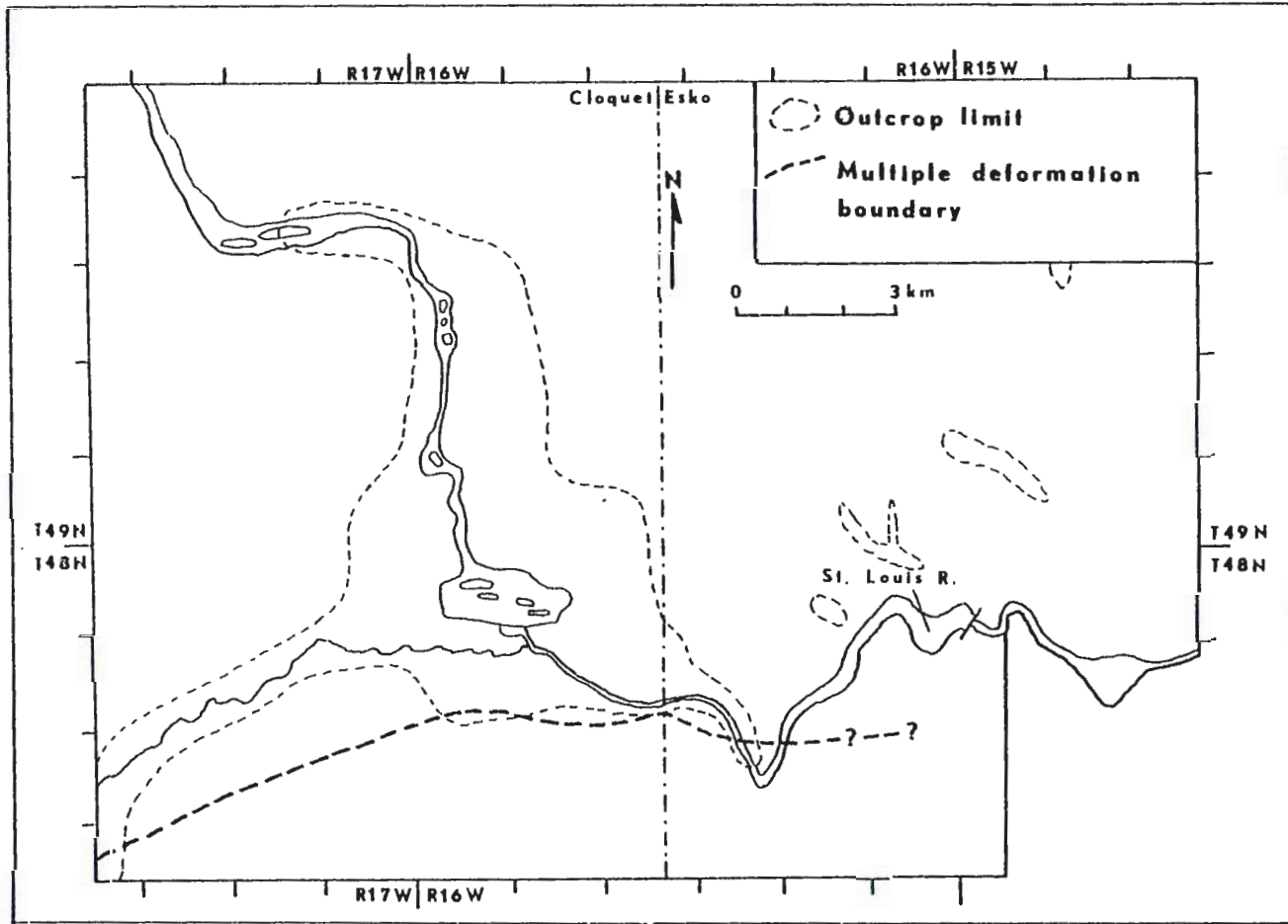


Fig. 58 Map showing the inferred location of the boundary between terranes affected by one (to the north) and two (to the south) Penokean deformations in the study area.

boundary can be delineated near the southwestern corner of the field area where outcrops containing one and two cleavages are separated by less than 1.5 kilometers (Craddock, Mudrey and Holst, 1983; Holst, 1984c). The boundary extends east-northeastwardly for nearly seven kilometers beneath glacial cover before it is located again between two railroad cuts on the old Northern Pacific grade. It then trends eastwardly just south of the St. Louis River (intersecting exposed outcrop in places) to the Oldenburg Point area of Jay Cooke State Park after which it disappears beneath glacial cover.

Scattered areas show the effects of a third, much less intense deformation. This deformation includes the formation of kink-bands and the 'readjustment' of cleavage (as discussed in the structural interpretation chapter), jointing and faulting and is probably the result of Keweenawan and not Penokean tectonic activity.

Evidence for at least two major Penokean deformations has been described in most of the Thomson Formation to the south of the study area. Early bedding-parallel (or nearly so) foliation is prevalent throughout the southern portion and is seen to be axial-planar to small (outcrop-size), isoclinal, recumbent folds (Connolly, 1981; Hyrkas, 1982; Holst, 1982) (Fig. 59). This early foliation and bedding were later refolded into open, upright folds with an axial-planar crenulation cleavage with the same orientation as the one cleavage at the type locality.

Thus, the first phase of Penokean deformation resulting in the development of isoclinal, recumbant folds accompanied by axial-planar bedding-parallel foliation affected only the southern two-thirds of the

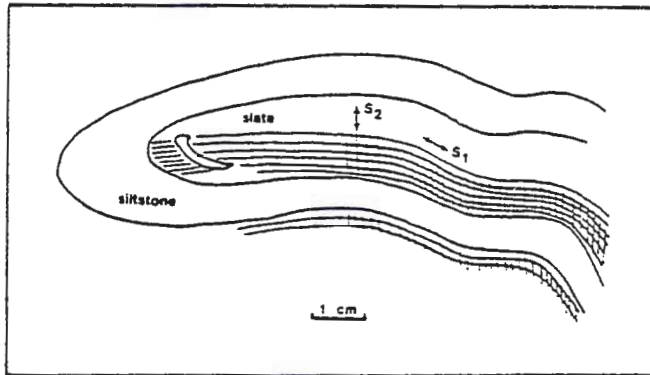


Fig. 59 Sketch of a small fold near Atkinson (10 km SW of the study area) showing the axial-planar  $S_1$  slaty cleavage parallel with bedding on the limb of the fold and the intersection of the  $S_1$  cleavage with the hinge of the fold. (Holst, 1982).

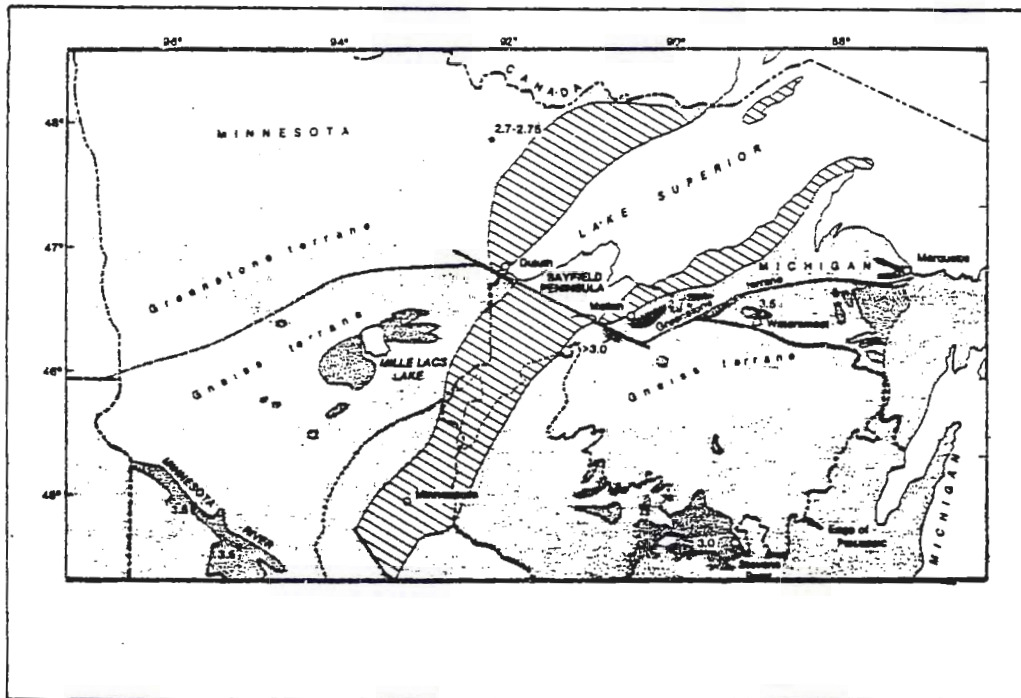


Fig. 60 Map showing the location of the boundary between the Archean granite-greenstone and gneiss terranes in Minnesota, Wisconsin and Michigan. (After Morey and Sims, 1976).

Thomson Formation. The second phase of deformation forming the open, upright folds with nearly vertical axial-planar cleavage (crenulation cleavage in the south) affected the entire Thomson Formation and is the only Penokean deformation visible at Thomson Dam.

Evidence of multiple deformation during the Penokean orogeny has also been observed in Middle Precambrian rocks in Upper Michigan (Cannon, 1973; Klasner, 1978) and in Wisconsin (Maass and others, 1980; Maass, 1983).

Structures attributable to Keweenawan activity such as kink-bands and [readjusted] cleavage have not been described to date in the southern exposures of the Thomson Formation. The fact that these structures are found only in the northern area is probably due to the area's proximity to the Keweenawan-age intrusions.

#### Influences of basement rocks

It has been recognized that there is a geologic boundary between two Archean terranes that extends in an east-northeastwardly direction across Minnesota (Morey and Sims, 1976). In northern Minnesota 2700 m.y. granite-greenstone complexes make up the bedrock whereas in southern Minnesota older (>3500 m.y.) granulite-facies gneisses form the basement bedrock. The metavolcanic and metasedimentary rocks of the granite-greenstone terrane are thought to have accumulated adjacent to the pre-existing gneiss terrane which was at that time part of a sialic protocontinent. The addition of 2700 m.y. granitic material welded the two terranes sufficiently to support a Proterozoic sedimentary basin (Sims, 1976; Morey and Sims, 1976). This fundamental difference in Archean basement terranes has been noted to extend to the

east through northern Wisconsin and northern Michigan (Sims, 1980) (Fig. 60).

The boundary between Archean terranes coincides in location with the Great Lakes tectonic zone of Sims and others (1980) which is a 30 to 60 km wide zone of distinctive tectonism affecting both Archean and Proterozoic rocks.

#### Intracratonic model

The intracratonic model of the Penokean orogeny suggests that deformation was strongly influenced by the location of the Archean basement boundary and the different nature of the two Archean terranes. This model suggests that Early Proterozoic sedimentary successions developed in an intracratonic basin that was located with its axis over the boundary between the two Archean basement types. Crustal foundering in an extensional environment (as indicated by the presence of Early Proterozoic dikes parallel to the basement boundary and to the Great Lakes tectonic zone) initiated basin development (Sims, 1980; Sims and others, 1980; Sims and Peterman, 1983; Morey, 1983). The continuity of Early Proterozoic sedimentary rocks across the basement boundary and the lack of a simatic basement in Minnesota has been cited as evidence that this rifting was intracratonic and no oceanic crust was involved (Sims and others, 1980; Morey, 1983). Sedimentation in the northern portion of the basin consisted of thin, miogeosyncline-like deposits. With continued foundering and subsidence of the basin, deep-water turbidite sheets (the Thomson Formation) and tholeiitic and calc-alkalic volcanic rocks similar to a eugeosynclinal environment

were deposited in the southern part of the basin (Sims, 1976; Morey, 1979; 1983).

Deposition ended with the compression of the basin during the Penokean orogeny. Deformation was asymmetric across the basin, being most intense in the southern portion where both the gneissic basement and the overlying supracrustal rocks were deformed together (Fig. 61). Deformation in the northern portion of the basin underlain by the granite-greenstone basement was much less intense resulting in the mild folding of only the supracrustal rocks (Sims, 1976; Sims and others, 1980; Morey, 1983). This contrast in deformational style has been explained by the differential mobility of the two Archean basement terranes. The deformation is proposed to have resulted from the alternating contraction and expansion (uplift) of the mobile gneiss terrane with corresponding lateral transport of overlying supracrustal rocks against the relatively stable granite-greenstone terrane to the north. That is, the Penokean orogeny was caused mostly by vertical tectonics; there is very little evidence of plate-tectonic processes being involved (Sims, 1976; 1980; Sims and others, 1980; Morey, 1983).

Vertical remobilization of the Archean basement has also been suggested as the cause of Penokean deformation in northern Michigan (Cannon, 1973; Klasner, 1978). Small sedimentary basins with complex depositional histories (as compared to the larger, simpler Animikie basin of Minnesota) were deformed into structural troughs such as the Marquette trough or the Republic trough during the Penokean orogeny (Larue and Sloss, 1980). The deformation involved two stages: an initial period of folding caused by gravity sliding northward off of an

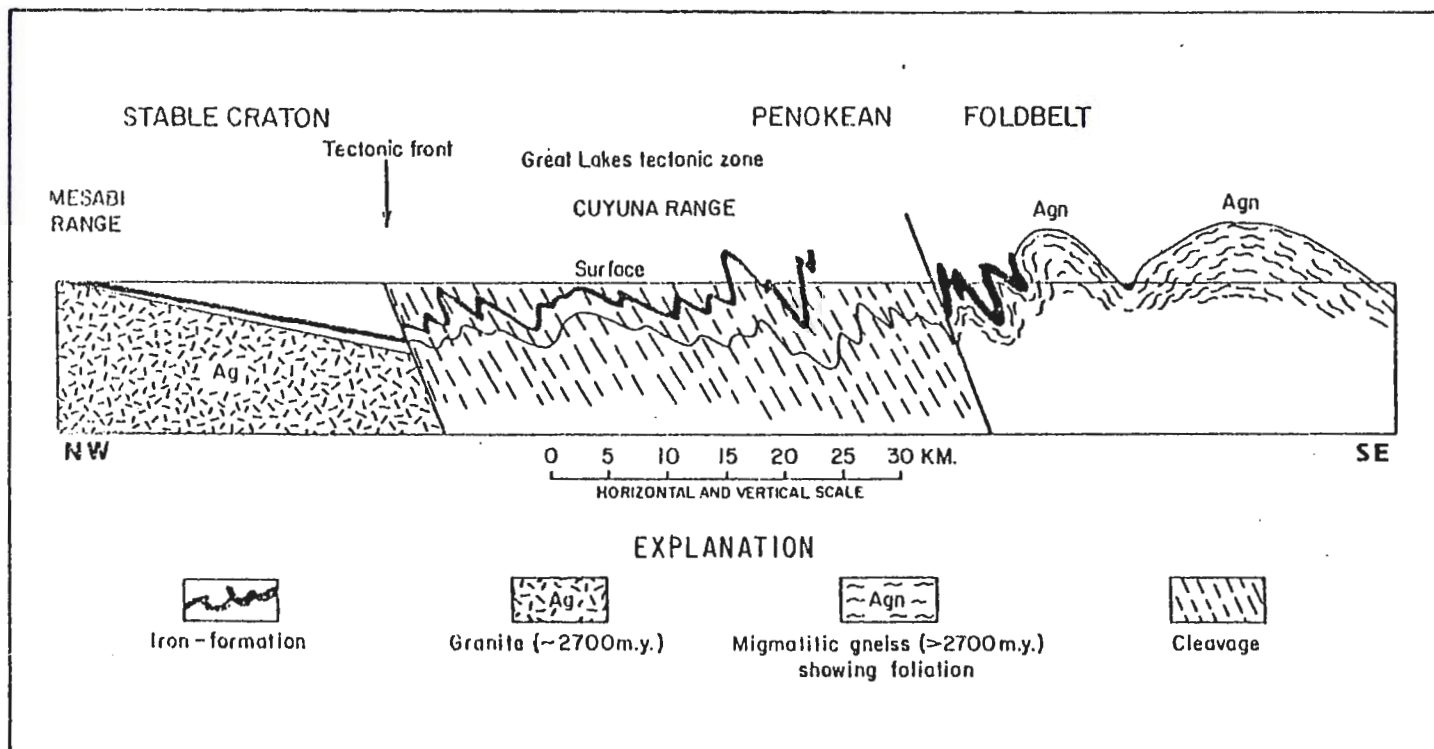


Fig. 61 Geologic section across the Animikie basin in Minnesota showing the asymmetric nature of the deformation. (Morey, 1983).



ancestral Penokean range in central Wisconsin and a later period of uplift of rigid Archean basement blocks or gneiss domes (depending on the plasticity of the basement gneiss (Sims, 1976)) forming grabens and causing passive folding of the overlying Proterozoic rocks (Fig. 62) (Cannon, 1973; Klasner, 1978). As with the intracratonic model for Minnesota, regional horizontal compressive forces are thought to be of only minimal importance.

#### Plate-tectonic models

The Penokean orogeny has also been explained by various plate-tectonic models. These models suggest that the Archean basement rocks had no direct influence on structural development in the overlying Proterozoic succession, but instead, some type of converging plate environment was responsible for deformation.

A converging plate-tectonic event has been proposed for the rocks of Wisconsin and northern Michigan. Cambray (1977, 1978) suggested that the sequence of events in northern Michigan is similar to that for a continental margin of a spreading ocean that later became part of a convergent plate environment similar to that proposed by Van Schmus (1976). This model proposes that the Penokean orogeny involved a north-dipping subduction zone that was located to the south of exposed Precambrian rocks in Wisconsin (Fig. 63). The volcanic-plutonic rocks of northern and central Wisconsin represent the island-arc region and the Animikie Group of Minnesota and the Marquette Range Supergroup of Michigan represents a part of the back-arc basin.

Other possible convergent plate-margin interpretations that attempt to account for the ages and distribution of rocks related to

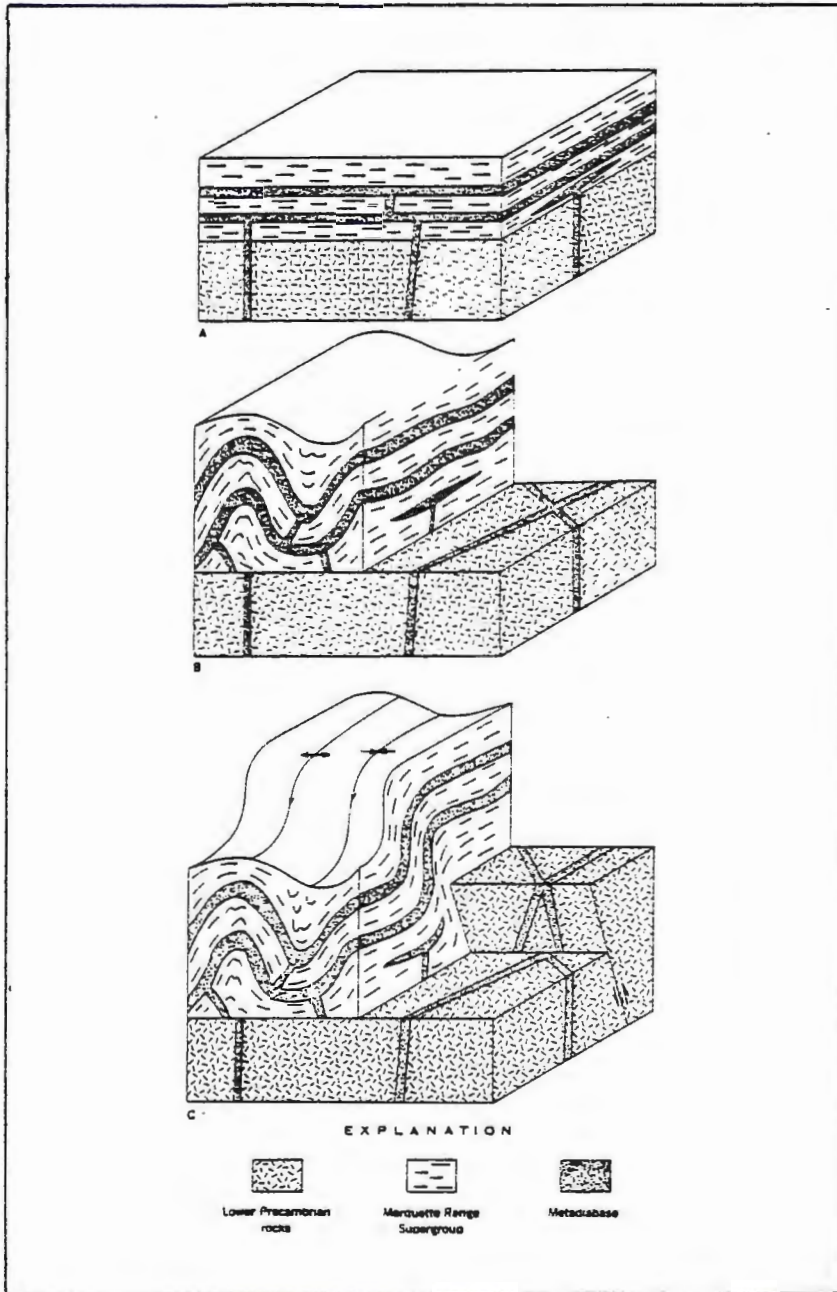


Fig. 62 Schematic block diagram illustrating the behavior of sedimentary and basement rocks in northern Michigan. Sedimentary rocks undergo deformation by gravity sliding whereas basement rocks remain undeformed (b). Later block faulting of the basement produces passive draping of the earlier folds (c). (Cannon, 1973).

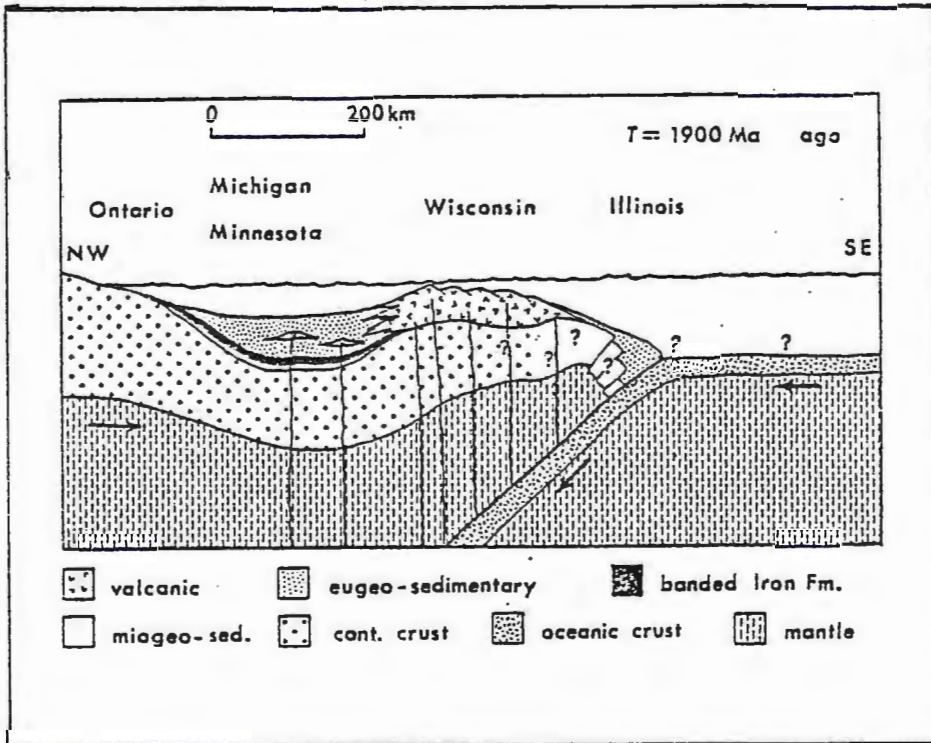


Fig. 63 A possible reconstruction of the Great Lakes area during the early stages of the Penokean orogeny. (Van Schmus, 1976).

the Penokean orogeny have been proposed by Van Schmus (1981). The first possibility is that of two successive south-dipping subduction zones. The first zone created an oceanic island-arc that collided with the Superior craton. The second subduction zone formed further to the south under another Archean microcontinent which later collided with the first arc complex. The second possibility suggests that three successive subduction zones were involved. The first zone, again a south-dipping zone, created an oceanic island-arc that collided with the Superior craton. Then a north-dipping subduction zone formed under the island-arc and was active until it consumed all of the oceanic crust between it and an Archean microcontinent to the south which subsequently collided against the arc. This added igneous material to the arc complex. Another north-dipping subduction zone then formed to the south under the microcontinent creating igneous rocks in the Archean terrane of central Wisconsin.

There has been some objection to plate-tectonic models for the Penokean orogeny because certain characteristics of modern plate-tectonics have not been described (until recently) in the Precambrian rocks of the Great Lakes region. The lack of rocks that are typical of oceanic crustal rocks has been cited as evidence that the rifting during the Early Proterozoic depositional stage never developed to the point where oceanic crust was formed (Sims and others, 1980; Morey, 1983), thus precluding the existence of a subducted oceanic plate. The apparent lack of ophiolite sequences (Van Schmus and Bickford, 1981; Morey, 1983), paired metamorphic belts (Morey, 1979), large foreland-directed overthrusts and other structures with largely horizontal

components (Morey, 1979; 1983; Brown and Greenberg, 1981) and the intimate association of Penokean metamorphic nodes with plutons and sites of intense local deformation (typical of non-plate-tectonic granite-greenstone terranes) (Greenberg and Brown, 1983) is additional evidence that plate-tectonic processes may not have been active.

Several recent studies, however, have provided considerable support to the convergent plate boundary model for the Penokean orogeny. Geochemical studies on the mafic Quinnesec Formation of northeastern Wisconsin have shown that these Penokean-age volcanic rocks are indeed of the island-arc or back-arc type indicative of a collisional event (Schulz, 1983). Holst (1984a, 1984b, 1984c) has cited compelling evidence that northward-directed nappes (involving a significant horizontal shortening component) developed in the Thomson Formation during an early stage of folding during the Penokean orogeny. Strain measurements on the rocks of the Thomson Formation (Holst, 1983) indicate a horizontal shortening perpendicular to the east-west vertical cleavage in excess of 60% during the second phase of Penokean deformation. The intracratonic model for the Penokean orogeny with its largely vertical remobilization of underlying basement rocks is incompatible with the large amount of horizontal shortening that took place during nappe and cleavage formation that occurred during deformation (Craddock, Mudrey and Holst, 1983).

#### Nappes in the Thomson Formation

As mentioned previously, there is considerable evidence to suggest that nappes developed in the Thomson Formation during the Penokean

orogeny (Holst, 1984a; 1984b; 1984c). It has been noted that Penokean deformation in the Thomson Formation involved two major phases of folding: an early phase of isoclinal, recumbent folding with a well-developed, axial-planar, usually bedding-parallel foliation in the southern portion and a later phase of open, upright folding with a well-developed, axial-planar, vertical foliation throughout the entire formation.

The pervasive  $S_1$  foliation is nearly always parallel to bedding due to the isoclinal nature of the  $F_1$  folds. The only exceptions to this are a few rare hinges of small-scale (less than one meter in amplitude) folds (Fig. 59) and a few outcrops where the  $S_1$  foliation is strongly refracted across lithologic contacts (Holst, 1982). The rarity of these hinge areas, the lack of larger mesoscopic folds and the pervasive nature of the bedding-parallel foliation implies that the entire southern portion of the Thomson Formation is located on the upper limb of a very large isoclinal fold or folds (nappes) (Holst, 1984c).

Studies of the structural facing of the  $F_2$  folds also provide additional evidence that the entire southern Thomson Formation is on the upper limb of large isoclinal folds; that is, the folds are thrust nappes or have extremely attenuated lower limbs (Holst, 1984c). Only upward-facing  $F_2$  folds were observed; no downward-facing  $F_2$  folds were seen as would be expected if the  $F_1$  folds are 'normal' small-scale isoclinal folds.

The cleavage refracton pattern that occurs in an outcrop less than 0.5 km west of the southwest corner of the study area (located near the

boundary between one and two deformations) also supports the nappe model. The  $S_1$  foliation dips steeply in the coarser units and is more nearly horizontal in the finer units. By removing the effects of the strain of the second deformation (measured at the type locality (Holst, 1983)) it can be seen that the resulting cleavage refraction pattern is what would be expected on the upper limb and near the hinge of an isoclinal, recumbent fold (Fig. 64) (Holst, 1984c). The cleavage-bedding relationships developed in several outcrops in the study area that show the effects of two deformations is similar to that just described. These outcrops are located very near to the boundary between one and two deformations (the nappe front) (Fig. 58), and they generally contain an  $S_1$  cleavage that is at a distinct angle to bedding much as would be expected near the hinge of an isoclinal fold or nappe (Fig. 64).

Lithologic differences across the nappe front provide additional support for the existence of nappes in the Thomson Formation. Metavolcanic rocks, carbonate beds and graphitic units are common in areas to the south (Connolly, 1981; Hyrkas, 1982), but are absent in areas to the north of the nappe front. Carbonate concentrations in the metasediments located just south of the nappe front in the study area contain significantly more calcite outside of concretions than those in the north. This difference in lithology is probably the result of tectonic transport of rock from initially distant parts of the Animikie basin during nappe development.

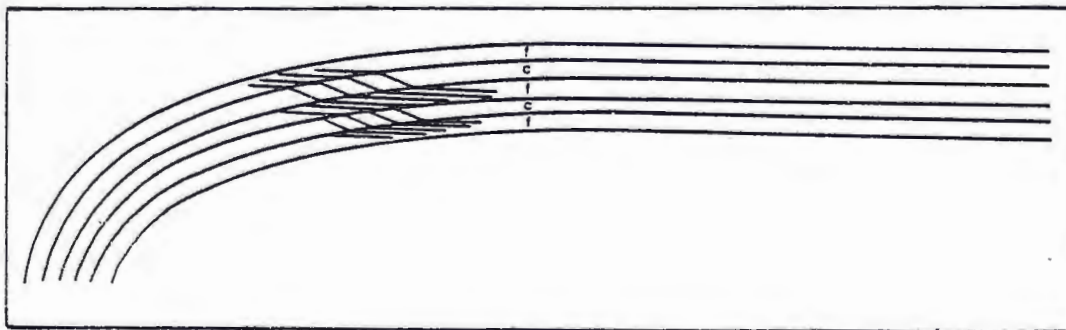
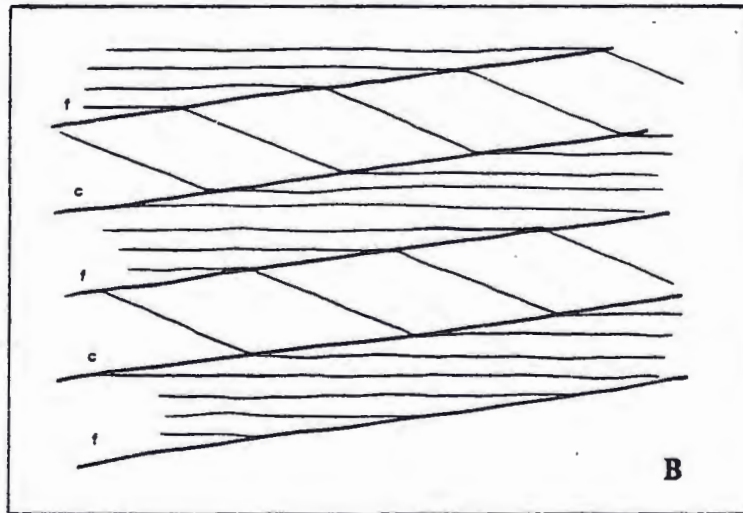
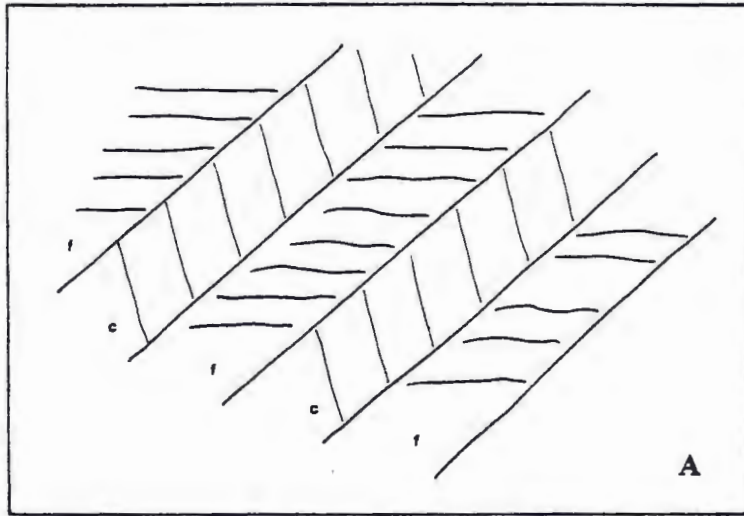


Fig. 64 Geometric aspects of bedding-cleavage relationships near Mahtowa (7.6 km SW of Carlton) as it is now (a) and after the  $D_2$  strain is removed (b). This outcrop is inferred to be near the hinge of a large-scale, isoclinal, recumbent fold (c). (Holst, 1984c).



## Conclusions

The Penokean deformation of the Thomson Formation is probably the result of a collisional orogeny due to plate-tectonic processes. This caused the formation of northward-directed nappes with the corresponding nappe front extending through the study area (Fig. 65) and the development of two phases of cleavage in most parts of the Thomson Formation with subsequent large amounts of horizontal shortening. The evidence presented is compatible with a plate-tectonic model with at least one south-dipping subduction zone. The oceanic crust associated with such an environment has probably been entirely consumed by subduction, and the Middle Precambrian igneous rocks of east-central Minnesota may represent the roots of a continental-arc or island-arc adjacent to a microcontinent located to the south (Fig. 66). The plate-tectonic processes active during the Penokean orogeny are probably not strictly analogous to Phanerozoic plate-tectonics, but instead, they may be transitional between Archean-style tectonics (with small, thin, mobile protocontinents with largely vertical tectonic transport) and modern-style plate-tectonics.

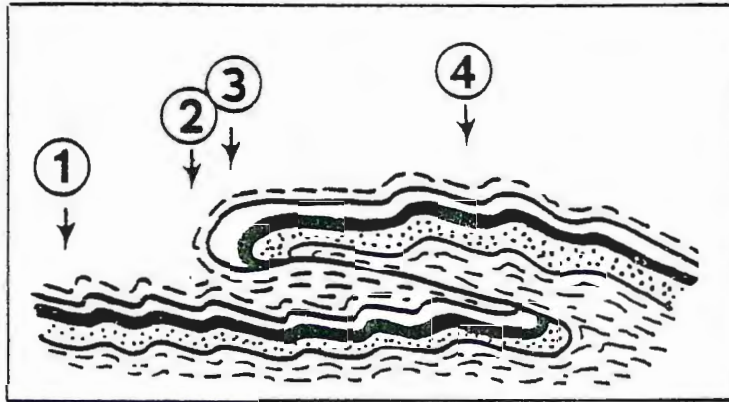


Fig. 65 Diagrammatic cross-section of the Thomson Formation. 1 = Thomson Dam. 2 = nappe front. 3 = location of outcrop shown in Fig. 64. 4 = southern area of multiple deformation. (Holst, 1984c).

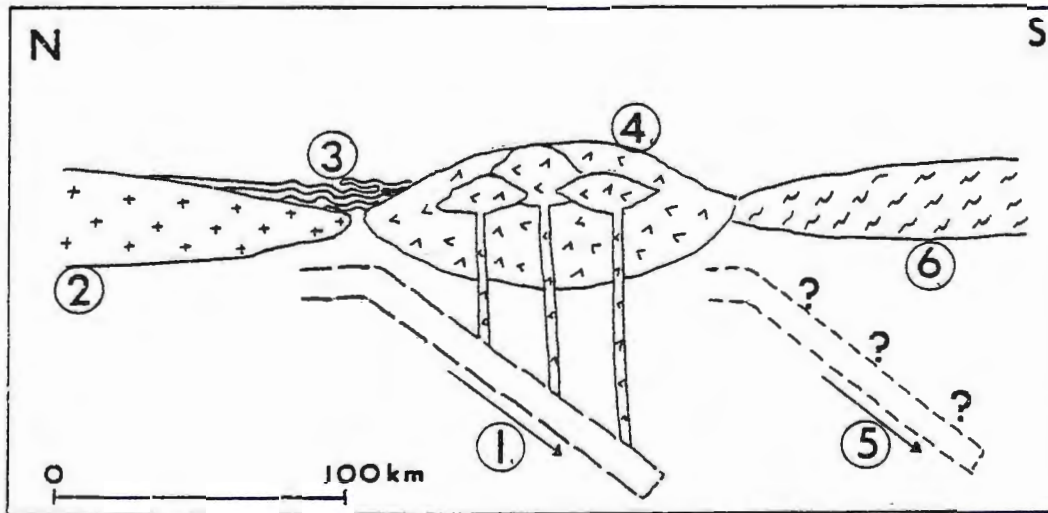


Fig. 66 A possible reconstruction of the Penokean orogeny in east-central Minnesota. A south-dipping subduction zone (1) with the oceanic plate completely subducted brings the granite-greenstone terrane (2) near the deformed Animikie sedimentary rocks (with northward-directed nappes (3)). Partial melting of the subducted plate produces the igneous rocks of east-central Minnesota (4). Another south-dipping subduction zone (5) with a completely subducted oceanic plate may have brought a microcontinent to the south (6) into proximity with the igneous rocks. (After Van Schmus, 1981).

## CHAPTER VII

### SUMMARY

The Thomson Formation in the Cloquet and Esko quadrangles consists of interbedded slate, slaty greywacke and metagreywacke generally striking approximately east-west and dipping to the south at 40 to 70 degrees or less commonly to the north at slightly higher angles. These rocks were later intruded by numerous N30E-S30W striking, Keweenawan diabase dikes.

The rocks were folded during the Penokean orogeny into open, upright, subhorizontal folds with fold axes usually plunging less than 20 degrees to nearly due east or west although plunges of up to 50 degrees were seen locally. These folds contain an axial-planar cleavage that strikes nearly east-west and dips vertically or steeply to the south.

The cleavage is a well-developed, continuous slaty cleavage in the slate and a poorly to well-developed, type A, type B or type C rough cleavage in the slaty greywacke. A poorly-developed crenulation cleavage that strikes S85E-N85W and dips nearly vertically is present in a few outcrops in the extreme southern portion of the study area. A pressure solution origin for the cleavages is likely.

Kink-bands striking approximately N70E-S70W and dipping 20 degrees to the south are present at Thomson Dam. They appear to have formed by processes involved with both the rotation and the joint-drag models of kinking. They probably formed late in the structural history of the area; possibly as a result of Keweenawan activity.

Numerous areas show the effects of other late-stage deformation

such as faulting, jointing and the deformation or "readjustment" of the earlier cleavage. These structures are probably a result of late Penokean or Keweenawan activity.

There is a boundary between terranes affected by one (to the north) and two (to the south) Penokean deformations that extends across the southern portion of the study area. This has also been noted by Holst (1984c) in his paper dealing with the existence of nappes in the southern Thomson Formation. Recent geochemical studies in Wisconsin and the identification of probable nappes suggest that plate tectonic processes may have been responsible for Penokean deformation in the Thomson Formation.

### References cited

- Anderson, T. B., 1964, Kink-bands and related geologic structures: Nature, V. 202, pp. 272-274.
- Beutner, E. C., 1978, Slaty cleavage and related strain in Martinsburg Slate, Delaware Water Gap, New Jersey: Am. J. Sci., V. 278, pp. 1-23.
- Beutner, E. C., 1980, Slaty cleavage unrelated to tectonic dewatering: The Siamo and Michigamme Slates revisited: Geol. Soc. Am. Bull., Pt. 1, V. 91, pp. 171-178.
- Borradaile, G. J., 1978, Transected folds: A study illustrated with examples from Canada and Scotland: Geol. Soc. Am. Bull., V. 89, pp. 481-493.
- Borradaile, G. J., 1982, Chlorite-mica blasts in slate with continuous cleavage, in Borradaile, G. J., Bayley, M. B., and Powell, C. McA., eds., Atlas of Deformation and Metamorphic Rock Fabrics: Springer-Verlag, New York, pp. 458-459.
- Bouma, A. H., 1962, Sedimentology of some Flysch Deposits: Elsevier Pub. Co., Amsterdam, 168 pp.
- Braddock, W. A., 1970, The origin of slaty cleavage: Evidence from Precambrian rocks in Colorado: Geol. Soc. Am. Bull., V. 81, pp. 589-600.
- Brown, B. A. and Greenberg, J. A., 1981, Middle Proterozoic deformation in northern and central Wisconsin (abs.): 27th Institute on Lake Superior Geology, East Lansing, p. 8.
- Cambray, F. W., 1977, Field guide to the Marquette District, Michigan: Michigan Basin Geol. Soc. Ann. Meeting, 62 pp.
- Cambray, F. W., 1978, Plate tectonics as a model for the environment of deposition and deformation of the Early Proterozoic (Precambrian X) of northern Michigan (abs.): Geol. Soc. Am. Abs. with Programs, V. 10, p. 376.
- Cannon, W. F., 1973, The Penokean orogeny in northern Michigan, in Young, G. M., ed., Huronian stratigraphy and sedimentation: Geol. Assoc. Can. Sp. Paper 12, pp. 211-249.
- Clifford, P. M., 1968, Kink-band development in the Lake St. Joseph area, northwestern Ontario, in Baer, A. J. and Norris, D. K., eds. Proceedings of conference on research in tectonics (kink-bands and brittle deformation): Can. Geol. Surv. Paper 68-52, pp. 229-241.
- Connolly, M. R., 1981, The geology of the Middle Precambrian Thomson

Formation in southern Carlton County, east-central Minnesota: unpub. M.S. thesis, Univ. Minn.-Duluth.

Cosgrove, J. W., 1976, The formation of crenulation cleavage: J. Geol. Soc. Lond., V. 132, pp. 155-178.

Craddock, C., Mudrey, M. G., and Holst, T. B., 1983, Precambrian geology south of Lake Superior (Field trip 4): Geol. Soc. Am. Ann. Meeting, Indianapolis.

Davidson, D. M., Jr., 1979, Some structural attributes of Lower and Middle Precambrian rocks, Carlton and Pine Counties, Minnesota, in Balaban, N. H., ed., Field trip guidebook for stratigraphy, structure and mineral resources of east-central Minnesota: Minn. Geol. Surv., Guidebook series #9, pp. 29-41.

De la Beche, H. T., 1838, Report on the Geology of Cornwall, Devon and West Somerset: Longmans, London, 648 pp.

Dewey, J. F., 1965, Nature and origin of kink-bands: Tectonophysics, V. 1, pp. 459-494.

Dewey, J. F., 1969, The origin and development of kink-bands in a foliated body: Geol. J., V. 6, Pt. 2, pp. 193-216.

Dickinson, W. R., 1970, Interpreting detrital modes of greywackes and arkose: J. Sed. Pet., V. 40, pp. 695-707.

Donath, F. A., 1968, Experimental study of kink-band development in Martinsburg Slate, in Baer, A. J. and Norris, D. K., eds., Proceedings of conference on research in tectonics (kink-bands and brittle deformation): Can. Geol. Surv. Paper 68-52, pp. 255-288.

Donath, F. A. and Parker, R. B., 1964, Folds and folding: Geol. Soc. Am. Bull., V. 75, pp. 45-62.

Durney, D. W., 1972, Solution transfer, an important geological deformation mechanism: Nature, V. 235, pp. 315-317.

Durney, D. W., 1976, Pressure solution and crystallization deformation, in Ramsey, J. G. and Wood, D. S., eds., A discussion on natural strain and geological structure: Phil. Trans. Roy. Soc. Lond., V. A283, pp.229-240.

Fletcher, R. C., 1977, Quantitative theory for metamorphic differentiation in development of crenulation cleavage: Geol., V. 5, pp. 185-187.

Geiser, P. A., 1975, Slaty cleavage and the dewatering hypothesis - An examination of some critical evidence: Geol., V. 3, pp. 717-720.

- Goldich, S. S., Nier, A. O., Baadsgaard, H., Hoffman, J. H., and Krueger, H. W., 1961, The Precambrian geology and geochronology of Minnesota: Minn. Geol. Surv. Bull. 41, 193 pp.
- Gray, D. R., 1977a, Differentiation associated with discrete crenulation cleavages: Lithos, V. 10, pp. 89-101.
- Gray, D. R., 1977b, Some parameters which affect the morphology of crenulation cleavages: J. Geol., V. 85, pp. 763-780.
- Gray, D. R., 1978, Cleavages in deformed psammitic rocks from southeastern Australia: Their nature and origin: Geol. Soc. Am. Bull., V. 89, pp. 577-590.
- Gray, D. R., 1979a, Microstructure of crenulation cleavages: An indication of cleavage origin: Am. J. Sci., V. 279, pp. 97-128.
- Gray, D. R., 1979b, Geometry of crenulation-folds and their relationship to crenulation cleavage: J. Struct. Geol., V. 1, pp. 187-205.
- Gray, D. R. and Durney, D. W., 1979a, Investigations into the mechanical aspects of crenulation cleavage: Tectonophysics, V. 58, pp. 35-79.
- Gray, D. R. and Durney, D. W., 1979b, Crenulation cleavage differentiation: Implications of solution-deposition processes: J. Struct. Geol., V. 1, pp. 73-80.
- Greenberg, J. K. and Brown, B. A., 1983, Lower Proterozoic volcanic rocks and their setting in the southern Lake Superior district: Geol. Soc. Am. Memoir 160, pp. 67-83.
- Greenhalgh, 1979, Studies with a small seismic array in east-central Minnesota: Unpub. Ph.D. thesis, Univ. Minn.
- Gregg, W. J., 1979, The redistribution of pre-cleavage clastic dikes by folding at New Paltz, New York: J. Geol., V. 87, pp. 99-104.
- Groshong, R. H., Jr., 1976, Strain and pressure solution in Martinsburg Slate, Delaware Water Gap, New Jersey: Am. J. Sci., V. 276, pp. 1131-1146.
- Grout, F. F., Gruner, J. W., Schwartz, G. M., and Thiel, G. A., 1951, Precambrian stratigraphy of Minnesota: Geol. Soc. Am. Bull., V. 62, pp. 1017-1078.
- Hall, C. W., 1901, Keewatin area of eastern and central Minnesota: Geol. Soc. Am. Bull., V. 12, pp. 343-376.
- Harder, E. C. and Johnson, A. W., 1918, Preliminary report on the geology of east-central Minnesota including the Cuyuna iron-ore

- district: Minn. Geol. Surv. Bull. 15, 178 pp.
- Holst, T. B., 1982, Evidence for multiple deformation during the Penokean orogeny in the Middle Precambrian Thomson Formation, Minnesota: Can. J. Earth Sci., V. 19, pp. 2043-2047.
- Holst, T. B., 1983, Implications of strain measurements from Early Proterozoic rocks in Minnesota (abs.): Geol. Soc. Am. Abs. with Prog., V. 15, p. 598.
- Holst, T. B., 1984a, The Early Proterozoic Penokean orogeny as a convergent plate boundary: Structural evidence from the Thomson Formation of Minnesota (abs.): Geol. Assoc. Can. Symposium, Plate Tectonics in the Proterozoic.
- Holst, T. B., 1984b, Penokean tectonics: Constraints from the structural geology in east-central Minnesota (abs.): Institute of Lake Superior Geology, Wausau, Wisc.
- Holst, T. B., 1984c, Evidence for nappe development during the early Proterozoic Penokean orogeny, Minnesota: Geol., V. 12, pp. 135-138.
- Hyrkas, J., 1982, Structural geology and sedimentology of the Middle Precambrian Thomson Formation, central Carlton County, Minnesota: Unpub. M.S. thesis, Univ. Minn. - Duluth.
- Irving, R. D., 1883, The copper-bearing rocks of Lake Superior: U. S. Geol. Surv. Mon. 5, 464pp.
- Keighen, C. W., Morey, G. B., and Goldich, S. S., 1972, East-central Minnesota, in Sims, P. K. and Morey, G. B., eds., The Geology of Minnesota: A centennial volume: Minn. Geol. Surv., pp. 240-255.
- Kilburg, J. A. and Morey, G. B., 1977, Reconnaissance geologic map of the Esko quadrangle, St. Louis and Carlton Counties, Minnesota: Minn. Geol. Surv. Misc. Map Series M-25.
- Klasner, J. S., 1978, Penokean deformation and associated metamorphism in the western Marquette Range, northern Michigan, Geol. Soc. Am. Bull., V. 89, pp. 711-722.
- Larue, D. K. and Sloss, L. L., 1980, Early Proterozoic sedimentary basins of the Lake Superior region - Summary: Geol. Soc. Am. Bull., Pt. 1, V. 91, pp. 450-452.
- Leith, C. K., 1903, The Mesabi iron-bearing district of Minnesota: U. S. Geol. Surv. Mon., V. 43, 316 pp.
- Maass, R. S., 1983, Early Proterozoic tectonic style in central Wisconsin: Geol. Soc. Am. Memoir 160, pp. 85-95.



- Maass, R. S., Medaris, L. G., and Van Schmus, W. R., 1980, Penokean deformation in central Wisconsin: Geol. Soc. Am. Sp. Paper 182, pp. 147-157.
- March, A., 1932, Mathematische Theorie der Regelung nach der Korngestalt bei affiner Deformation: Z. Kristallogr., V. 81, pp. 285-297.
- Maxwell, J. C., 1962, Origin of slaty and fracture cleavage in the Delaware Water Gap area, New Jersey and Pennsylvania, in Engel, A. E. J. and others, eds., Petrologic Studies: Boulder, Colo., Geol. Soc. Am., pp. 281-311.
- Means, W. H., 1975, Natural and experimental microstructures in deformed micaceous sandstones: Geol. Soc. Am. Bull., V. 86, pp. 1221-1229.
- Morey, G. B., 1972, General geologic setting, in Sims, P. K. and Morey, G. B., eds., Geology of Minnesota: A centennial volume: Minn. Geol. Surv., pp. 199-203.
- Morey, G. B., 1978, Lower and Middle Precambrian stratigraphic nomenclature for east-central Minnesota: Minn. Geol. Surv. Report of Invest. 21, 52 pp.
- Morey, G. B., 1979, Stratigraphic and tectonic history of east-central Minnesota, in Balaban, N. H., ed., Field trip guidebook for stratigraphy, structure and mineral resources of east-central Minnesota: Minn. Geol. Surv., Guidebook Series #9, pp. 13-28.
- Morey, G. B., 1983, Lower Proterozoic stratified rocks and the Penokean orogeny in east-central Minnesota: Geol. Soc. Am. Memoir 160, pp. 97-112.
- Morey, G. B. and Ojakangas, R. W., 1970, Sedimentology of the Middle Precambrian Thomson Formation, east-central Minnesota: Minn. Geol. Surv. Report Invest. 13, 32 pp.
- Morey, G. B., Olsen, B. M., and Southwick, D. L., 1981, Geologic map of east-central Minnesota: Minn. Geol. Surv., scale 1:250,000.
- Morey, G. B. and Sims, P. K., 1976, Boundary between two Precambrian W terranes in Minnesota and its geologic significance: Geol. Soc. Am. Bull., V. 87, pp. 141-152.
- Neuman, S., in prep., Lower and Middle Precambrian geology of the Denham area, northern Pine County, east-central Minnesota: Unpub. M.S. thesis, Univ. Minn. - Duluth.
- Ojakangas, R. W., 1976, Uranium potential in Precambrian rocks of Minnesota: U.S. Dept. of Energy Open-file Report GJBX-62(76), Grand

- Junction Office, Colorado, 267 pp.
- Ojakangas, R. W., 1983, Tidal deposits in the Early Proterozoic basin in the Lake Superior region - The Palms and Pokegama Formations: Evidence for subtidal-shelf deposition of Superior-type banded iron formations: Geol. Soc. Am. Memoir 160, pp. 49-66.
- Paterson, M. S. and Weiss, L. E., 1962, Experimental folding of rocks: Nature, V. 195, pp. 1046-1048.
- Paterson, M. S. and Weiss, L. E., 1966, Experimental deformation and folding in phyllite: Geol. Soc. Am. Bull., V. 77, pp. 343-374.
- Potter, P. E. and Pettijohn, F. J., 1977, Paleocurrent and Basin Analysis: New York, Springer-Verlag, 425 pp.
- Powell, C. McA., 1969, Intrusive sandstone dykes in the Siamo Slate near Negaunee, Michigan: Geol. Soc. Am. Bull., V. 80, pp. 2585-2594.
- Powell, C. McA., 1972, Tectonic dewatering and strain in the Michigamme Slate, Michigan: Geol. Soc. Am. Bull., V. 83, pp. 2149-2158.
- Powell, C. McA., 1979, A morphologic classification of rock cleavage: Tectonophysics, V. 58, pp. 24-34.
- Ramsey, J. G., 1967, Folding and Fracturing of Rocks: McGraw-Hill, New York, 568 pp.
- Ramsey, J. G. and Wood, D. S., 1973, The geometric effects of volume change during deformation processes: Tectonophysics, V. 16, pp. 263-277.
- Sandberg, A. E., 1938, Section across Keewenawan lavas at Duluth, Minnesota: Geol. Soc. Am. Bull., V. 49, pp. 795-830.
- Schulz, K. J., 1983, Geochemistry of the volcanic rocks of northeastern Wisconsin (abs.): 29th Institute on Lake Superior Geology, Houghton, MI, pp. 39-40.
- Schwartz, G. M., 1942a, Structures in the Thomson Formation, Minnesota: Econ. Geol., V. 37, pp. 39-63.
- Schwartz, G. M., 1942b, Correlation and metamorphism of the Thomson Formation, Minnesota: Geol. Soc. Am. Bull., V. 53, pp. 1001-1020.
- Schwartz, G. M., 1942c, Concretions of the Thomson Formation, Minnesota: Am J. Sci., V. 240, pp. 491-499.
- Sims, P. K., 1976, Precambrian tectonics and mineral deposits, Lake Superior region: Econ. Geol., V. 71, pp. 1092-1127.

- Sims, P. K., 1980, Boundary between Archean greenstone and gneiss terranes in northern Wisconsin and Michigan: Geol. Soc. Am. Sp. Paper 182, pp. 113-124.
- Sims, P. K., Card, K. D., Morey, G. B., and Peterman, Z. E., 1980, The Great Lakes tectonic zone - A major crustal structure in central North America: Geol. Soc. Am. Bull., Pt. 1, V. 91, pp. 690-698.
- Sims, P. K. and Peterman, Z. E., 1983, Evolution of the Penokean foldbelt, Lake Superior region, and its tectonic environment: Geol. Soc. Am. Memoir 160, pp. 3-14.
- Sims, P. K. and Viswanathan, S., 1972, Giants Range Batholith, in Sims, P. K. and Morey, G. B., eds., The Geology of Minnesota: A centennial volume: Minn. Geol. Surv., pp. 220-239.
- Spurr, J. E., 1894, The stratigraphic position of the Thomson slates: Am. J. Sci., V. 48, pp.159-166.
- Van Hise, C. R. and Leith, C. K., 1911, The geology of the Lake Superior region: U. S. Geol. Surv. Mon. 52, 641 pp.
- Van Schmus, W. R., 1976, Early and Middle Proterozoic history of the Great Lakes area, North America: Phil. Trans. R. Soc. Lond., V. 280, pp. 605-628.
- Van Schmus, W. R., 1980, Chronology of igneous rocks associated with the Penokean orogeny in Wisconsin: Geol. Soc. Am. Sp. Paper 182, pp.159-168.
- Van Schmus, W. R., 1981, Possible interpretations of the Penokean orogeny (abs.): Int'l Proterozoic Symposium, Univ. Wisc. - Madison, p. 44.
- Van Schmus, W. R. and Bickford, M. E., 1981, Proterozoic chronology and evolution of the Midcontinent region, North America, in Kroner, A., ed., Precambrian plate-tectonics: Elsevier, pp. 261-296.
- Verbeek, E. R., 1978, Kink-bands in the Somport Slates, west-central Pyrenees, France and Spain: Geol. Soc. Am. Bull., V. 89, pp. 814-824.
- Walker, R. G., 1967, Turbidite sedimentary structures and their relationship to proximal and distal depositional environments, J. Sed. Pet., V. 37, pp. 25-43.
- Weiblen, P. W., 1964, A preliminary study of the metamorphism of the Thomson Formation: Unpub. M.S. thesis, Univ. Minn., Minneapolis 153 pp.

- White, S. H. and Knipe, R. J., 1978, Microstructure and cleavage development in selected slates: Contrib. Min. Pet., V. 66, pp. 165-174.
- Williams, P. F., 1972, Development of metamorphic layering and cleavage in low-grade metamorphic rocks of Bermagui, Australia: Am. J. Sci., V. 272, pp. 1-47.
- Wright, H. E., Mattson, L. A., and Thomas, J. A., 1970, Geology of the Cloquet quadrangle, Carlton County, Minnesota: Minn. Geol. Surv. Geol. Map GM-3 (with text), 30 pp.